Associate Editor Decision: Reconsider after major revisions (14 Oct 2020) by Martin De Kauwe

Dear Martin de Kauwe, dear referees,

We thank the reviewers for their time and effort to review our revised manuscript. We are very pleased that reviewer #1 was satisfied with our revision and recommended to accept our revised manuscript. We have inserted all of his minor points and suggestions in the 2nd revision (now manuscript version #5 in the BG file system; "bg-2020-97-manuscript-version5.pdf"). Regarding the continued criticism of reviewer #2 to our revised manuscript, we show in our response below that we already had in large part addressed his concern with our first revision of the manuscript and highlight this once more in our point-by-point response below. Furthermore, we now made additional changes to emphasize our storyline. We apologize that we did not upload a manuscript version showing all changes in track-changes mode with the first revision, which may have partly contributed to the difficulties for reviewer #2 not being able to see the in-depth revision that we had already undertaken. We have pasted the track changes version at the end of our response letter, which marks all the changes we made in the entire revision process.

In this author response, the editor comments are marked in *italic,* our response to the editor and reviewers is inserted in blue in the point-by-point response below.

Summary:

Both of the original reviewers have read your revised manuscript and arrive at contrasting positions. R1 is satisfied with your revisions but highlights some minor points to address. R2 is less convinced by the scope of the revision and raises some very important issues. I think it is important to address all of their points. For me they make two key points:

1. A better explanation of the motivation - why do we need variable rooting depth? This feels fairly straightforward but is an important element of the narrative for any reader.

Thank you for raising this point. In our view, the manuscript clearly introduces a hypothesis which we want to test. Testing this hypothesis is the motivation for implementing variable roots. Proving this hypothesis true is the reason why we need variable rooting depth. We have made additional changes to the current manuscript version #5 to clarify our logic. Here are our key points which can also be found in our detailed response to reviewer #2 below:

We would like to take the opportunity to explain our reasoning and refer also to our first author response letter. We show where in the revised manuscript we have made the requested changes:
Reviewer #2 claims that our "main motivation is to introduce variable rooting strategies" per se without wanting to "explain some phenomenon". We find that right in the beginning of the introduction the reader is introduced to a hypothesis and respective phenomenon, namely that "tree rooting depth is regarded as a crucial variable to explain the geographical distribution of main phenology strategies such as evergreen and deciduous, as well as the observed local to continental pattern of productivity, biomass storage, evapotranspiration (ET)" (line 39-42 last manuscript version #4). This is the hypothesis which aims at explaining the phenomenon why evergreen tropical forests have the observed geographical extent and why rates of ET and productivity are often high during the dry season. To further underline that this is the hypothesis we want to test, we now write "In this study we revisit the hypothesis that tree rooting depth is a crucial variable to explain the geographical distribution of main phenology

strategies such as evergreen and deciduous, as well as the observed local to continental pattern of productivity, biomass storage, evapotranspiration (ET) and consequently moisture recycling" (line 39-42 current manuscript version #5).
Next, we introduce the reader to the fact that most models have a prescribed constant shallow rooting depth which is regarded as a reason why they have problems "reproducing the extent of South-America's tropical evergreen forests, as well as its seasonal productivity and ET especially in regions with seasonal rainfall" (line 50-52 last manuscript version #4, line 51-53 current manuscript version #5). This addresses "the inability of previous models to explain the wide distribution of evergreen types" and represents a strong argument to support the hypothesis. To underline the latter point we now write "In favor of the rooting depth hypothesis, most DGVMs in the past had problems reproducing the extent of South-America's tropical evergreen forests, as well as its seasonal productivity and ET especially in regions with seasonal rainfall" (line 51-53 manuscript version #5).
In the following paragraph, we introduce several examples of modelling approaches trying to solve this problem and mention their positive results (line 52-63 manuscript version #4; line 53-64 manuscript version #5), i.e. another strong argument in favor of the hypothesis. Next we introduce the conceptual shortcomings of all those previous modelling approaches which could undermine the results of the respective studies (line 64-92 last manuscript version #4; line 65-93 current manuscript version #5). This is a strong argument against the hypothesis and we therefore now write "… some assumptions of the underlying models might decrease the liability of their results and therefore pose arguments against the rooting depth hypothesis" (line 65-67 current manuscript version #5). We then continue to explain how our modelling approach overcomes these shortcomings (line 93-100 last manuscript version #4; line 94-101 current manuscript version #5). We finish the introduction with a clear statement that our study wants to "re-evaluate the hypothesis that varying tree rooting depth is key to explain major patterns of evapotranspiration, productivity and the geographical distribution of tropical evergreen forests in South America" (line 101-104 last manuscript version #4; line 102-105 current manuscript version #5). We give a clear summarizing answer regarding this re-evaluation of the hypothesis in the conclusion saying: "We here show for the first time that mean tree rooting depth across South-America can indeed explain the spatial distribution of tropical evergreen forests and their spatio-temporal pattern of ecosystem fluxes (ET and NEE) even when the competition of tree rooting strategies, carbon investment into gradually growing roots, and a spatially explicit soil depth are considered." (line 617-619 last manuscript version #4; line 583-585 current manuscript version #5). We furthermore now explicitly mention the hypothesis in the abstract (line 29-31 current manuscript version #5).

In summary we make it very clear that our "main motivation" is neither to introduce variable roots per se, nor to increase model quality per se (as suggested by reviewer #2), but to test this hypothesis. This is also in accordance with the requests from the first reviews to introduce a more biology oriented objective or research question that we want to answer with this study.

With this explanation and evidence from the revised manuscript we hope to have now made our reasoning clear which we had explained in our author response to reviewer #2 during the first round of revision. We hope that the introduction now clearly explains our justification of including variable roots to the reader and also explains the biology of the system.

2. I felt the reviewers point about not understanding why variable root depth leads to predicting a wider distribution of evergreens was very important. It is important this is clearly explained in the revision.

Our revised manuscript version 2 had already addressed this point in great detail, by addressing comments of reviewer #1 who had raised this issue in his/her first review. We had produced a detailed answer also in our first author response to reviewer #1. We explain again this point in our point-by-point explanation below. We have double-checked in our revised manuscript version #5, that this point is clearly explained and understandable to a wide audience. We have also answered new points raised by reviewer #2 of his second review in our response below and cross-checked this is clearly described and explained in the revised manuscript version #5. This also includes the explanation of the model differences in our method section. We hope to have now clarified the last remaining open questions in our revised manuscript version #5. Here are our key points which can also be found in our detailed response to reviewer #2 below:

Our answer on main issue of not understanding why deeper roots lead to better reproducing measured rates of evapotranspiration and distributions of PFTs:

We agree that this is an important point in improving the manuscript and so we take the opportunity to explain why variable rooting depth has an effect on the spatial distribution of evergreen trees.

An evergreen plant needs a minimum water supply all year round. When models use the standard maximum rooting depth of around 1 m they fail to reproduce evapotranspiration rates and the distribution of tropical evergreen rainforest. When we allow for variable rooting depth (even with investment trade-offs and root growth) results of evapotranspiration and evergreen distribution come close to observations. By weighting rooting depth with NPP contribution (Fig. 5) and plotting this rooting depth vs. an index of dry season strength (MCWD) and annual precipitation (Fig. 6), we show how the simulated vegetation adjusts to those climatological conditions. As deep roots are costly, any adjustment towards deeper roots must mean that deeper rooted PFTs are more productive, hence more competitive. And this adjustment makes only sense when the general growing strategy is “evergreen”. So, the ultimate answer for “why are the results improving?” is, because the evergreen PFT has access to deep water in the dry season and gains a competitive advantage. We refer to lines 480-490, 503-516, 537-548 and 555-564 in the discussion section in the current manuscript version #5, where we discuss all these implications. Responding to the first review of reviewer #2, we put much emphasis on this explanation in our first manuscript revision. We have inserted background information on how water percolation is simulated in the LPJmL model (line 137-152 current manuscript version #5) as was requested by reviewer #2. Related to this, we also inserted a new Appendix figure (now Fig. A9 referred to in line 564 current manuscript version #5) both in the manuscript but also directly in the last response letter which irrefutable shows how the deep roots in LPJmL4.0-VR extract water from deep soil layers during the dry season in comparison to LPJmL4.0-VR-base. This level of evidence and explanation makes, in our view, a convincing set of arguments. We also refer to our response to the point below on a related topic. We would like to emphasize that we wrote a

comprehensive paragraph specifically focusing on this topic in the last response letter to reviewer #2.

Our answers on questions regarding differences between model versions related to doubting that rooting depth is the reason for reproducing measured rates of evapotranspiration and distributions of PFTs:

We thank the reviewer for raising this point, which reviewer #1 also raised in his/her first review. Therefore, we had already explained this point in the revised manuscript version 2 in our previous resubmission. We would like to refer to our author response letter to reviewer #1 (p. 9 in bg-2020-97-AC1_version2.pdf), where he/she had commented on Fig. 12 which is now Fig. 10. We provide a high detail explanation, in response to the first review of reviewer#1, in the current manuscript version #5 in lines 503-516. It resolves all these new questions of reviewer #2. In summary our explanation in the revised manuscript comprises the following points:

LPJmL4.0 has 1) a constant shallow root distribution for both tropical tree PFTs and 2) no dominance dependent establishment of PFTs. Here the evergreen PFT is slightly more abundant in the wetter tropics and the deciduous slightly more abundant in the drier tropics (now Fig. 10g-h). Since there is no real mechanism rewarding one tree strategy over the other over time in the LPJmL4.0 model (including the spin-up simulation phase), both PFTs can be found about 50/50 in the Amazon region. LPJmL4-VR-base also has 1) constant shallow root distribution for both tropical tree PFTs, but 2) a dominance-dependent establishment of PFTs (LPJmL4.0-VR-base is equal to LPJmL4.0-VR except that it allows for shallow roots only as explained in line 287-292 current manuscript version #5). These two criteria reveal under which climate conditions, each PFT outcompetes the other over time, if trees could grow shallow roots only. Therefore, there is a clear dominance pattern of either PFT using LPJmL4.0-VR-base (even though this pattern is far away from matching evaluation data). Now in LPJmL4-VR, the addition of variable roots (which is the only difference to LPJmL4.0-VR-base), broadens the geographical extent where the evergreen PFT is clearly dominant. In this sense, LPJmL-VR-base does not go a "considerable way to explaining the wide distribution of evergreens", but only reveals the true dominance pattern of PFTs when performance is rewarded. Acceptable results are only achieved when adding variable roots, i.e. with LPJmL4.0-VR.
The dominance-dependent tree establishment and its consequences are mentioned at different occasions in the manuscript, e.g. in the discussion in line 503-513 (current manuscript version #5). We think we made sure that this point is now clearly explained in the revised manuscript.

I am recommending further major revisions to allow you time to fully address the concerns of R2.

Thank you for reconsidering our manuscript. Please find our detailed answers regarding the comments of reviewer #1 & #2 below.

Referee #1: Anonymous

The authors revised the manuscript substantially and it is now much clearer and more concise. All my comments and suggestions were adequately considered and included in the revised manuscript. I don't have additional major comments, only a few minor points and suggestions.

Thank you for your positive evaluation and important remarks. We have addressed all your points.

l. 35: often have access
Changed accordingly in line 35.
l. 66: maybe mention timing of what
We changed the word "timing" to "temporal growth" to be more specific now in line 67.
l. 131: but extend this scheme
Changed accordingly in line 131.
l. 133: computational demand. Further, I assume that this demand increase because deeper soil implies more soil layers that need to be updated. (in principle it would also be possible to keep the number of soil layers but change their thickness.
Changed accordingly now in line 134. You are right. In principle any soil layer thickness can be applied. Choosing thicker soil layers would decrease the computational demand, but would decrease the vertical resolution of root shapes as well as the temporal resolution of water percolation and temporal resolution of root growth. We chose the general soil layer partitioning of LPJmL4.0 of 1 m, in order to keep differences between model versions as small as possible. We now indicate this reason in line 132.
l. 194: when considering coarse roots
Changed accordingly now in line 195-196.
l. 371: explain the geographical pattern
Changed accordingly now in line 372.
l. 428: and more seasonal climates
Changed accordingly now in line 429.
l. 441: negative correlation
Changed accordingly now in line 442.
l. 456: other two models
Changed accordingly now in line 457.
l. 478: delete header, there is no 3.4.2
Thank you for pointing out this mistake. The whole section regarding simulated biomass has been moved to the Appendix.
l. 529: climatic envelope
Changed accordingly now in line 514.
l. 530: which coincides with

Changed accordingly now in line 515.

Referee #2: Daniel Falster, daniel.falster@unsw.edu.au

I reviewed a previous version of this paper, which introduces a scheme for variable rooting depths into the LPJmL4.0 DGVM. While generally enthusiastic about the idea, I found the previous version too long and unfocussed, which prevented any deep engagement and understanding. Both reviewers felt similarly and requested a more focussed narrative.

While the revised paper is a little clearer and has benefited from some minor improvements, my major criticisms have only been superficially addressed. The authors have clarified their goals only a little by adding a few lines of text in the introduction. Otherwise the introduction and methods seems almost identical, and we still have 12 figures, most with multiple panels.

We have pasted the track changes version of the manuscript version #5 at the end of our response letter, which marks all the changes we made in the entire revision process. We apologize for this confusion so that the reviewer could not retrace the modifications. We have compiled this now together with the minor changes from reviewer #1 which illustrates that the revision was indeed in-depth.
In the first revision, we reduced the number of figures from 15 to 12. Because we aim to enhance readability also for non-modelers, we want to emphasize that Fig. 1-3 are methodological figures which we regard as being essential for readers who are less familiar with modelling techniques to follow our logic. For the current manuscript version #5 we now additionally transferred Fig. 11-12 and the respective results and discussion section to the Appendix, which reduces the number of figures to 10 and shortens the manuscript. The remaining figures we regard as crucial results and very important for the storyline. Those figures show simulated rooting depths, evapotranspiration rates and forest type cover, which are essential variables to support the findings of our study.

The authors really need to do more to streamline the paper and tell a convincing story about the biology of the system.
The way it currently reads, the main motivation is to introduce variable rooting strategies. But this is the solution. The motivation should be to explain some phenomenon: I'd suggest focussing on the inability of previous models to explain the wide distribution of evergreen types in the Amazon. While the authors do mention this in paragraph two, this material seems to come second to the goal of modelling variable rooting depths, and then gets lost amongst the many plots and attention given to biomass and ET.

The significance of the problem relating to evergreens vs deciduous doesn't really hit until we reach Figure 10, which shows just how bad the standard LPJ model does in predicting the distribution of evergreen vs deciduous types. Perhaps these panels could be introduced in the introduction, to motivate the study? Then variable rooting depth introduced as a potential solution?

We would like to take the opportunity to explain our reasoning and refer also to our first author response letter. We show where in the revised manuscript we have made the requested changes:

Reviewer #2 claims that our "main motivation is to introduce variable rooting strategies" per se without wanting to "explain some phenomenon". We find that right in the beginning of the introduction the reader is introduced to the hypothesis and respective phenomenon, namely

that “tree rooting depth is regarded as a crucial variable to explain the geographical distribution of main phenology strategies such as evergreen and deciduous, as well as the observed local to continental pattern of productivity, biomass storage, evapotranspiration (ET)” (line 39-42 last manuscript version #4). This is the hypothesis which aims at explaining the phenomenon why evergreen tropical forests have the observed geographical extent and why rates of ET and productivity are often high during the dry season. To further underline that this is the hypothesis we want to test, we now write “In this study we revisit the hypothesis that tree rooting depth is a crucial variable to explain the geographical distribution of main phenology strategies such as evergreen and deciduous, as well as the observed local to continental pattern of productivity, biomass storage, evapotranspiration (ET) and consequently moisture recycling” (line 39-42 current manuscript version #5).
Next, we introduce the reader to the fact that most models have a prescribed constant shallow rooting depth which is regarded as a reason why they have problems “reproducing the extent of South-America’s tropical evergreen forests, as well as its seasonal productivity and ET especially in regions with seasonal rainfall” (line 50-52 last manuscript version #4, line 51-53 current manuscript version #5). This addresses “the inability of previous models to explain the wide distribution of evergreen types” and represents a strong argument to support the hypothesis. To underline the latter point we now write “In favor of the rooting depth hypothesis, most DGVMs in the past had problems reproducing the extent of South-America’s tropical evergreen forests, as well as its seasonal productivity and ET especially in regions with seasonal rainfall” (line 51-53 current manuscript version #5).
In the following paragraph, we introduce several examples of modelling approaches trying to solve this problem and mention their positive results (line 52-63 last manuscript version #4; line 53-64 current manuscript version #5), i.e. another strong argument in favor of the hypothesis. Next we introduce the conceptual shortcomings of all those previous modelling approaches which could undermine the results of the respective studies (line 64-92 last manuscript version #4; line 65-93 current manuscript version #5). This is a strong argument against the hypothesis and we therefore now write “… some assumptions of the underlying models might decrease the liability of their results and therefore pose arguments against the rooting depth hypothesis” (line 65-67 current manuscript version #5). We then continue to explain how our modelling approach overcomes these shortcomings (line 93-100 last manuscript version #4; line 94-101 current manuscript version #5). We finish the introduction with a clear statement that our study wants to “re-evaluate the hypothesis that varying tree rooting depth is key to explain major patterns of evapotranspiration, productivity and the geographical distribution of tropical evergreen forests in South America” (line 101-104 last manuscript version #4; line 102-105 current manuscript version #5). We give a clear summarizing answer regarding this re-evaluation of the hypothesis in the conclusion saying: “We here show for the first time that mean tree rooting depth across South-America can indeed explain the spatial distribution of tropical evergreen forests and their spatio-temporal pattern of ecosystem fluxes (ET and NEE) even when the competition of tree rooting strategies, carbon investment into gradually growing roots, and a spatially explicit soil depth are considered.” (line 617-619 last manuscript version #4; line 583-585 current manuscript version #5). We furthermore now explicitly mention the hypothesis in the abstract (line 29-31 current manuscript version #5).

In summary we make it very clear that our “main motivation” is neither to introduce variable roots per se, nor to increase model quality per se (as suggested by reviewer #2), but to test this hypothesis. This is also in accordance with the requests from the first reviews to introduce a more biology oriented objective or research question that we want to answer with this study. The storyline is oriented along this hypothesis and delivers an ecological derivation of our main conclusion, by a) first showing that in our modelling approach the

rooting strategies align along the environmental gradients, which then leads to being able to reproduce b) observed rates of evapotranspiration productivity as well as c) observed distributions of plant functional types.

With this explanation and evidence from the revised manuscript we hope to have now made our reasoning clear which we had explained in our author response to reviewer #2 during the first round of revision. We hope that the introduction now clearly explains our justification of including variable roots to the reader and also explains the biology of the system.

After reading the paper several times, I still can't say why variable rooting depth leads the LPJmL4.0-VR version to predict wider distribution of evergreens. I see that it does, but don't understand why.

We agree that this is an important point in improving the manuscript and so we take the opportunity to explain why variable rooting depth has an effect on the spatial distribution of evergreen trees:

An evergreen plant needs a minimum water supply all year round. When models use the standard maximum rooting depth of around 1 m they fail to reproduce evapotranspiration rates and the distribution of tropical evergreen rainforest. When we allow for variable rooting depth (even with investment trade-offs and root growth) results of evapotranspiration and evergreen distribution come close to observations. By weighting rooting depth with NPP contribution (Fig. 5) and plotting this rooting depth vs. an index of dry season strength (MCWD) and annual precipitation (Fig. 6), we show how the simulated vegetation adjusts to those climatological conditions. As deep roots are costly, any adjustment towards deeper roots must mean that deeper rooted PFTs are more productive, hence more competitive. And this adjustment makes only sense when the general growing strategy is “evergreen”. So, the ultimate answer for “why are the results improving?” is, because the evergreen PFT has access to deep water in the dry season and gains a competitive advantage. We refer to lines 480-490, 503-516, 537-548 and 555-564 in the discussion section in the current manuscript version #5, where we discuss all these implications. Responding to the first review of reviewer #2, we put much emphasis on this explanation in our first manuscript revision. We have inserted background information on how water percolation is simulated in the LPJmL model (line 137-152 current manuscript version #5) as was requested by reviewer #2. Related to this, we also inserted a new Appendix figure (now Fig. A9 referred to in line 564 current manuscript version #5) both in the manuscript but also directly in the last response letter which irrefutable shows how the deep roots in LPJmL4.0-VR extract water from deep soil layers during the dry season in comparison to LPJmL4.0-VR-base. This level of evidence and explanation makes, in our view, a convincing set of arguments. We also refer to our response to the point below on a related topic. We would like to emphasize that we wrote a comprehensive paragraph specifically focusing on this topic in the last response letter to reviewer #2.

That said, the results suggest it's not only about variable rooting depth. I was interested to see in Figure 10 that that the LPJmL4.0-VR-base model actually goes a considerable way to explaining the wide distribution of evergreens. So there seems to be two changes making a

difference: from LPJmL4.0 -> LPJmL4.0-VR-base, then from LPJmL4.0-VR-base -> LPJmL4.0-VR. The authors need to explain the biological mechanism causing LPJmL4.0 and LPJmL4.0-VR-base to differ and perhaps temper their claims about variable rooting accordingly.

We thank the reviewer for raising this point, which reviewer #1 also raised in his/her first review. Therefore, we had already explained this point in the revised manuscript version 2 in our previous resubmission. We would like to refer to our author response letter to reviewer #1 (p. 9 in bg-2020-97-AC1_version2.pdf), where he/she had commented on Fig. 12 which is now Fig. 10. We provide a high detail explanation, in response to the first review of reviewer#1, in the current manuscript version #5 in lines 503-516. It resolves all these new questions of reviewer #2. In summary our explanation in the revised manuscript comprises the following points:

LPJmL4.0 has 1) a constant shallow root distribution for both tropical tree PFTs and 2) no dominance dependent establishment of PFTs. Here the evergreen PFT is slightly more abundant in the wetter tropics and the deciduous slightly more abundant in the drier tropics (now Fig. 10g-h). Since there is no real mechanism rewarding one tree strategy over the other over time in the LPJmL4.0 model (including the spin-up simulation phase), both PFTs can be found about 50/50 in the Amazon region. LPJmL4-VR-base also has 1) constant shallow root distribution for both tropical tree PFTs, but 2) a dominance-dependent establishment of PFTs (LPJmL4.0-VR-base is equal to LPJmL4.0-VR except that it allows for shallow roots only as explained in line 287-292 current manuscript version #5). These two criteria reveal under which climate conditions, each PFT outcompetes the other over time, if trees could grow shallow roots only. Therefore, there is a clear dominance pattern of either PFT using LPJmL4.0-VR-base (even though this pattern is far away from matching evaluation data). Now in LPJmL4-VR, the addition of variable roots (which is the only difference to LPJmL4.0-VR-base), broadens the geographical extent where the evergreen PFT is clearly dominant. In this sense, LPJmL-VR-base does not go a "considerable way to explaining the wide distribution of evergreens", but only reveals the true dominance pattern of PFTs when performance is rewarded. Acceptable results are only achieved when adding variable roots, i.e. with LPJmL4.0-VR.
The dominance-dependent tree establishment and its consequences are mentioned at different occasions in the manuscript, e.g. in the discussion in line 503-513 (current manuscript version #5). We think we made sure that this point is now clearly explained in the revised manuscript.

Unfortunately, the LPJmL4.0-VR-base model is never really introduced or explained in any detail, so we can only guess why it predicts a wider distribution of evergreens than LPJmL4.0. I also note strong differences between LPJmL4.0 and LPJmL4.0-VR-base in Tables A6 and A7. My naive expectation is that LPJmL4.0 and LPJmL4.0-VR-base should produce near identical results, as they mostly do in Tables A3-A5. Why is this the case, if there's no variance in rooting depth?

Here, we would like to stress that reviewer #2 is raising a new issue which we are happy to explain. Parts of these points are already addressed in our response above and had been answered in the first review. The other points are explained here:

Regarding the claim of reviewer #2 that LPJmL4.0-VR-base has never been introduced in the manuscript, we would like to refer to line 287-292 where LPJmL4-VR-base was perfectly introduced in the manuscript in section "2.4. Model versions and simulation protocol" since

our first submission. Moreover, the features of LPJmL4.0-VR-base are again explained in the discussion of the revised manuscript version #5 now in line 560-564.

Reviewer #2 claims that one "can only guess why it [LPJmL4.0-VR-base] predicts a wider distribution of evergreens than LPJmL4.0" and that numbers in Tables A3-A7 do not add up with our logic. However, the numbers in Tables A3-A7 are perfectly in line with our argumentation and the coherences are explained throughout the manuscript. As mentioned in our points above there must be differences between LPJmL4.0 and LPJmL4.0-VR-base, because one model rewards PFT performance over time and the other one does not (as explained in detail in line 503-513 current manuscript version #5). Again (as explained in our points above), therefore LPJmL4.0 shows no clear dominance pattern of PFTs, whereas LPJmL4.0-VR-base does show clear dominance pattern. That is why in Table A6 (comparing regional PFT dominance to validation data) and Table A7 (comparing regional biomass to validation data) the differences between the models are large. The reason why Table A3-A5 show nearly identical results for LPJmL4.0 and LPJmL4.0-VR-base is, because here simulation results are compared to regional/local monthly rates of evapotranspiration and local monthly net ecosystem exchange evaluation data. These monthly variables are highly dependent on PFT water access and therefore rooting depth. Because LPJmL4.0 and LPJmL4.0-VR-base have the same constant rooting depth (unlike LPJmL4.0-VR with variable rooting depth), regardless of the underlying PFT type, similar simulation results are obtained. In this sense, reviewer #2 is correct that there is no variance in rooting depth, but this is anticipated by our study design to show the reader 1) the effect of dominance-dependent tree establishment and 2) the effect of introducing variable roots.

We hope that with the current revision and additional explanations we have finally addressed all concerns of reviewer #2 and have hopefully provided a coherent and understandable manuscript.

Yours sincerely,
Boris Sakschewski on behalf of all co-authors.

Variable tree rooting strategies ~~improve tropical~~ are key to model distribution, productivity and evapotranspiration ~~in a dynamic global vegetation model~~of tropical evergreen forests

Boris Sakschewski[1], Werner von Bloh[1], Markus Drüke[1], Anna A. Sörensson[2, 3], Romina Ruscica[2, 3], Fanny Langerwisch[4, 5], Maik Billing[1], Sarah Bereswill[6], Marina Hirota[7, 8], Rafael S. Oliveira[8], Jens Heinke[1], Kirsten Thonicke[1]

[1]Potsdam Institute for Climate Impact Research, Potsdam, 14473, Germany
[2]Universidad de Buenos Aires - Consejo Nacional de Investigaciones Científicas y Técnicas, Centro de Investigaciones del Mar y la Atmósfera (CIMA/UBA-CONICET), Buenos Aires, Argentina.
[3]Institut Franco-Argentin d'Etudes sur le Climat et ses Impacts, Unité Mixte Internationale (UMI-IFAECI/CNRS-CONICET-UBA), Argentina
[4]Czech University of Life Sciences Prague, Department of Water Resources and Environmental Modeling, 165 00 Praha 6 – Suchdol, Czech Republic
[5]Palacký University Olomouc, Department of Ecology and Environmental Sciences, 78371 Olomouc, Czech Republic
[6]University of Potsdam, Potsdam, 14469, Germany
[7]Federal University of Santa Catarina (UFSC), Campus Universitário Reitor João David Ferreira Lima Trindade – Florianópolis – SC, CEP: 88040-900, Santa Catarina, Brazil
[8]University of Campinas (UNICAMP) Cidade Universitária "Zeferino Vaz" CEP 13083-970, Campinas-SP, Sao Paulo, Brazil

Correspondence to: Boris Sakschewski (boris.sakschewski@pik-potsdam.de)

Abstract. ~~Tree water access via roots is crucial for forest functioning and therefore forests have developed a vast variety of rooting strategies across the globe. However, Dynamic Global Vegetation Models (DGVMs), which are increasingly used to simulate forest functioning, often condense this variety of tree rooting strategies into biome scale averages, potentially under- or overestimating forest response to intra- and inter-annual variability in precipitation. Here we present a new~~A variety of modelling studies have suggested tree rooting depth as a key variable to explain evapotranspiration rates, productivity and the geographical distribution of evergreen forests in tropical South America. However, none of those studies acknowledged resource investment, timing and physical constraints of tree rooting depth within a competitive environment, undermining the ecological realism of their results. Here we present an approach of implementing variable rooting strategies and dynamic root growth into the LPJmL4.0 DGVM and apply it to tropical and sub-tropical South-America under contemporary climate conditions. We show how competing rooting strategies which underlie the trade-off between above- and below-ground carbon investment lead to more ~~realistic~~realistically simulated intra-annual productivity and evapotranspiration, and consequently forest cover and spatial biomass distribution. We find that climate and soil depth determine a spatially heterogeneous pattern of mean rooting depth and belowground biomass across the study region. Our findings support the hypothesis that the ability of evergreen trees to adjust their rooting systems to seasonally dry climates is crucial to explain the current dominance, productivity and evapotranspiration of evergreen forests in tropical South America.

1 Introduction

Tropical evergreen forest is the naturally dominant biome type in South-America over a large climatic range including regions with a marked dry season (Hirota et al., 2011; Xiao et al., 2006). To withstand seasonal shortages of precipitation and sustain productivity, trees with evergreen phenology often ~~gain~~ have access to deep soil water via deep roots (Brum et al., 2019; Canadell et al., 1996; Johnson et al., 2018; Kim et al., 2012; Markewitz et al., 2010). Consequently, recent studies suggest a heterogeneous spatial pattern of maximum rooting depth across tropical forest biomes in South-America which differs over the order of magnitudes depending on local groundwater, soil and climate conditions (Canadell et al., 1996; Fan et al., 2017). ~~Therefore,~~ In this study we revisit the hypothesis that tree rooting depth is ~~regarded as~~ a crucial variable to

explain the geographical distribution of main phenology strategies such as ~~"~~evergreen~~"~~ and ~~"~~deciduous~~",~~ as well as the observed local to continental pattern of productivity, biomass storage, evapotranspiration (ET) and consequently moisture recycling (Fan et al., 2017; Jobbágy and Jackson, 2000; Kleidon and Heimann, 2000; Langan et al., 2017; Nepstad et al., 1994; Stahl et al., 2013). To test this hypothesis, dynamic global vegetation models (DGVMs) seem to be promising tools, as those models are suitable to project the development of vegetation formation and ecosystem functioning systematically and on large spatial scales~~While these variables and processes are in the focus of model based earth system sciences projecting the development of vegetation formation and ecosystem functioning worldwide (Huntingford et al., 2013; Liu et al., 2018; Weber et al., 2009),~~ (Huntingford et al., 2013; Liu et al., 2018; Weber et al., 2009). However, most DGVMs ~~and land surface models (LSMs) still~~ do not represent the diversity of rooting depth or tree rooting strategies (Warren et al., 2015a). In general these models condense the diversity of such functional ~~plant~~tree traits ~~to biome scale averages, to simulate~~into so called plant functional types (PFTs~~))~~, which ~~reflect~~represent average ~~plant individuals of a biome~~tree growing strategies on scales as large as biomes. Here, often a shallow rooting depth for tree PFTs is assumed, i.e. most roots are distributed downwards to a few meters of depths at maximum (Arora and Boer, 2003; Best et al., 2011; Guimberteau et al., 2017; Lawrence et al., 2011; Ostle et al., 2009; Schaphoff et al., 2018; Smith et al., 2014).

In favour of the rooting depth hypothesis, most~~By ignoring natural local adaptations of rooting depth,~~ DGVMs ~~and LSMs~~ in the past had problems reproducing the extent of South-America's tropical evergreen forests, as well as its seasonal productivity and ET especially in regions with seasonal rainfall (Baudena et al., 2014; Liu et al., 2018, 2017; Restrepo-Coupe et al., 2017).

So far different ~~attempts~~approaches were ~~carried out~~presented trying to solve this problem in DGVMs and similar models by allowing for variable rooting strategies. ~~More than 20 years ago~~In a pioneering study ~~by~~more than 20 years ago, Kleidon and Heimann (1998) systematically searched for rooting strategies which yield highest net primary productivity over South America in a DGVM to explain intra-annual rates of ET and vegetation cover. Follow up studies further underlined the importance of deep roots for the climate system of South America (Kleidon and Heimann, 2000). Lee *et al.* (2005) found that allowing for deep roots and hydraulic redistribution of water in the soil column in a general circulation model enhances Amazon forest productivity and evapotranspiration (ET) in the dry season. Baker *et al.* (2008) came to similar results when introducing deep roots in a land surface model. Ichii *et al.*, (2007) found that constraining rooting depth across the Amazon based on satellite data yields similar results in a terrestrial ecosystem model. More recently, Langan, Higgins and Scheiter (2017) showed for the same study area how diverse rooting strategies in a tree individual and trait-based DGVM can improve simulated intra-annual productivity and ET and better explain patterns of different tropical biome types and biomass in connection with fire.

While these studies are important steps to acknowledge the diversity of tree rooting strategies and its effects, some assumptions of the underlying models might decrease the liability of their results and therefore pose arguments against the rooting depth hypothesis. These assumptions are related to 1) resource investment, 2) ~~timing~~ temporal growth and 3) physical constraints of rooting depth. 1) Most models so far do not account for coarse roots (Warren et al., 2015a) even though they can make up the majority of total root biomass (Xiao et al., 2003). This approach may be sufficient when employing shallow tree rooting strategies only, but with increasing rooting depth, costs for coarse roots increases substantially. Since the amount of resources trees can allocate to their processes and structures is finite, a local adaptation of tree rooting depth must follow a trade-off between above- and below-ground resource investment (Nikolova et al., 2011). Generally, above-ground investments into leaf and stem growth can increase light absorption and CO_2 uptake, while below-ground investments can increase the uptake of water and nutrients. Depending on local environmental and competitive conditions one or the other ~~direction~~allocation strategy might be more advantageous, eventually leading to substantial regional variation in the mean below-ground to above-ground biomass ratios (Leuschner et al., 2007; Mokany et al., 2006). Therefore, the simulated spectrum of tree rooting strategies which can survive and co-exist should be in accordance with this

crucial trade-off. 2) In contrast to above-ground stem growth, most DGVMs so far do not simulate gradual root growth (Warren et al., 2015a). Instead PFTs are assigned a constant relative distribution of fine roots throughout the soil column at any point in space and time (Best et al., 2011; Lawrence et al., 2011; Schaphoff et al., 2018; Smith et al., 2014). As under the above~~-~~-mentioned simplification under 1), this approach may be sufficient when accounting for shallow rooting strategies only, but when the maximum tree rooting depth of PFTs strongly diverges, it is questionable that the time needed to reach this depth is negligible, especially when accounting for PFT competition. Rooting depth increases rather gradually and non-linear over a tree's lifetime with a velocity driven by a mix of plastic optimization and allometric determination (Brum et al., 2019; Brunner et al., 2015; Nikolova et al., 2011; Poorter et al., 2012; Warren et al., 2015b). ~~While the knowledge base for a mechanistic bottom-up modelling approach of plastic~~Even though non-DGVM related models have implemented root optimization schemes in the past (Schymanski et al., 2008), the knowledge base for a mechanistic bottom-up modelling approach of plastic root optimization is very sparse ~~(Jenik, 2010; Poorter et al., 2012; Warren et al., 2015b);~~(Jenik, 2010; Poorter et al., 2012; Warren et al., 2015b) and knowledge on certain allometric rules (Brum et al., 2019; Eshel and Grünzweig, 2013; Mokany et al., 2006) seems enough to be applied in DGVMs. 3) Most DGVMs so far do not account for a location~~-~~-dependent soil depth, but apply a constant soil depth across the globe (Best et al., 2011; Guimberteau et al., 2017; Lawrence et al., 2011; Ostle et al., 2009; Schaphoff et al., 2018; Smith et al., 2014). Again, this approach may be sufficient when accounting for shallow rooting strategies only, but allowing for deep tree rooting strategies should go in parallel with their potential physical barriers. Recent data products on global soil depth now enable to better constrain rooting depth in DGVMs (Pelletier et al., 2016).

Here we overcome the above mentioned limitations and present a new approach of diversifying tree rooting strategies in the DGVM LPJmL4.0 (Lund-Potsdam-Jena managed Lands; Schaphoff *et al.*, 2018) which increases the ecological liability with the following aspects: 1) Maximum rooting depth is restricted to a recent global product of soil depth, 2) simulated tree rooting strategies were chosen to represent a wide range of maximum rooting depth between 0.5 and 18 m, 3) ~~this spectrum of~~ all tree rooting strategies ~~grows~~of this spectrum grow in competition and ~~tree~~PFT performance determines dominance, 4) dominance is supported by best performing rooting strategies ~~producing more offspring~~increasing their establishment rate, 5) ~~trees~~PFTs have to invest into coarse roots as well, i.e. acknowledging the trade-off between growing deeper roots and allocating available carbon to other compartments (stem and leaf growth), and 6) tree PFT roots are growing deeper over time depending on tree height~~. The objectives of this study are to describe an approach of how to diversify tree rooting strategies in a DGVM and to evaluate its effect on simulated evapotranspiration, productivity, biomass and spatial distribution of evergreen and deciduous tropical forests using different sources of validation data~~.

Given these new model developments we here re-evaluate the hypothesis that varying tree rooting depth is key to explain major patterns of evapotranspiration, productivity and the geographical distribution of tropical evergreen forests in South America, as we acknowledge a diversity of different competing tree rooting strategies as well as resource investment, temporal growth and physical constraints of rooting depth. Therefore, we compare several model versions of LPJmL4.0 differing in the above~~-~~-mentioned model developments and evaluate simulated evapotranspiration, productivity, biomass and spatial distribution of evergreen and deciduous tree PFTs using different sources of validation data.

2 Materials and Methods

~~In the method sections below we describe the implementation of a new tree rooting scheme in LPJmL4.0 (Sect. 2.2) where maximum rooting depth is constrained by a recent map on maximum soil/sediment thickness (Sect. 2.3). We apply the model to several historical climate input data (Sect. 2.7) with details of the simulation protocol described in Sect. 2.9. The Evaluation of the new model version is described in Sect. 2.10.~~

~~All data processing and statistical analysis described in the methods sections were performed with the commercial software MATLAB® (MATLAB and Statistics Toolbox Release 2012b; The MathWorks, Inc., Natick, MA, USA).~~

2.1 The LPJmL4.0 model

LPJmL4.0 is a process-based Dynamic Global Vegetation Model (DGVM) which simulates the surface energy balance, water fluxes, fire disturbance, carbon fluxes and stocks of the global land (Schaphoff et al., 2018). Plant productivity is modelled on the basis of leaf-level photosynthesis responding to climatic and environmental conditions, atmospheric CO_2 concentration, canopy conductance, autotrophic respiration, phenology and management intensity. Fire disturbance is modelled using the simple fire module Glob-FIRM (Thonicke et al., 2001) which relates the length of the fire season to fractional annual area burnt. The model ~~employs~~simulates 11 plant functional types (PFTs), 3 bioenergy functional types (BFTs) and 12 crop functional types (CFTs), to represent average plants of ~~biomes~~natural vegetation, bioenergy plantations and agriculture, respectively. Three PFTs represent the natural vegetation of the tropics and sub-tropics namely the "tropical broadleaved evergreen tree" mainly representing tropical evergreen forest, the "tropical broadleaved deciduous tree" representing tropical dry forest and the woody component of savanna and "tropical herbs" representing the herbaceous layer in grasslands, savanna and forests.

The standard spatial model resolution is a 0.5° x 0.5° longitude-latitude grid. For each grid cell the fractional coverage of bioenergy and agricultural BFTs and CFTs follows a prescribed land-use data set, whereas in the remaining grid-cell area natural PFTs grow in competition.

2.2 A new tree rooting scheme for LPJmL4.0

In this section we describe the new basic scheme for soil layer partitioning, the new tree rooting scheme, the simulation of belowground carbon investment, and how different tree rooting ~~schemes~~strategies (implemented in the new scheme) compete. All changes made to LPJmL4.0 described in ~~the methods below~~this section result in a new sub-version of LPJmL4.0 which we call LPJmL4.0-VR hereafter (where "VR" stands for variable roots).

2.2.1 Scheme for soil layer partitioning

LPJmL4.0 employs a globally universal soil depth of 3 m. For LPJmL4.0-VR we extended the general maximum soil depth to 20 m (but restrict it to local soil depth information at spatial model resolution; Sect. 2.3.2). We applied the same basic scheme for soil layer partitioning from LPJmL4.0 (Schaphoff et al., 2018), in order ~~but extend~~continue this scheme down to ~~20 m~~to keep model differences small (~~Tab. 1~~Table A1). We chose a maximum of 20 m soil depth to considerably increase the maximum soil depth compared to constant 3 m in LPJmL4.0, while keeping the increment of computational ~~intensiveness~~ demand connected to adding more soil layers within an acceptable range. ~~As for LPJmL4.0, a general soil texture information is applied to the whole soil column.~~ Equal to LPJmL4.0 (Schaphoff et al., 2018)~~.~~, we use a grid cell specific soil texture information which is applied to the whole soil column.

2.2.2 Water balance, infiltration and percolation

We here provide a very brief description of LPJmL's water balance and soil hydrology. A detailed description can be found in Schaphoff et al. (2018).

Hydraulic conductivity and water holding capacity (water content at permanent wilting point, at field capacity, and at saturation) for each grid cell are derived from information on soil texture from the Harmonized World Soil Database (HWSD) version 1 (Nachtergaele et al., 2009) and relationships between texture and hydraulic properties from Cosby et al. (1984). Each soil layer's (Sect. 2.2.1) water content can be altered by infiltrating rainfall and percolation. The soil water content of the first soil layer determines the infiltration rate of rain and irrigation water. The excess water that does not

infiltrate generates surface water runoff. Water percolation through the soil layers is calculated by the storage routine technique (Arnold et al., 1990) as used in regional hydrological models such as SWIM (Krysanova et al., 1998). Water percolation thus depends on the hydraulic conductivity of each soil layer and the soil water content between field capacity and saturation at the beginning and the end of the day for all soil layers. Similar to water infiltration into the first soil layer, percolation in each soil layer is limited by the soil moisture of the following lower layer. Excess water over the saturation levels forms lateral runoff in each layer and contributes to subsurface runoff. Surface and subsurface runoff accumulate to river discharge. The routines for water balance, infiltration and percolation were not changed for LPJmL4.0-VR. Thus the routines now apply for soil columns of up to 20 m depth (Sect. 2.2.1).

2.2.3 Diversifying general tree rooting strategies ~~in LPJmL4.0-VR~~

In LPJmL4.0 the tree rooting strategy of a PFT is reflected by a certain prescribed vertical distribution of fine roots throughout the soil column. Each soil layer l is assigned a PFT specific relative amount of fine roots $rootdist_l$:

$$rootdist_l = rootdist(z_l) - rootdist(z_{l-1}) \quad \text{Eq. (1)}$$

where z_l is the soil layer boundary depth in cm of each soil layer l and $rootdist(z_l)$ is the relative amount of fine roots between the forest floor and the boundary of soil layer l. The function $rootdist(z)$ is defined following Jackson *et al.* (1996):

$$roodist(z) = \frac{1-\beta^z}{1-\beta^{z_{bottom}}} \quad \text{Eq. (2)}$$

where β is a constant parameter shaping the vertical distribution of fine roots and therefore determining the tree rooting strategy and z_{bottom} is the maximum soil depth in cm. In LPJmL4.0 each PFT is assigned a different β-value reflecting the average tree rooting strategy on this broad ~~biome~~PFT scale (Schaphoff et al., 2018).

To quantify the maximum rooting depth of PFTs that actually results from this approach (Eq. 1&2) we here calculate the depth at which ~~is reached by 95% of~~ the cumulated fine root biomass from the soil surface downwards is 95% (D_{95_max}) as follows:

$$D_{95\_max} = \frac{log(1-0.95\cdot(1-\beta^{z_{bottom}}))}{log\,(\beta)} \quad \text{Eq. (3)}$$

In LPJmL4.0 the β-values of tropical tree PFTs are set to 0.962 for the ~~evergreen PFT and 0.961 for the deciduous PFT.~~tropical broadleaved evergreen tree and to 0.961 for the tropical broadleaved deciduous tree following Jackson et al. (1996). According to Eq. 3 both PFTs have a D_{95_max} smaller than 1 m. For LPJmL4.0-VR we extended this representation of tree rooting strategies by splitting both tropical tree PFTs into 10 sub-PFTs and assigned each with a different β-value. These values were chosen to cover a range of different D_{95_max} values between 0.5 and 18m (~~Tab.~~Table 1). We chose 18 m as the largest D95_max value in order to avoid that roots of the respective sub-PFT significantly exceed the maximum soil depth of 20 m (see also 2.2.5). Fig. 1 shows the new maximum distribution of fine roots throughout the soil column ~~according to~~for the ~~chosen~~different β-values ~~(Tab. 2~~chosen (Table 1).

2.2.~~3~~4 Belowground carbon investment

Tropical trees can avoid water stress under seasonally dry climate by growing relatively deep roots (Brum et al., 2019; Fan et al., 2017) which goes along with increased below-ground carbon investment. Thus, the need for deep water access creates a trade-off between below-ground and above-ground carbon investment. Therefore, a new ~~tree rooting~~carbon allocation scheme for LPJmL4.0-VR was necessary to account for this trade-off in order to reproduce observed local to regional patterns and distributions of tree rooting strategies instead of prescribing them. ~~Therefore,~~In LPJmL4.0-VR we introduced two new carbon pools ~~in LPJmL4.0-VR~~, namely root sapwood and root heartwood. Like stem sapwood in LPJmL4.0, also root sapwood in LPJmL4.0-VR needs to satisfy the assumptions of the pipe model (Shinozaki et al., 1964; Waring et al., 1982). The pipe model describes, that for a certain amount of leaf area a certain amount of water conducting tissue must be available. In LPJmL4.0 the cross-sectional area of stem sapwood needs to be proportional to the leaf area LA_{ind} as follows:

$$LA_{ind} = k_{la:sa} \cdot SA_{ind} \quad \text{Eq. (4)}$$

where $k_{la:sa}$ is a constant describing the ratio of leaf area and stem sapwood cross-sectional area (SA_{ind}). In LPJmL4.0-VR we also apply the pipe model to root sapwood. Root sapwood cross-sectional area ~~must be proportional~~in the first soil layer is equal to stem sapwood cross-sectional area, ~~but is decreasing with soil depth, depending on~~as all water must be transported through the root sapwood within this soil layer. In the following soil layers downwards, root sapwood cross-sectional area decreases by the relative amount of fine roots in ~~each~~all soil ~~layer~~layers above (Fig. 2). Root sapwood is turned into root heartwood at an equal rate as stem sapwood is turned into stem heartwood, i.e. 5% per year as implemented in LPJmL4.0 (see Schaphoff *et al.*, 2018).

2.2.~~4~~5 Root growth

In LPJmL4.0 (Schaphoff et al., 2018) no vertical root growth is simulated, thus the relative distribution of fine roots over the soil column is constant over space and time. It means that PFTs starting from bare ground in a sapling stage display the same relative distribution of fine roots throughout the soil column as a full-grown forest which contradicts the principles of dynamic root growth over a tree's lifetime. Applied to LPJmL4.0-VR, the belowground biomass of an initialized deep rooting-strategy sub-PFT would exceed its aboveground biomass (AGB) by order of magnitudes when ~~acknowledging~~ considering coarse roots. Consequently, deep rooting strategies would always be disadvantageous, calling for modelling gradual root growth in LPJmL4.0-VR. Unfortunately, little is known about how roots of tropical trees grow over time, given the fact that this research field is strongly time and resource demanding, and at the same time the variety of tree species, rooting strategies and environmental conditions are large (Jenik, 2010). A recent promising study by Brum *et al.* (2019) was able to capture the effective functional rooting depth (EFRD) of different size classes of 12 dominant tree species in a seasonal Amazon forest where tree roots grow considerably deep with maximum values reaching below ~~30m~~30 m. To our knowledge this is the only study capturing the relation between the size of tropical trees and their maximum rooting depth in a high spatial resolution covering sufficient tree-height classes in order to derive a ~~function.~~functional relation between tree height and rooting depth. Following the findings of Brum *et al.* (2019), we here implemented a logistic root growth function, which calculates a general maximum conceivable tree rooting depth D depending on tree height:

$$D = \frac{S}{e^{-kSh}} \cdot \left(\frac{S}{D_0} - 1\right) \quad \text{Eq. (5)}$$

where S is the maximum soil depth in the model (20 m), k is the growth rate (set to 0.02), h is the average tree height of a PFT in m and D_0 is the initial rooting depth of tree PFT saplings (set to 0.1 m; tree saplings in LPJmL4.0-VR are initialized with a height of 0.45 m as in LPJmL4.0). The distribution of fine root biomass of each sub-PFT in the soil column is then adjusted according to D at each time step, by restricting z_{bottom} in Eq. 2. Every time D crosses a specific soil layer boundary (Sect. 2.2.1) z_{bottom} is assigned the value of the next soil layer boundary. Thus, z_{bottom} increases in discrete steps. Consequently, each tree rooting strategy allowed for in this study (Sect. 2.2.~~2~~3) shows a logistic growth of rooting depth which is dependent on ~~tree~~the sub-PFT height and which saturates towards its specific maximum rooting depth (Fig. 3). Therefore, limitations of aboveground ~~tree~~sub-PFT growth due to below-ground carbon investment of different tree rooting strategies (Sect. 2.2.~~3~~4) are equal in the ~~tree~~ sapling phase of all sub-PFTs (starting from bare ground) and start to diverge with increasing ~~tree~~sub-PFT height. In the case D exceeds the grid cell specific local soil depth (as prescribed by the soil thickness input, see Sect. 2.3.2) all the respective fine root biomass exceeding this ~~grid cell specific~~ soil depth is transferred to the last soil layer ~~which matches~~matching this soil depth (see also Fig. 2 right panel and Supplementary Video 1 for a visualization of root growth under http://www.pik-potsdam.de/~borissa/LPJmL4_VR/Supplementary_Video_1.pptx).

The parameter k in Eq. 5 was chosen to preserve the slope of the 75%ile function describing the relation between tree height and ~~effective functional rooting depth (EFRD)~~EFRD as found in Brum *et al.* (2019). We could not implement any of the original functions as suggested in Brum *et al.* (2019) since they deliver unrealistic low values of rooting depth (between 0 and 10cm) for trees <= 10 m, which results in a strong competitive disadvantage against herbaceous PFTs in LPJmL4.0-VR.

We decided for the slope of the 75%ile function ~~since we wanted~~ to ~~apply~~allow for root growth rates close to the maximum which also allows for the largest D_{95_max} values in this study (Sect. 2.2.~~1~~3) to be reached.

Note that Brum *et al.* (2019) originally propose a relation between tree diameter at breast height (*DBH*) and EFRD. For our purposes we related rooting depth to tree height (h), which is calculated from DBH in in LPJmL4.0 according to ~~(Huang et al., 1992)~~Huang et al. (1992):

$$h = k_{allom2} \cdot DBH^{k_{allom3}} \quad \text{Eq. (6)}$$

where k_{allom2} and k_{allom3} are constants set to 40 and 0.67, respectively (Schaphoff et al., 2018).

2.2.~~5~~6 Competition of rooting strategies

In each grid-cell all sub-PFTs of the evergreen and deciduous tree PFTs compete for light and water following LPJmL4.0's approach to simulate plant competition. ~~To allow for environmental filtering of tree rooting strategies which are best adapted to local environmental conditions, we changed the tree establishment scheme of LPJmL4.0-VR.~~ In LPJmL4.0, the number of new PFT saplings per unit area (est_{PFT} in ind m^{-2} a^{-1}) which are established each year is proportional to a maximum establishment rate k_{est} and to the sum of foliage projected cover (FPC; a relative number between 0 and 1) of all tree PFTs present in a grid cell (FPC_{TREE}). It declines in proportion to canopy light attenuation when the sum of woody FPCs exceeds 0.95, thus simulating a decline in establishment success with canopy closure (Prentice et al., 1993):

$$est_{PFT} = k_{est} \cdot (1 - e^{(-5 \cdot (1 - FPC_{TREE}))}) \cdot \frac{1 - FPC_{TREE}}{n_{est_{TREE}}} \quad \text{Eq. (7)}$$

where $n_{est_{TREE}}$ is the number of established tree individuals ~~per m² per year. In LPJmL4.0-VR, establishment rates of sub-PFTs (est_{sub_PFT}) are additionally weighted by~~(ind m^{-2} a^{-1}). It is important to note that LPJmL4.0 does not simulate individual trees. As a common method of DGVM's, tree saplings enter the average individual of a PFT as described in Schaphoff et al. (2018).

To allow for environmental filtering of tree rooting strategies which are best adapted to local environmental conditions, we changed the standard tree establishment scheme in LPJmL4.0-VR. Now, the establishment rates of sub-PFTs (est_{sub_PFT}) are additionally weighted by the local dominance of each sub-PFT as follows:

$$est_{sub\_PFT} = k_{est} \cdot \left(1 - e^{-5 \cdot (1 - FPC_{TREE})}\right) \cdot \frac{1 - FPC_{TREE}}{n_{est_{TREE}}} \cdot \frac{FPC_{sub\_PFT}}{FPC_{TREE}} \cdot n_{est_{TREE}} \quad \text{Eq. (8)}$$

where FPC_{sub_PFT} is the FPC of each sub-PFT. The new term ~~allows productive sub-PFTs~~leads to ~~establish more offspring~~a higher establishment rate for productive sub-PFTs relative to their spatial dominance and vice versa, without changing the overall establishment rate as set by ~~(Prentice et al., 1993)~~Prentice et al. (1993). This function has the effect that non-viable sub-PFTs are outcompeted over time.

2.2.~~5~~7 Background mortality

In LPJmL4.0 background mortality is modelled by a fractional reduction of PFT biomass, which depends on growth efficiency (Schaphoff et al., 2018). This annual rate of mortality is limited by a constant maximum mortality rate of 3% of tree individuals per year which is applied to all tree PFTs. In other words, the fastest total biomass loss of a tree PFT due to low growth efficiency can happen within ~~1/0.03 =~~ about 33 simulation years. In general, this maximum mortality rate can be regarded as a global tuning parameter of biomass accumulation as it caps the maximum biomass loss. Since many mechanisms influencing tree mortality in the real world, e.g. hydraulic failure (Johnson et al., 2018), are not yet implemented in most DGVMs including LPJmL4.0 (Allen et al., 2015), the parameterization of a background tree mortality remains a challenging topic. Under the current model status of LPJmL4.0 maximum mortality rates are a necessary feature, while future model development must overcome the concept of applying a maximum mortality rate by refining and implementing most important mechanisms that influence tree mortality.

~~The new features of LPJmL4.0-VR head in this direction. Here tree PFTs can access water in soil depths which were formally inaccessible. This enhances the general growth efficiencies of tree PFTs and consequently decreases their overall background mortality. Since global biomass pattern simulated with LPJmL4.0 are already in an acceptable range, we increased the maximum background mortality in LPJmL4.0-VR to 7% in order to counter-balance increased survival rates and therefore biomass accumulation. This value keeps simulated mortality rates in real world boundaries, as a recent study comprising data of 167 forest plots finds that actual annual stem mortality rates generally do not exceed 6% across Amazonia (Johnson et al., 2016). We regard increasing the maximum mortality rate as a step into the right direction as its value can eventually be set close to 100% when model development progresses.~~

In LPJmL4.0-VR tree PFTs can access water in soil depths which were formerly inaccessible. This enhances the general growth efficiencies of tree PFTs and consequently decreases their overall background mortality. Since global biomass pattern simulated with LPJmL4.0 were already in acceptable range, the maximum background mortality in LPJmL4.0-VR was calibrated and is now increased to 7% in order to counter-balance increased survival rates and therefore biomass accumulation.

2.3 Model input data

2.3.1 Climate ~~and land-use~~ input data

All versions of LPJmL used in this study (~~see~~ Sect. 2.4) were forced with 4 different climate inputs each ~~based on single or multiple available data products~~ delivering the climate variables air temperature, precipitation, long-wave and shortwave downward radiation at daily or monthly resolution:

1) WATCH Forcing Data (WFD) + WATCH Forcing Data methodology applied to ERAInterim data. A combination of the WATCH data set (Weedon et al., 2011) and the WFDEI data set (Weedon et al., 2014) as used in the ISIMIP project (https://www.isimip.org/gettingstarted/input-data-bias-correction/details/5/). This input data set is called WATCH+WFDEI hereafter.

2) Global Soil Wetness Project Phase 3 (GSWP3) (Kim *et al.*, no date; http://hydro.iis.u-tokyo.ac.jp/GSWP3/index.html).

3) NOAH Global Land Assimilation System version 2.0 (GLDAS, Rodell *et al.*, 2004).

4) Climate forcing as in Schaphoff *et al.* (2018) with monthly precipitation provided by the Global Precipitation Climatology Centre (GPCC Full Data Reanalysis version 7.0; (Becker et al., 2013), daily mean temperature from the Climate Research Unit (CRU TS version 3.23, University of East Anglia Climatic Research Unit, 2015; Harris *et al.*, 2014), shortwave downward radiation and net downward radiation reanalysis data from ERA-Interim (Dee et al., 2011), and number of wet days from (New et al., 2000) used to allocate monthly precipitation to individual days.

This input data set is called CRU hereafter.

2.3.2 Soil and sediment thickness

~~We~~For this study, we regridded a global 1 x 1 km soil and sediment thickness product (Pelletier et al., 2016) to the 0.5° x 0.5° spatial resolution of LPJmL4.0-VR, set the global maximum value to 20 m according to the maximum soil depth chosen for LPJmL4.0-VR (Sect. 2.2.1), and used the resulting map as grid cell specific model input (Fig. ~~4).~~ A4). Regridding was done using the software R (R Core Team, 2019) with the package "raster" (Hijmans and van Etten, 2016). We used the aggregate function to calculate the average value of all Pelletier et al. (2016) data entries falling into the coarser 0.5° grid of LPJmL.

2.4 Model versions and simulation protocol

In order to investigate the impact of simulating variable rooting strategies and root growth, we employ 3 model versions of LPJmL in this study: 1) LPJmL4.0, 2) LPJmL4.0-VR, and 3) LPJmL4.0-VR-base ~~with~~. LPJmL4.0-VR-base has the same

settings as LPJmL4.0-VR ~~but without~~except variable rooting strategies, i.e. using the 2 β-values of LPJmL4.0 for the respective 10 sub-PFTs of the tropical broadleaved evergreen PFT (β = 0.962) and the tropical broadleaved deciduous PFT (β=0.961~~) for all the respective 10 sub-PFTs.~~). We regard ~~the latter model version~~LPJmL4.0-VR-base as ~~a~~the baseline model of this study, because comparisons to LPJmL4.0-VR enable to investigate differences ~~which are~~ caused by the ~~amount~~presence or absence of ~~considered~~variable tree rooting strategies ~~only~~.

~~Each simulation was initialized with 5000 simulation years of spin up from bare ground without land use by randomly recycling the first 30 years of respective climate data (1901-1930 for WATCH+WFDEI, GSWP3, CRU and 1948-1977 for GLDAS) and a pre industrial atmospheric CO_2 level of 278ppm, in order to ensure that carbon pools and local distribution of PFTs and sub-PFTs are in equilibrium with climate. This first spin up phase was followed by another spin up phase of 390 years using the same climate data, but employing historical land use data (reshuffling the first 30 years 1851-1880). Land-use input and routines were carried out according to the standard settings of LPJmL 4.0 as described in (Schaphoff et al., 2018). This second spin up phase was followed by transient simulations (1901-2010 for WATCH+WFDEI, GSWP3, CRU and 1948-2010 for GLDAS) with respective land use change and changing levels of atmospheric CO_2 concentration.~~

~~At the beginning of the spin-up phase~~Each simulation was initialized with 5000 simulation years of spin up from bare ground without land-use by ~~–~~periodically cycling the first 30 years of the respective climate data set (1901-1930 for WATCH+WFDEI, GSWP3, CRU and 1948-1977 for GLDAS) and using a pre-industrial atmospheric CO_2 level of 278 ppm. The first spin-up ensures that carbon pools and local distributions of PFTs and sub-PFTs are in equilibrium with climate (Schaphoff et al., 2018). In a second spin~~–~~up phase cycling the same 30 years of climate data, historical land-use and changing levels of atmospheric CO_2 concentration are introduced. The second spin-up starts in the year 1700 and ends with the first year available in each climate data set. Land-use is updated annually as described in Schaphoff et al. (2018). Before the year 1840 a constant pre-industrial atmospheric CO_2 concentration of 278 ppm is prescribed. After this year atmospheric CO_2 increases annually based on data of Tans and Keeling (2015) as described in Schaphoff et al. (2018). After the second spin up, transient simulations start with the first year available in each climate data set and end in 2010. Land-use and atmospheric CO_2 are consistently updated annually continuing to follow the same data sets as used in the second spin-up.

At the beginning of the first spin-up, all sub-PFTs in LPJmL4.0-VR and LPJmL4.0-VR-base have the same chance to establish, i.e. tree rooting strategies are uniformly distributed. During the spin-up ~~simulations~~simulations local environmental ~~conditions lead to environmental~~ filtering ~~supported by~~and competition ~~and~~in connection with PFT-dominance dependent establishment rates (Sect. ~~2.2.4).~~2.2.6) determine which tree rooting strategies are best adapted and which are outcompeted. Therefore, the ~~following~~ transient simulations already start with distinct distributions of tree rooting strategies.

2.5 Model validation

2.5.1 Validation data

Regional biomass pattern

~~For evaluation of simulated regional pattern of AGB we compare the results of all LPJmL model versions used in this study to two remote sensing based biomass maps (Avitabile et al., 2016a; Saatchi et al., 2011) regridded to the spatial resolution of the LPJmL models.~~

~~*Inventory based biomass*~~

~~Because of the contradicting spatial pattern of currently available AGB maps, we also perform a direct comparison of our modelled AGB patterns to inventory based biomass estimates provided by (Brienen et al., 2015). The general problem of such a comparison is that AGB estimates from DGVMs represent large scale (0.5 x 0.5 degree) averages, while inventory based AGB estimates are representative for forest plots of a typical size of ~1 ha. Because of the smaller spatial scale, plot estimates are affected by spatial variability and random measurement errors (Chave et al., 2004), which causes plot estimates to differ from large scale average AGB. Thus, even a simulated AGB pattern that perfectly matches the real large scale~~

~~pattern would not yield a correlation coefficient of one when compared to small-scale plot observations. To address this problem, we apply the method from Rammig *et al.* (2018), which was specifically developed to compare spatial patterns of simulated large scale ecosystem properties (Y) to ground based observations (X). The method assumes that a small scale "point" measurement consists of two components: the large scale average and a normally distributed random component originating from small scale variability and measurement error. The standard deviation of the random component can be estimated from the data by analyzing differences among neighboring observation point, and then be used to obtain an estimate of the standard deviation of the underlying large scale AGB pattern $\sigma_{x,LS}$ and to calculate a modified correlation coefficient r_{LS} that accounts for differences in the large scale patterns by removing the diminishing effect of the random component in point observations. The subscript LS for $\sigma_{x,LS}$ and r_{LS} indicates that they represent estimates of the true large scale variability and the true correlation coefficient of the large scale patterns. The uncertainty ranges for these two properties as well as for the pattern average $\underline{x}$ (which does not require a correction and therefore no differentiation of 'large scale') are estimated by bootstrapping. For further details on the underlying methodology see (Rammig et al., 2018).~~

~~For the evaluation of the modeled large scale AGB pattern (Y) against inventory based biomass estimates (X) we employ three metrics to detect deviations in important pattern properties: 1. The ratio of means ($\overline{y}/\overline{x}$) as a measure for the agreement of pattern average. 2. The ratio of standard deviations of large scale AGB patterns ($\sigma_y/\sigma_{x,LS}$) as a measure for the agreement of pattern amplitude (the differences between grid cells). 3. The modified 'large scale' Pearson correlation coefficient (r_{LS}) as a measure for the agreement of large scale pattern shape (the location of maxima and minima).~~

For evaluation of simulated regional pattern of AGB we compare the results of the 3 LPJmL model versions used in this study to two remote sensing based biomass maps (Avitabile et al., 2016; Saatchi et al., 2011) which were regridded to the spatial resolution of the LPJmL models. Data of Avitabile et al. (2016) was regridded using the software R (R Core Team, 2019) with the package raster (Hijmans and van Etten, 2016). We used the aggregate function to calculate the average value of all Avitabile et al. (2016) data entries falling into the coarser 0.5° grid of LPJmL. Regridded data of Saatchi et al. (2011) was taken from Carvalhais et al. (2014).

Local scale evapotranspiration and productivity

To evaluate ~~the performance of~~ simulated local ET and net ecosystem exchange (NEE) of the 3 LPJmL versions used in this study, we compare Fluxnet eddy covariance measurements of ET at 7 sites and NEE at ~~3sites~~3 sites across the study region (Bonal *et al.*, 2008; Saleska *et al.*, 2013, ~~table 3~~Table A2) to respective simulated rates of local ET and NEE. We used only 3 sites for NEE comparisons, because only those sites provided continuous data covering more than 2 years. Fluxnet data was downloaded from https://fluxnet.fluxdata.org (under DOI: 10.18140/FLX/1440032 and DOI: 10.18140/FLX/1440165) in October 2017 and from https://daac.ornl.gov/LBA/guides/CD32_Brazil_Flux_Network.html in November 2019.

Continental scale gridded evapotranspiration products and selection of regions

To evaluate the simulated ET over large regions and during a long period (1981-2010), we use three global gridded datasets: Global Land Data Assimilation System Version 2 (Rodell et al., 2004), ERA-Interim/Land (ERAI-L, Balsamo *et al.*, 2015) and Global Land Evaporation Amsterdam Model v3.2 (GLEAM, Miralles *et al.*, 2011; Martens *et al.*, 2017).

GLDAS and ERAI-L are ~~land-~~reanalysis products, meaning that they are land surface models forced with meteorological data that has been corrected with observations to give better estimates of land surface variables. The selection of these two products is based on the study of Sörensson and Ruscica (2018), who found that they have a better performance over South America than other reanalysis and satellite-based ET products. GLDAS uses the land surface model Noah (Ek et al., 2003) forced by Princeton meteorological dataset version 2.2 -(Sheffield et al., 2006). The soil depth of Noah is 2 m and the model uses four soil layers and vegetation data from University of Maryland (http://glcf.umd.edu/data/landcover/). ERAI-L uses the land surface model HTESSEL (Hydrology-Tiled ECMWF Scheme for Surface Exchanges over Land, Balsamo *et al.*, 2009) forced by ERA-Interim atmospheric data with a GPCP based correction of monthly precipitation. The soil depth of ERAI-L is 2.89 m, the model uses four soil layers and vegetation data from ECOCLIMAP (Masson et al., 2003).

GLEAM uses the Priestley-Taylor equation to estimate the potential ET and a set of algorithms with meteorological and vegetation satellite data as input to calculate the actual ET. The version used here, GLEAMv3.2a (Martens *et al.*, 2017, downloaded from https://www.gleam.eu/#downloads) uses precipitation input from MSWEP v1.0 (Beck et al., 2017), vegetation cover from the MODIS product MOD44B, remotely sensed Vegetation Optical Index from CCI-LPRM (Liu et al., 2013) and assimilates soil moisture from both remote sensing (ESA CCI SM v2.3, Liu *et al.*, 2012) and land-reanalysis (GLDAS Noah, Rodell *et al.*, 2004). The original spatio-temporal resolution of GLDAS and GLEAM is 0.25º x 0.25º while for ERAI-L it is 0.75º x 0.75º. Monthly time series were calculated from daily values for the three datasets. Hereafter, we use the short names GLDAS, ERAI-L and GLEAM for the described reference datasets.

For the temporal analysis of ET we used five climatological regions across the study area ~~called~~: Northern South America (NSA), Equatorial Amazon West (EQ W), Equatorial Amazon East (EQ E), Southern Amazon (SAMz), and South American Monsoon System region (SAMS) (see ~~Figure 11f~~Fig. 9f). These regions result from a K-means clustering analysis of the annual cycles of the main drivers of ET: precipitation and surface net radiation (for details see Sörensson and Ruscica, 2018). ~~For the purpose of this study~~Additionally we divided the large EQ region used by Sörensson and Ruscica (2018) in two smaller (EQ W and EQ E) at 60ºW, since this is the approximate division between regimes that have a maximum climatological water deficit (MCWD; Sect. 2.5.3) of around -200 mm per year (EQ W), and of around -500 mm per year (EQ E~~). MCWD is an indicator of seasonal water stress (see section 2.5.3~~)~~.

~~The original spatio-temporal resolution of GLDAS and GLEAM is 0.25º x 0.25º while for ERAI-L it is 0.75º x 0.75º. Monthly time series were calculated from daily values for the three datasets. Hereafter, we use the short names GLDAS, ERAI-L and GLEAM for the described reference datasets.~~

Spatial distribution of vegetation types

To evaluate the simulated regional distribution of simulated biome types ~~in all~~of the 3 LPJmL versions we compare our results to satellite-derived vegetation composition maps from ESA Land cover CCI V2.0.7 (Li et al., 2018) which were reclassified to the PFTs of LPJmL from Forkel *et al.* (2014). In this dataset PFT dominance is indicated by foliage projected cover (FPC) which is also a standard output variable of ~~all~~the 3 LPJmL ~~models enabling~~model versions allowing a direct comparison ~~of~~to model results.

Spatial pattern of rooting depth

We compare regional patterns of mean rooting depth simulated with LPJmL4.0-VR to a maximum depth of root water uptake map (Fan et al., 2017) which was regridded to the 0.5° x 0.5° spatial resolution of LPJmL4.0-VR. This product was inversely modelled by taking the dynamically interacting variables soil water supply and plant water demand into account. ~~Here, supply was based on climate, soil properties and topography and demand on plant transpiration deduced from satellite based~~In Fan et al. (2017) supply was based on climate, soil properties and topography and demand of plant transpiration deduced from remotely sensed reanalysis of atmospheric water fluxes and leaf area index (LAI) data.

2.5.2 Validation metrics

Except for inventory biomass all statistical evaluations of model results were based on 1) Pearson Correlation and 2) normalized mean squared error (NME; Kelley *et al.*, 2013). NME is calculated as:

$$NME = \frac{\sum_{i=1}^{N} |y_i - x_i|}{\sum_{i=1}^{N} |x_i - \bar{x}|} \quad \text{Eq. (9)}$$

where y_i is the simulated and x_i the reference value in the grid cell or time step i. $\bar{x}$ is the mean reference value. NME takes the value 0 at perfect agreement, 1 when the model performs as well as the reference mean and values > 2 indicate complete disagreement.

2.5.3 Maximum cumulative water deficit as indicator of seasonal water stress

~~For this study~~To analyse and explain the geographical pattern of rooting depth, ET and productivity we use the maximum cumulative water deficit (MCWD) as an ~~explanatory variable, since it~~independent indicator of potential seasonal water demand of vegetation. MCWD is a widely used indicator for seasonal water stress ~~for studies~~of tropical and sub-tropical forests in South America (Aragão et al., 2007; Lewis et al., 2011; Malhi et al., 2009). MCWD captures the seasonal difference of ET and precipitation in a cumulative way and therefore ~~reveals~~comprises dry season strength and duration. Here we calculate MCWD on a monthly basis. Therefore, we first calculate the cumulative water deficit CWD_n of each month n as:

$$CWD_n = CWD_{n-1} - PET_n + P_n \quad \text{Eq. (10)}$$

where PET is the potential monthly ET and P the monthly sum of precipitation. CWD is constrained to values <=0 and is set to 0 at the end of each hydrological year, here the last day of September, as in Lewis *et al.* (2011). We use P from climate input used for model forcing (Sect. 2.3.1) and PET as it is simulated by LPJmL4.0 (Schaphoff et al., 2018) which is only dependent on net surface radiation and air temperature, therefore remaining an explanatory variable independent of vegetation dynamics. We chose this PET ~~over~~instead of using the commonly used constant ET of 100 mm/month to calculate CWD (Aragão et al., 2007; Lewis et al., 2011; Malhi et al., 2009), because in this way, the CWD better corresponds to the actual climatological conditions in the different LPJmL model versions used in this study (~~see~~ Sect. 2.4). MCWD is then calculated as:

$$MCWD_y = min\,(CWD_{October,y-1}, \dots, CWD_{September,y}) \quad \text{Eq. (11)}$$

where y indicates the calendrical year.

3 Results

3. 1 Local and regional pattern of tree rooting strategies

~~The results of LPJmL4.0-VR show a high variation in dominance and compositions of tree rooting strategies across the study region. The~~In LPJmL4.0-VR the contribution of each tree rooting strategy to the overall net primary productivity (NPP) appears highly dependent on local environmental conditions. Comparisons at the local scale show that shallow-rooted (deep-rooted) sub-PFTs contribute more to the overall NPP under generally wetter (drier) and less (more) seasonal climate conditions (Fig. ~~5~~4). At the Fluxnet site MAN K34, which exhibits a mean annual precipitation (MAP) of 2609 mm and a mean MCWD of -222 mm under CRU climate input (2001-2010), the sub-PFT with a maximum rooting depth (D_{95_max}) of 0.5 m contributes most to overall NPP and the whole distribution of NPP weighted D_{95_max} classes shows a mean of 1.52 m (Fig. 5a). At the Fluxnet site STM K67, which exhibits a lower MAP of 2144 mm and a stronger dry season reflected in a mean MCWD of -465 mm, the NPP weighted distribution of D_{95_max} shows a peak at 10 m and a corresponding mean of 10.26 m (Fig. ~~5b~~4b). Since both sites have a soil ~~thickness~~depth of 20 m (according to the soil depth input; Sect. 2.3.2, Fig. A1) differences in rooting strategy compositions must emerge from the climatic differences~~.~~ of those sites. It is important to note that D_{95_max} values in Fig. ~~5~~4 (i.e. the bins on the x-axes) do not necessarily reflect the true achieved rooting depth of each sub-PFT, but ~~the~~their maximum value. For reasons of visual clarity for this figure we kept the bins of the x-axes as chosen in ~~Tab.~~Table 1.

Based on ~~this NPP~~the information of how much NPP each sub-PFT contributes in each grid cell, we derived maps of mean rooting depth over the whole study region for the time span 2001-2010 for each climate input used in this study (Fig. ~~6~~5). In contrast to Fig. ~~5~~4 we computed the mean of the actually achieved D_{95} of each sub-PFT (evergreen and deciduous combined) weighted by the respective relative NPP contribution of each sub-PFT to total forest NPP (we call $\overline{D_{95}}$). ~~The~~ Apparently, the regional pattern of $\overline{D_{95}}$ ~~is a result of environmental filtering and sub-PFT competition, reflecting~~reflects the effects of climate

and ~~sediment thickness~~soil depth. A general East to West gradient of $\overline{D_{95}}$ over the Amazon region follows climatic gradients of precipitation and MCWD (Fig. ~~S1-2)~~A2-A3), while soil depth (Fig. ~~4~~A1) constrains $\overline{D_{95}}$ especially in the South-~~eastern~~Eastern Amazon ~~(compare Fig. 4 & 6).~~ In general, areas with higher mean annual rainfall and weaker dry season show lower $\overline{D_{95}}$ and vice versa. This pattern holds true under all climate inputs, with some minor local differences and is in line with an inversely modelled global gridded product of maximum depth of root water uptake (MDRU in Fan et al. 2017). Nevertheless, we find considerable absolute differences between MDRU and $\overline{D_{95}}$ (Fig. A4), which can easily emerge from different model settings and assumptions, e.g. related to differences in spatial model resolution, simulated water percolation and underlying vegetation features.

Focussing on the climatological clusters (~~see~~ Sect. 2.5.1 and Fig. 9f) under CRU climate input, the western Amazon (EQ-W), with a MAP of 2708 mm and mean MCWD of -163 mm, displays an overall mean $\overline{D_{95}}$ of 1.14 m and a maximum of 5.47 m, despite considerably deeper soils present. In this cluster Fan et al. (2017) find a respective mean and maximum MDRU of 1.26 and 17.95 m. In the Northern, Western and Southern Amazon clusters (NSA, EQ E, SAMz) with lower MAP of 2299, 2190 and 2035 mm and considerably lower MCWD of -488, -438 and -497 mm ~~(meaning higher seasonality),~~ respectively, mean $\overline{D_{95}}$ increases to 2.32, 3.20 and 2.68 m, respectively~~.~~ (mean MDRU of 1.85, 2.84 and 3.28 m). Here, maximum $\overline{D_{95}}$ values respectively reach 11.97, 11.27 and 9.04 m~~.~~ (maximum MDRU of 14.28, 13.47 m and 16.57 m). In the monsoon dominated region (SAMS) displaying the lowest MAP of 1449 mm and MCWD of -649 mm, mean $\overline{D_{95}}$ decreases to 1.37 m~~.~~ (mean MDRU 2.61 m). The maximum $\overline{D_{95}}$ of this region reaches 11.17 m located at the border to SAMz~~.~~ (maximum MDRU 49.37 m).

~~Comparing our results to an inversely modelled global gridded product of maximum depth of root water uptake (MDRU; Fan et al. 2017) we find considerable absolute differences to simulated $\overline{D_{95}}$ while overall patterns coincide (Fig. 7). As $\overline{D_{95}}$ (Fig. 6) also the original product by Fan et al. (2017) regridded to LPJmL4.0 VR's spatial resolution (Fig. 7a) shows a northwest to southeast gradient of MDRU across the Amazon region. Lowest mean MDRU is found in cluster EQ W with 1.38 m, followed by NSA with 2.98 m, SAMz with 5 m, SAMS with 5.47 m and EQ E with 5.88 m. All cluster have a maximum MDRU > 20 m with the highest value found in SAMS with 64.4 m. Fig. 7c shows a difference map between MDRU and simulated $\overline{D_{95}}$ using CRU climate input. Largest differences are found over a wide area (most pronounced in EQ E, SAMz and SAMS) especially where MDRU exceeds $\overline{D_{95}}$. It appeared that for many grid cells in this area MDRU even exceeds the soil depth input used in this study (2.3.2) substantially. To overcome this technical bias we set MDRU to our soil depth input values in cases where MDRU exceeded them (Fig. 7b) to make MDRU and $\overline{D_{95}}$ more comparable. The differences between this adjusted MDRU and $\overline{D_{95}}$ are more likely caused by model architecture than prescribed abiotic limits, enabling for a more meaningful comparison. After this adjustment mean and maximum values of MDRU in the clusters converge to results of LPJmL4.0 VR by decreasing to 1.85 and 14.28 m for NSA, 1.26 and 17.95 m for EQ W, 2.84 and 13.47 m for EQ E, 3.28 and 16.57 m for SAMz, and 2.61 and 49.37 m for SAMS. Consequently, the geographical pattern of $\overline{D_{95}}$ and adjusted MDRU shows a better agreement (Fig. 7d). Largest differences remain in north western NSA, eastern EQ W, along the Amazon River in EQ E and in eastern SAMz where $\overline{D_{95}}$ exceeds MDRU. On the other hand MDRU substantially exceeds $\overline{D_{95}}$ in south western SAMz and south western SAMS. These differences might easily emerge from different model settings and assumptions, e.g. related to differences in spatial model resolution, simulated water percolation and underlying vegetation features.~~

The regional ~~validation~~simulation of $\overline{D_{95}}$ now allows us to generalize which tree rooting strategies occupy which climate space. Using MCWD and MAP to define a climate space we find a clear ~~separation~~adjustment of $\overline{D_{95}}$ (Fig. ~~8~~6). A core region with deep-rooted forests (mean ~~D_{95}~~ $\overline{D_{95}}$ > 4 m) is found where MCWD ranges between -1300 and -400 and where MAP is at least 1500 mm (see also maps of MCWD and MAP in Fig. ~~S1-2) if soil depth allows for it.~~A2-3). This core region is surrounded by a small band of medium rooting depth forests (mean $\overline{D_{95}}$ ~ 2-4 m) forming a crescent shape. Rather

shallow-rooted forests (mean $\overline{D_{95}}$< 2 m) are found in increasingly drier climates where MAP is less than 1000 mm and in more ~~increasingly~~ seasonal climates where MCWD is below -500 mm~~, i.e. in increasing seasonally dry climates with MAP at the edge to support closed tropical evergreen forest~~. Shallow-rooted forests are also simulated in very wet conditions where MCWD is greater than -300 mm and MAP is 1200 mm or higher.

3.2 Evapotranspiration rates and productivity

3.2.1 Local evapotranspiration

Differences of intra-annual ET rates between ~~LPJmL4.0, LPJmL4.0 VR and LPJmL4.0 VR base~~ the 3 LPJmL model versions are most pronounced at Fluxnet sites ~~showing a~~with high seasonality of rainfall (Fig. ~~9b~~7b, e, g and Fig. ~~10b~~8b, e, g). Here, ~~the results of LPJmL4.0 VR show how~~ variable tree rooting strategies (LPJmL4.0-VR) lead to a major improvement ~~of matching~~ in reproducing measured Fluxnet NEE and ET, also expressed in reduced NME and increased r^2-values (Table ~~4 and 5). This improvement arises from an important new model behaviour:~~A3-A4). Whereas, constant tree rooting strategies (LPJmL4.0-VR-base and LPJmL4.0) simulate decreasing ET and increasing NEE during dry seasons at these sites, which is anticorrelated to Fluxnet measurements, variable tree rooting strategies (LPJmL4.0-VR ~~shows~~) follow the ~~opposite and follows the~~intra-annual Fluxnet signals. ~~This means LPJmL4.0 VR's variable rooting strategies buffer precipitation deficits by usage of deep water. Together with a generally lower mean cloud cover during the dry season, this leads to an increase of productivity and ET as suggested by numerous studies (Nemani et al., 2003; da Rocha et al., 2004).~~ Most pronounced improvements are found at STM K67 and STM K83, where the NME of ET and NEE drop below or close to 1, and where r²-values considerably increase compared to the other 2 model versions (Table ~~4-5~~A3-A4). For STM K67, the r² of NEE is higher under LPJmL4.0 and LPJmL4.0-VR-base, but this refers to a significant negative ~~anti-~~correlation. At STM K77 (Fig. ~~9f)~~ 7f) local circumstances show the influence of variable rooting strategies ~~is reversely demonstrated.~~on ET in a different way. This former rainforest site was converted to pasture before Eddy covariance measurements began. This local land-use at STM K77 is not representative for the respective 0.5° grid cell, and thus all 3 LPJmL model versions simulate mainly natural ~~forest. In this case~~vegetation instead of pasture. Therefore, the shallow rooting systems of LPJmL4.0 and LPJmL4.0-VR-base show a better match to ET measurements~~. Nevertheless,~~ at STM K77. The site STM K83~~,~~ (Fig. 7g) is a selectively logged primary forest site which shares the same model grid cell as STM K77 due to their geographical proximity~~, LPJmL4.0 VR is the~~. Again, here only ~~model reproducing~~ simulations with variable tree rooting strategies (LPJmL4.0-VR) reproduce increased ET and decreased NEE during the dry season. At sites with weaker to no dry season (Fig. ~~9c~~7c, d, h) differences between model versions become less pronounced, as water availability is more stable throughout the year leading to less ~~variability in~~variable ET. ~~Generally, all models show a better match with ET than with NEE, most likely explainable by the fact that DGVMs a) miss or underestimate important mechanisms driving seasonal productivity and respiration and b) have a coarse spatial resolution and therefore miss site specific environmental factors. The latter might also explain why LPJmL4.0 VR overestimates ET at GF GUY in the dry season. Here the soil depth input for the corresponding grid cell most likely exceeds the soil depth at this site, thus the model overestimates rooting depth and resulting ET.~~

3.2.2 Continental Evapotranspiration

Results of regional ET are in line with results of site-specific ET. The climatological clusters within the Amazon region which undergo the strongest dry season (EQ E and SAMz) show the largest differences between variable (LPJmL4.0-VR) and ~~the other 2 models~~constant tree rooting strategies (LPJmL4.0-VR-base and ~~also here~~LPJmL4.0). In those clusters LPJmL4.0-VR shows ~~a higher~~highest agreement with validation data (Fig. ~~11c~~9c, d and Table ~~6). Improvement~~A5). Agreement is largest for EQ E where NME and r² show values of 0.62 and 0.91, respectively, whereas constant rooting systems in the other ~~2~~two ~~models show~~models lead to values of NME >= 1.92 and r² <= 0.21~~. As expected in~~ (Table A5). In

NSA and EQ W model differences ~~become~~are less pronounced as annual precipitation deficits are lower and deep rooting systems play a lesser role~~, but still there is noticeable improvement e.g.~~. Still, variable rooting systems lead to noticeably higher agreement in NSA between January and April~~,~~ (Fig. 9a), where monthly precipitation is lower ~~than during~~compared to the rest of the year. In the monsoon dominated cluster SAMS outside the Amazon region (~~SAMS)~~Fig. 9e), model differences are least pronounced, since shallow rooting forests ~~in LPJmL4.0-VR~~ dominate this area in LPJmL4.0-VR (Fig. 5) which are very similar to the forests with constant tree rooting ~~systems~~strategies in the other 2 model versions.

~~3.3 Biome distributions~~

3.3 Distribution of plant functional types

The simulated relative dominance of tropical tree PFTs across the study area differs substantially between model versions (Fig. ~~12). More~~10). In simulations with LPJmL4.0, more than half of the grid cells ~~of LPJmL4.0~~ show the evergreen and deciduous PFTs equally dominant (Fig. ~~11g~~10g-h). Only in areas outside tropical moist climate regions the model ~~shows~~tends towards a ~~clear~~ dominance of the deciduous PFT, whereas e.g. in the Amazon region, the evergreen and deciduous PFTs co-exist in almost equal abundance. These patterns strongly differ ~~to~~from satellite-derived ~~vegetation composition maps~~geographical PFT distributions (Fig. ~~12a~~10a-b) and therefore yield in respective comparisons the highest NME values among all models (Table ~~7~~A6). In contrast LPJmL4.0-VR and LPJmL4.0-VR-base show clear dominance patterns of both tropical tree PFTs across the study area (Fig. ~~12c-f). This can be attributed to the dominance dependent PFT establishment introduced in this study (Sect. 2.2.5) and applied to LPJmL4.0-VR and LPJmL4.0-VR-base, which makes it possible that one PFT (or sub-PFT) can fully outcompete others.~~10c-f). Nevertheless, differences between LPJmL4.0-VR and LPJmL4.0-VR-base are quite substantial. In LPJmL4.0-VR-base the tropical evergreen PFT dominates the North-Western Amazon region only, negligibly extending further than the borders of climatological clusters NSA and EQ W combined. Beyond these borders the tropical deciduous PFT ~~is dominating.~~dominates (Fig. 10e-f). In contrast, in LPJmL4.0-VR (Fig. ~~12e~~10e-f) the evergreen tree PFT ~~dominance extends closer to its observed borders~~dominates the entire Amazon region including EQ E and SAMz, and the deciduous PFT is pushed towards drier and more seasonal climate (including parts of SAMS). Therefore, LPJmL4.0-VR yields lowest NME values in comparison to satellite-derived ~~vegetation composition maps~~PFT distributions (Table ~~7~~A6).

~~3.4 Regional pattern of simulated above- and belowground~~Aboveground biomass

~~3.4.1 Regional AGB pattern~~

~~The simulated mean AGB pattern (2001-2010) of LPJmL4.0-VR (Fig. 13c) shows how deep water access produces a contiguous high biomass over the Amazon region. Especially towards the borders of the South Eastern Amazon region in the climatological clusters EQ E and SAMz AGB values appear rather homogenous in contrast to the other 2 model versions (Fig. 13d-e). In connection with the significantly improved underlying vegetation composition (Fig. 12) it is clear that LPJmL4.0 VR is the only model version capable of simulating high AGB evergreen rainforests across the climatic gradient of the Amazon region (Fig. S1-2). This pattern is suggested by one satellite derived AGB product chosen for evaluation of our model results (Saatchi *et al.*, 2011; Fig 12b) which yields a corresponding NME close to 0 (Table 8), even though this is true for all model versions. Surprisingly, for the other AGB validation product (Avitabile *et al.*, 2016b; Fig. 12a) LPJmL4.0-VR base yields a smaller NME than LPJmL4.0 VR. Taking into account the significantly less accurate underlying vegetation composition of LPJmL4.0 VR base (Fig. 12) we regard the comparison as obsolete in this context. The same holds true for LPJmL4.0. A known problem with AGB maps for South America is their poor overall agreement especially in the Amazon region (Mitchard et al., 2014), making it hard to interpret such geographical evaluations. The divergence~~

between the 2 AGB evaluation products chosen for this study clearly displays this problem (Fig. 13a-b). Therefore, we also conducted a site specific AGB comparison with results in the following section (Sect. 3.4.2).

3.4.2 AGB at specific sites

For site specific comparisons of simulated and observed AGB we calculated 3 indicators, 1) the ratio of means ($\overline{y}/\overline{x}$) as a measure for the agreement of pattern average, 2) the ratio of standard deviations of large scale AGB patterns ($\sigma_y/\sigma_{x,LS}$) as a measure for the agreement of pattern amplitude (the differences between grid cells), and 3) the modified 'large scale' Pearson correlation coefficient (r_{LS}) as a measure for the agreement of large scale pattern shape (the location of maxima and minima).

Fig. 14 shows a site specific AGB comparison for LPJmL4.0, LPJmL4.0 VR and LPJmL4.0 VR base for the four climate input data sets used in this study against inventory data from Brienen *et al.* (2015). We find that for all climate datasets, LPJmL4.0 tends to overestimate and LPJmL4.0 VR base tends to underestimate average AGB across forest plots in the Amazon region. Except for GLDAS, average AGB from LPJmL4.0 VR lies between these two cases, showing the closest match with average AGB derived from forest plots. However, uncertainties in average AGB from forest plots is quite large (as indicated in spread of violine) so that for all but two cases (LPJmL4.0 VR base with GSWP3 and WATCH+WFDEI) $\overline{y}/\overline{x} = 1$ falls within the 95 % confidence interval of $\overline{y}/\overline{x}$.

With regard to the pattern's amplitude (σ), we find that for all climate datasets all model versions tend to overestimate AGB differences across the Amazon, but only for LPJmL4.0 with GSWP3 and WATCH+WFDEI unity is outside the 95 % confidence interval of $\sigma_y/\sigma_{x,LS}$. In other words the spatial difference between grid cell biomass is generally larger than observations imply. Nevertheless, pattern amplitude decreases with increasing model complexity (from LPJmL4.0 over LPJmL4.0 VR base to LPJmL4.0 VR) so that for LPJmL4.0 VR unity falls within the interquartile range of $\sigma_y/\sigma_{x,LS}$ for all climate datasets. Note, however, that for GLDAS median $\sigma_y/\sigma_{x,LS}$ for LPJmL4.0 VR is slightly larger than for LPJmL4.0 VR base but the 25 % percentile is lower for LPJmL4.0 VR due to the wider uncertainty distribution.

Evaluation of the shape of the large scale average AGB pattern shows that median r_{LS} increases with increasing model complexity. In other words LPJmL4.0 VR matches large scale maxima and minima of biomass across the Amazon forests best. Highest median r_{LS} are found for LPJmL4.0 VR with 0.43 for CRU, GSWP3, and WATCH+WFDEI and 0.51 for GLDAS (upper bounds of the 95 % interval are 0.61 for CRU, 0.68 for GLDAS, and 0.48 for GSWP3 and WATCH+WFDEI).

In summary, we conclude that LPJmL4.0 VR reproduces the 'observed' large scale AGB pattern in the Amazon in all three relevant aspects (pattern mean, amplitude and shape) better than either of the two other model versions. Still LPJmL4.0 VR cannot completely reproduce all features of the large scale AGB pattern in the Amazon, which points to bias in model input connected to climate and soil depth as well as insufficient representation of other important processes for modelling carbon dynamics in tropical forests such as tree mortality (Pillet et al., 2018), gap dynamics (Espírito Santo et al., 2014), and nutrient limitation (Quesada et al., 2012). However, it is important to acknowledge that AGB estimates derived from inventory plots may be subject to large errors and spatial biases themselves (Saatchi et al., 2015).

3.5 Belowground biomass

Simulations with LPJml4.0 VR enable an unprecedented analysis of root carbon pools due to the implementation of belowground carbon investment into tree coarse root structures (Sect. 2.2.3). Fig. 15 shows the mean sum (2001-2010) of coarse and fine root carbon pools of tropical evergreen and deciduous tree PFTs under CRU climate over the study region. As expected the pattern follows simulated mean rooting depth (Fig. 6) as coarse root carbon investment increases accordingly. In the Amazon region drier and more seasonal climate selects for sub PFTs with deeper tree rooting strategies

~~which comes with higher investments into below-ground root structures, implying lower growth rates of these forests compared to wetter and less seasonal regions.~~

4 Discussion

~~This study demonstrates a generalizable approach to improve the representation of tree root system diversity in a DGVM by employing gradual root growth and a trade-off between below- and aboveground carbon investment. A major advance of the new sub-model version LPJmL4.0-VR is that simulations start with a uniform input distribution of tree rooting strategies for each PFT (tropical evergreen and deciduous) in each location, thus ensuring that all tree rooting strategies have the same chance to establish. This uniform distribution then shapes into a local distribution of abundance driven by local environmental conditions and competition (Fig. 5). Therefore, these distributions are not a pre-selected input, but a model output, enabling to investigate patterns like mean rooting depth over the study region (Fig. 6, 7). Since the simulated vegetation can now adjust its root systems to environmental conditions, the quality of simulated biome distributions (Fig. 12) and subsequently the quality of simulated ET and NEE fluxes (Fig. 9-11) and state variables like AGB (Fig. 13-14) is considerably increased.~~

4.1 Climate and soil depth determine dominant tree rooting strategies

The geographical patterns of simulated $\overline{D_{95}}$ are very similar under 4 different climate input data sets (Fig. 5). This gives confidence to the general robustness of our results and modelling approach as differences in climate data do not lead to substantially different model behaviour. This is further supported by similar regional rates of ET simulated under the different climate data inputs (Fig. 9).

Simulated $\overline{D_{95}}$ (Fig. ~~6~~5) clearly follows climate gradients and soil depth ~~of~~found in the study region (Fig. 4~~,~~ A1-A3). Here, MAP and MCWD can serve as explanatory variables of simulated $\overline{D_{95}}$ (Fig. ~~S1). Our~~6). These findings are in line with the general ecological expectation and former studies that seasonal water depletion of upper soil layers, as a combination of annual precipitation ~~sums~~ and dry season length and strength, is positively correlated with the rooting depth of tropical evergreen trees (Baker et al., 2009; Ichii et al., 2007; Kleidon and Heimann, 1998, 1999). We also find lower thresholds for MAP and MCWD ~~were~~where $\overline{D_{95}}$ strongly decreases again (Fig. 6) which can be explained by different mechanisms leading to a regime shift from the evergreen to the deciduous ~~growing strategy~~tree PFT as discussed below (see 4.2).

~~In this study, we focus on the NPP-weighted mean rooting depth ($\overline{D_{95}}$) to detect the tree rooting strategies which are most important for water and carbon fluxes (ET, NEE) as well as biomass. The comparisons of mapped mean MDRU of Fan *et al.* (2017) to $\overline{D_{95}}$ (Fig. 9) should be treated with caution as the latter does not necessarily reflect the productivity nor the dominance of certain tree rooting strategies. Fan *et al.* (2017) back-calculate the necessary water uptake depth to meet observed plant productivity derived from satellites while our results are based on DGVM simulations which yield communities of different tree rooting systems. A number of additional general differences of both approaches and underlying assumptions could have easily led to the observed mismatches: 1) Fan *et al.* (2017) use a different soil depth input, i.e. assuming a different physical boundary of maximum rooting depth. Even though we adjusted MDRU of Fan *et al.* (2017) to the soil depth input used in this study (Fig. 8b), this adjustment was only for cases where MDRU exceeds our soil depth input. Therefore, cases where adjusted MDRU exceeds simulated $\overline{D_{95}}$ in Fig. 8d, e.g. in western SAMz, could be caused by a higher soil depth input assumed in Fan *et al.* (2017) for the respective grid cells. 2) LPJmL4.0-VR simulates the growth and competition of (sub-)PFTs on the basis of leaf-level photosynthesis and allocation of accumulated carbon. Their traits, such as the rooting strategy, determine performance and subsequently competitiveness. Therefore, competition could lead to a different $\overline{D_{95}}$ as would be expected when considering water supply and demand of each (sub-)PFT alone. 3) Satellite-derived productivity of tropical vegetation can be biased, e.g. due to strong cloud cover all year round, potentially leading to biased~~

~~plant water demand and deduced MDRU. 4) Different water percolation schemes and soil textures in both models lead to different seasonal plant water supply determining MDRU and $\overline{D_{95}}$. 5) LPJmL4.0-VR does not employ a ground water model or static ground water table. By considering ground water aquifers the simulated dominance of tree rooting strategies and consequently $\overline{D_{95}}$ could locally shift towards lower values, e.g. in the EQ-E and SAMz cluster, if ground water depth would be lower than the simulated $\overline{D_{95}}$. Applying a ground water model in LPJmL4.0-VR is in the focus of future studies. 6) The tropical deciduous PFT of LPJmL4.0-VR avoids water stress during the dry season by shedding its leaves. Therefore the need for deeper roots to withstand a dry season is relatively low. Generally, areas where the deciduous PFT dominates, e.g. the most southwestern part of the study region (Fig. 6), display a low $\overline{D_{95}}$ whereas this area shows amongst the highest values of MDRU in Fan *et al.* (2017). Since deciduous tree types dominate this area also in reality (Fig. 12b), MDRU values might be overestimated. 7) LPJmL4.0-VR does account for tropical tree PFTs only. Bush and shrub PFT types which might be evergreen and gain access to deep water while stem size remains relatively small (Oliveira et al., 2005) are not accounted for. Implementing more general PFTs into LPJmL4.0-VR is in the focus of future studies.~~

~~For this study~~To evaluate our model results against empirical data, we checked the data availability on maximum rooting depth across South America in the TRY database (Kattge *et al.*, 2020; data downloaded September 2019). As it is also shown in Fan *et al.* (2017; Fig. 2) we found the number of sites within the TRY data base where maximum rooting depth has been measured in South America to be very low. Moreover, the number of data entries per site appeared very small, where 33 TRY sites falling within our study area showed a mean of ~9 and a median of 6 data entries, while 15 sites showed <=5 data entries. Therefore, we decided to not include site specific comparisons of rooting depth as it is not clear how representative these measurements are for the local forest communities. More research is necessary to increase the number of observation sites and improve the empirical basis of field-based rooting depth to allow for site-specific model evaluation. Nevertheless, as shown in Fan *et al.* (2017; Fig. ~~2) measured site-specific maximum rooting depth across the Amazon region seems to follow the expected climatic gradient and gives confidence to our results. More measurements gathered in openly available databases like TRY will help to evaluate future simulation results more sophistically.~~2) measured site-specific maximum rooting depth across the Amazon region expectedly follows the known climatic gradient (Fig. A2-A3). The same holds true for the inversely modelled MDRU of Fan *et al.* (2017; we show in Fig. A4), which gives confidence to our results.

4.2 Rooting depth influences the distribution, dominance and biomass of tropical ~~biomes and biomass~~plant functional types

~~Seasonal water deficit and annual precipitation are the main determinants of which tree rooting strategies perform best, are able co-exist and outcompete others in LPJmL4.0-VR (Fig. 8). Avoiding seasonal drought stress due to deep roots broadens~~In all 3 model versions used in this study the same land-use is applied (Sect. 2.4), which shapes the geographical extent ~~of simulated tropical evergreen forest. This~~ and maximum dominance of natural vegetation ~~type appears to be competitive over a substantially wider climatic range than anticipated when employing~~in our results. This is why FPC maps of all model versions show the ~~tree rooting strategies~~shape of ~~LPJmL4.0. With LPJmL4.0-VR,~~the Amazon region as a distinct pattern (Fig 10), even though it is less visible for LPJmL4.0-VR-base and one has to consider both tropical tree PFTs at the same time (Fig. 10e-f). Within the Amazon region, LPJmL4.0 simulates a similar dominance of the evergreen and deciduous PFT (Fig. 10g-h), which contradicts evaluation data (Fig. 10a-b) and indicates a similar performance of the 2 PFTs or missing mechanisms rewarding a better performance over time. We here find that introducing a performance dependent tree establishment rate (Sect. 2.2.6) clearly resolves this issue. This feature produces clear dominance pattern of either PFT in LPJmL4.0-VR and LPJmL4.0-VR-base. Apparently, by rewarding better performance, variable tree rooting strategies (LPJmL4.0-VR) become necessary to reproduce the dominance of the evergreen PFT throughout the Amazon region (Fig. 10e-f). To remain superior in drier and more seasonal environments ~~now appear suited for the evergreen PFT (Fig. 10).~~ in the South to South-Eastern Amazon region the evergreen PFT needs to access deep water by adjusting its

rooting depth (Fig. 5, 6). Clearly, this adjustment of rooting depth is only possible within a certain climatic ~~frame~~envelope. Below certain thresholds of ~~annual precipitation~~MAP (around 1000 mm) and ~~of~~ MCWD (around -500 mm) mean $\overline{D_{95}}$ decreases again~~, indicating~~ (Fig. 6), which ~~goes in parallel~~coincides with a transition from the evergreen to the deciduous ~~growing strategy or more open grasslands (Fig. 8). Whether this transition for each of those~~PFT. Those thresholds ~~is mainly caused by (a) environmental filtering of deep tree rooting strategies, (b) their competitive exclusion by shallow rooted deciduous tree types together with grass PFTs, (c) fire feedbacks or most probably, a combination of all is yet to be determined and in the focus of further studies.~~

~~The climatic thresholds of vegetation types we find are comparable~~are similar to thresholds between evergreen forests and ~~savannah~~savanna found by e.g. Malhi *et al.* (2009) at an annual precipitation of 1500 mm and at an MCWD of -300 mm. The substantially lower MCWD value found in this study can be explained by the differences in calculating CWD. While Malhi *et al.* (2009) assume a constant rate of ET per month of 100 mm, we use the monthly variable PET (Sect. 2.5.3). Since PET often is significantly higher than 100 mm our monthly CWD and therefore MCWD values are respectively lower.

Similarly to Malhi *et al.* (2009), Staver, Archibald and Levin (2011) find that the climatic thresholds for evergreen ~~tree cover appears to~~forest are not very distinct and savanna can simultaneously be ~~bi-modal within~~found in a climatic range ~~of MAP of 1000-2500 mm and~~ around the mean threshold. The authors ascribe this forest-savanna bi-stability to climate-fire-vegetation feedbacks. Many recent studies investigating potential forest-savanna bi-stability and tipping points of forests in and around the Amazon region rely solely on such climatic ranges of tropical biomes (Hirota *et al.*, 2011; Wuyts, Champneys and House, 2017; Zemp *et al.*, 2017; Staal *et al.*, 2018; Ciemer *et al.*, 2019). The results of LPJmL4.0-VR show that knowledge on local tree root adaptations is another important explanatory variable of vegetation cover reducing the uncertainty and width of anticipated climatic ranges where ~~evergreen tree cover can be bi-modal. This will help future studies to quantify climate-fire-vegetation feedbacks, forest resilience and potential individual tipping points of forests in the Amazon region in a new way.~~vegetation cover could be bi-stable. These findings are supported by a recent study that finds rooting depth more crucial than fire dynamics for explaining PFT dominance in South America (Langan et al., 2017).

~~Especially the current and potential extent of evergreen forests into drier and more seasonal environments can be better explained when considering local adaptations of tree rooting strategies. In these environments an evergreen growing strategy requires deeper root systems to access deep water. Deeper roots require higher BGB investments (Fig. 12) which on the one hand side has a~~Whether the transition between the evergreen and deciduous tree PFT for the thresholds of MAP and MCWD we find with LPJmL4.0-VR is mainly caused by (a) environmental filtering (including vegetation-fire feedbacks) of deep tree rooting strategies, (b) their competitive exclusion by shallow rooted deciduous sub-PFTs together with the tropical herbaceous PFT (Fig. A6), or most probably a combination of both is yet to be determined. Given that we used the most simplistic fire module of LPJmL (GlobFirm; Thonicke et al., 2001) and current land-use input to allow model evaluation against remotely sensed data in this study, investigating the natural mechanisms of tropical PFT shifts should be in the focus of further studies.

Regardless of the mechanisms that eventually lead to a PFT shift, we can state that neither costs for deep root investment nor a heterogeneous pattern of soil depth across the study region disproves that locally adapted tree rooting depth is key to explain the current geographical distribution of tropical evergreen forests in South-America. Given the large differences between LPJmL4.0-VR and LPJmL4.0-VR-base (Fig. 10) it is clear that in roughly half of the Amazon region the carbon balance of the evergreen PFT is superior to the deciduous PFT only when investing substantial amounts of carbon into deeper roots, i.e. belowground biomass (BGB; Fig. A8). On the one hand this investment has a direct negative effect on productivity, because during growth the allocation of assimilated carbon shifts towards respiring ~~BGB~~belowground biomass (BGB), while investments into productive AGB (Fig. A7) need to be reduced. On the other hand drier and more seasonal environments show less cloud cover during the dry season (Nemani et al., 2003), enhancing photosynthesis in this time of the year which increases productivity as long as water access is assured (Costa et al., 2010; Wu et al., 2016). The trade-off

between AGB and BGB investment most probably leads to a more homogenous AGB pattern across the Amazon region with similar values over a wide climatic range (compare EQ E and SAMz in Fig. ~~13c-e). This effect is also visible in lower amplitudes and higher correlation in the large scale AGB pattern from different evaluation sites (Fig. 14).~~A7c-e).

~~In fact comparisons of biomass pattern between all model versions of this study and different biomass products are difficult, since only LPJmL4.0-VR shows a reasonable geographical distribution of underlying biome types across the study area (Fig. 12, Table 7). Therefore, differences in biomass are not solely the consequence of different productivities directly related to diversity in tree rooting strategies, but also the consequence of simulated biome type which can be regarded as an indirect effect of diversity in tree rooting strategies. Concentrating on LPJmL4.0-VR only, the model matches substantially better with the gridded biomass product of Saatchi et al. In LPJmL4.0-VR the evergreen growing strategy dominates the entire Amazon region, which is more productive and accumulates more biomass than the deciduous growing strategy. The latter dominates EQ E and SAMz in LPJmL4.0-VR-base and is equally abundant throughout the Amazon region in LPJmL4.0.~~

~~Concentrating on LPJmL4.0-VR only, the model matches substantially better with the gridded biomass product of Saatchi et al. (2011b), since this product shows generally higher biomass values across the Amazon region which are more similar to LPJmL4.0-VR (Table 8). Therefore, the differences in NME are mainly caused by mean biomass values of rainforests across the whole study area rather than pattern divergence. Thus, we argue lowering overall biomass values in LPJmL4.0-VR would improve its match with (Avitabile et al., 2016b) which is a matter of adjusting overall maximum tree mortality rates (see Sect. 2.2.5). Differences to site specific measurements (Fig. 14) are rather caused by additional factors, such as a) the coarse model resolution leading to a different climate and soil information input than found at specific sites and b) insufficient representation of important processes forcing carbon dynamics in tropical forests such as tree mortality (Pillet et al., 2018), gap dynamics (Espírito-Santo et al., 2014), and nutrient limitation (Quesada et al., 2012).~~

4.3 Diverse tree rooting strategies improve simulated evapotranspiration and productivity

~~In-LPJmL4.0-VR~~LPJmL4.0-VR simulates rates of local ET and NEE which reasonably match respective measurements at different Fluxnet sites throughout the Amazon region (Fig. 7-8), even though we run the model with regionally gridded instead of locally measured climate data. While potentially lacking information on local short-term weather events, gridded climate input still seems to be sufficient to capture broad seasonal signals for our comparisons on a monthly basis. This increases the confidence in our results also on a regional scale.

Across large parts of the Amazon region variable tree rooting strategies decrease the intra-annual variability of ET and maintain high rates of NEE and ET during the dry season in accordance with the intra-annual trends suggested by evaluation data (Fig. 7-9~~-11~~). More than that simulated rates of ET and productivity can peak during the dry season e.g. in EQ E which ~~is~~has been explained by increased solar radiation ~~while trees having~~during this time of the year (Nemani et al., 2003; da Rocha et al., 2004). Especially, in EQ E and SAMz at least parts of the forest area must have access to ~~deep~~sufficient water in the model and in reality (Costa et al., 2010; Wu et al., 2016). ~~While recent parameter optimization against FAPAR data (Forkel et al., 2015) tried to improve the simulated productivity by adjusting phenology pattern in LPJmL4.0, the seasonal offset in simulated ET for Fluxnet sites in the Amazon region remained a challenge (Schaphoff et al., 2018). In this study we can~~Given that LPJmL4.0-VR and LPJmL4.0-VR-base are essentially identical models with the same soil depth input and subsequent hydrology over the whole soil column, their differences in simulated ET and NEE must emerge from their only difference which is the amount of simulated tree rooting strategies. Therefore, local root adaptations in LPJm4.0-VR can be regarded as a buffer against seasonal precipitation deficits by usage of deep water (exemplary shown for STM K67 in Fig. A9).

We can here quantify this water access for the first time on the basis of carbon investment and return, and limited by spatial heterogeneous soil depth. If soil depth was no limit to rooting depth throughout the study region, ET rates of seasonally dry climatological clusters would have most likely been overestimated. The same holds true if deeper roots would not require

additional below-ground carbon investment. Therefore, we argue that both factors are of great importance to explain regional rates of ET. This also means that forests in the same climatological cluster contribute very differently to the overall ET and therefore to the moisture transport across South America. We can here mechanistically explain this coherence as we show for the first time on the regional scale how PFTs with variable tree rooting strategies adjust to local environmental conditions and in return ~~improve~~lead to simulated rates of ET ~~and NEE~~very close to validation data (Fig. 7, 9~~-11).~~). The heterogeneous picture of $\overline{D_{95}}$ we find (Fig. 5) might provide a direct guideline where to put emphasis on forest conservation to maintain continental scale moisture recycling, as $\overline{D_{95}}$ directly scales with rates of ET.

Being able to mechanistically reproduce and explain ~~this~~the broad-scale stabilization of water fluxes into the atmosphere has wide implications for DGVM modelling frameworks and simulation of ET as moisture input to the atmosphere in Earth System Models (ESMs). Our approach can help to better quantify the role of forests for local-to-continental scale moisture recycling and to project the fate of forests under future climate and land-use change. The approach presented here is easily applicable for a wide range of DGVMs and ESMs which simulate fine root distribution in a similar way as the LPJmL model family (based on Jackson *et al.*, 1996). A first and easy to implement step for other models could be to prescribe the relative fine root distribution in a spatial explicit way in accordance to ~~the mean rooting depth ($\overline{D_{95}}$)~~$\overline{D_{95}}$ presented in this study.

5 Conclusions

~~In this study we~~We here show for the first time that ~~diverse~~mean tree rooting ~~strategies~~depth across South-America can indeed explain the spatial distribution of ~~biome types, biomass, as well as the spatial~~tropical evergreen forests and their spatio-temporal pattern of ~~the~~ ecosystem fluxes ~~of~~ (ET and NEE) even when the competition of tree rooting strategies, carbon investment into gradually growing ~~deep~~ roots, and ~~local~~a spatially explicit soil depth are considered. ~~Because~~In fact our findings suggest that roughly half of the evergreen forests in the Amazon region depend on investments into rooting systems which go deeper than the standard average PFT parameterization based on literature allows for.

A major advance of the new sub-model version LPJmL4.0-VR ~~allows for a whole spectrum of tree rooting strategies, where each strategy has the same theoretical chance to establish in every location, the simulated local~~ is that simulations start with uniform input distributions of tree rooting strategies ~~are an emergent simulation output which results from~~in each location which shape into a distribution of abundance driven by local environmental filtering and competition. ~~This enables~~Therefore, these distributions are not a pre-selected input, but an emergent simulation output.

The new model features enable to ~~estimate mean~~introduce local tree rooting depth ~~and below ground biomass on a continental scale as presented here, as well as future estimates of functional diversity of tree rooting strategies. Moreover, we conclude that tree root adaptation is~~ as a key explanatory variable ~~to explain forest cover and to estimate the climatic range of~~in future studies dealing with potential forest cover bi-stability in ~~connection with climate fire vegetation feedbacks in~~ tropical regions. Generally, we are convinced that our approach is of high importance to all modelling frameworks of DGVMs and Earth System Models (ESMs) aiming at quantifying continental scale moisture recycling, forest tipping points and resilience. So far the ~~continental scale~~ importance of local scale tree root adaptations for regional scale ecosystem functions shows that this potential treasure of below-ground functional diversity must be protected not only in the scope of future global change.

6 Code availability

In case of manuscript acceptance all model code and post-processing scripts will be made available. The first author of this manuscript is also willing to share all information with all reviewers upon request.

7 Data availability

In case of manuscript acceptance all simulation data will be made available. The first author of this manuscript is also willing to share all information with all reviewers upon request.

8 Author contribution

All authors helped in conceptualizing the model. BS and WvB developed the model code. BS, WvB, MD, AS, RR, FL, MB, SB, MH, RO, KT conceived the simulation experiments and BS carried them out. BS, MD, AS, RR and JH analysed model output data. BS prepared the manuscript with contributions from all co-authors.

9 Competing interests

The authors declare that they have no conflict of interest.

10 Acknowledgements

BS and KT acknowledge funding from the BMBF- and Belmont Forum-funded project "CLIMAX: Climate services through knowledge co-production: A Euro-South American initiative for strengthening societal adaptation response to extreme events", FKZ 01LP1610A. MD is funded by the DFG/FAPESP within the IRTG 1740/TRP 2015/50122-0. MH is supported by a grant from Instituto Serrapilheira/Serra 1709-18983. A. Sörensson and R. Ruscica acknowledge support from PICT-2018-02511 (ANPCyT, Argentina). This work used eddy covariance data acquired and shared by the FLUXNET community, including these networks: AmeriFlux, AfriFlux, AsiaFlux, CarboAfrica, CarboEuropeIP, CarboItaly, CarboMont, ChinaFlux, Fluxnet-Canada, GreenGrass, ICOS, KoFlux, LBA, NECC, OzFlux-TERN, TCOS-Siberia, and USCCC. The ERA-Interim reanalysis data are provided by ECMWF and processed by LSCE. The FLUXNET eddy covariance data processing and harmonization was carried out by the European Fluxes Database Cluster, AmeriFlux Management Project, and Fluxdata project of FLUXNET, with the support of CDIAC and ICOS Ecosystem Thematic Center, and the OzFlux, ChinaFlux and AsiaFlux offices.

11 References

Allen, C. D., Breshears, D. D. and McDowell, N. G.: On underestimation of global vulnerability to tree mortality and forest die-off from hotter drought in the Anthropocene, Ecosphere, 6(8), 1–55, doi:10.1890/ES15-00203.1, 2015.

Aragão, L. E. O. C., Malhi, Y., Roman-Cuesta, R. M., Saatchi, S., Anderson, L. O. and Shimabukuro, Y. E.: Spatial patterns and fire response of recent Amazonian droughts, Geophys. Res. Lett., 34(7), 1–5, doi:10.1029/2006GL028946, 2007.

Arnold, J. G., Williams, J. R., Nicks, A. D. and Sammons, N. B.: SWRRB; a basin scale simulation model for soil and water resources management., SWRRB; a basin scale Simul. Model soil water Resour. Manag., 1990.

Arora, V. K. and Boer, G. J.: A Representation of Variable Root Distribution in Dynamic Vegetation Models, Earth Interact., 7(6), 1–19, doi:10.1175/1087-3562(2003)007<0001:arovrd>2.0.co;2, 2003.

Avitabile, V., Herold, M., Heuvelink, G. B. M., Lewis, S. L., Phillips, O. L., Asner, G. P., Armston, J., Ashton, P. S., Banin, L., Bayol, N., Berry, N. J., Boeckx, P., de Jong, B. H. J., Devries, B., Girardin, C. A. J., Kearsley, E., Lindsell, J. A., Lopez-Gonzalez, G., Lucas, R., Malhi, Y., Morel, A., Mitchard, E. T. A., Nagy, L., Qie, L., Quinones, M. J., Ryan, C. M., Ferry, S. J. W., Sunderland, T., Laurin, G. V., Gatti, R. C., Valentini, R., Verbeeck, H., Wijaya, A. and Willcock, S.: An integrated pan-tropical biomass map using multiple reference datasets, Glob. Chang. Biol., 22(4), 1406–1420, doi:10.1111/gcb.13139, ~~2016a~~2016.

Avitabile, V., Herold, M., Heuvelink, G. B. M., Lewis, S. L., Phillips, O. L., Asner, G. P., Armston, J., Ashton, P. S., Banin, L., Bayol, N., Berry, N. J., Boeckx, P., de Jong, B. H. J., Devries, B., Girardin, C. A. J., Kearsley, E., Lindsell, J. A., Lopez-Gonzalez, G., Lucas, R., Malhi, Y., Morel, A., Mitchard, E. T. A., Nagy, L., Qie, L., Quinones, M. J., Ryan, C. M., Ferry, S. J. W., Sunderland, T., Laurin, G. V., Gatti, R. C., Valentini, R., Verbeeck, H., Wijaya, A. and Willcock, S.: An integrated pan-tropical biomass map using multiple reference datasets, Glob. Chang. Biol., 22(4), 1406–1420, doi:10.1111/gcb.13139, 2016b.

Baker, I. T., Prihodko, L., Denning, A. S., Goulden, M., Miller, S. and Da Rocha, H. R.: Seasonal drought stress in the amazon: Reconciling models and observations, J. Geophys. Res. Biogeosciences, 114(1), 1–10, doi:10.1029/2007JG000644, 2008.

Baker, I. T., Prihodko, L., Denning, A. S., Goulden, M., Miller, S. and Da Rocha, H. R.: Seasonal drought stress in the amazon: Reconciling models and observations, J. Geophys. Res. Biogeosciences, 114(1), 1–10, doi:10.1029/2007JG000644, 2009.

Balsamo, G., Viterbo, P., Beijaars, A., van den Hurk, B., Hirschi, M., Betts, A. K. and Scipal, K.: A revised hydrology for the ECMWF model: Verification from field site to terrestrial water storage and impact in the integrated forecast system, J. Hydrometeorol., 10(3), 623–643, doi:10.1175/2008JHM1068.1, 2009.

Balsamo, G., Albergel, C., Beljaars, A., Boussetta, S., Brun, E., Cloke, H., Dee, D., Dutra, E., Munõz-Sabater, J., Pappenberger, F., De Rosnay, P., Stockdale, T. and Vitart, F.: ERA-Interim/Land: A global land surface reanalysis data set, Hydrol. Earth Syst. Sci., 19(1), 389–407, doi:10.5194/hess-19-389-2015, 2015.

Baudena, M., Dekker, S. C., van Bodegom, P. M., Cuesta, B., Higgins, S. I., Lehsten, V., Reick, C. H., Rietkerk, M., Scheiter, S., Yin, Z., Zavala, M. A. and Brovkin, V.: Forests, savannas and grasslands: bridging the knowledge gap between ecology and Dynamic Global Vegetation Models, Biogeosciences Discuss., 11(6), 9471–9510, doi:10.5194/bgd-11-9471-2014, 2014.

Beck, H. E., Van Dijk, A. I. J. M., Levizzani, V., Schellekens, J., Miralles, D. G., Martens, B. and De Roo, A.: MSWEP: 3-hourly 0.25° global gridded precipitation (1979-2015) by merging gauge, satellite, and reanalysis data, Hydrol. Earth Syst. Sci., 21(1), 589–615, doi:10.5194/hess-21-589-2017, 2017.

Becker, A., Finger, P., Meyer-Christoffer, A., Rudolf, B., Schamm, K., Schneider, U. and Ziese, M.: A description of the global land-surface precipitation data products of the Global Precipitation Climatology Centre with sample applications including centennial (trend) analysis from 1901-present, Earth Syst. Sci. Data, 5(1), 71–99, doi:10.5194/essd-5-71-2013, 2013.

Best, M. J., Pryor, M., Clark, D. B., Rooney, G. G., Essery, R. . L. H., Ménard, C. B., Edwards, J. M., Hendry, M. A., Porson, A., Gedney, N., Mercado, L. M., Sitch, S., Blyth, E., Boucher, O., Cox, P. M., Grimmond, C. S. B. and Harding, R. J.: The Joint UK Land Environment Simulator (JULES), model description – Part 1: Energy and water fluxes, Geosci. Model Dev., 4(3), 677–699, doi:10.5194/gmd-4-677-2011, 2011.

Bonal, D., Bosc, A., Ponton, S., Goret, J., Burban, B., Gross, P., Bonnefonds, J. M., Elbers, J. A., Longdoz, B., Epron, D., Guehl, J. and Granier, A.: Impact of severe dry season on net ecosystem exchange in the Neotropical rainforest of French Guiana, , 14(8), 1917–1933 [online] Available from: https://edepot.wur.nl/1900, 2008.

Brienen, R. J. W., Phillips, O. L., Feldpausch, T. R., Gloor, E., Baker, T. R., Lloyd, J., Lopez-Gonzalez, G., Monteagudo-Mendoza, A., Malhi, Y., Lewis, S. L., Vásquez Martinez, R., Alexiades, M., Álvarez Dávila, E., Alvarez-Loayza, P., Andrade, A., Aragaõ, L. E. O. C., Araujo-Murakami, A., Arets, E. J. M. M., Arroyo, L., Aymard C., G. A., Bánki, O. S., Baraloto, C., Barroso, J., Bonal, D., Boot, R. G. A., Camargo, J. L. C., Castilho, C. V., Chama, V., Chao, K. J., Chave, J., Comiskey, J. A., Cornejo Valverde, F., Da Costa, L., De Oliveira, E. A., Di Fiore, A., Erwin, T. L., Fauset, S., Forsthofer, M., Galbraith, D. R., Grahame, E. S., Groot, N., Hérault, B., Higuchi, N., Honorio Coronado, E. N., Keeling, H., Killeen, T. J., Laurance, W. F., Laurance, S., Licona, J., Magnussen, W. E., Marimon, B. S., Marimon-Junior, B. H., Mendoza, C.,

Neill, D. A., Nogueira, E. M., Núñez, P., Pallqui Camacho, N. C., Parada, A., Pardo-Molina, G., Peacock, J., Penã-Claros, M., Pickavance, G. C., Pitman, N. C. A., Poorter, L., Prieto, A., Quesada, C. A., Ramírez, F., Ramírez-Angulo, H., Restrepo, Z., Roopsind, A., Rudas, A., Salomaõ, R. P., Schwarz, M., Silva, N., Silva-Espejo, J. E., Silveira, M., Stropp, J., Talbot, J., Ter Steege, H., Teran-Aguilar, J., Terborgh, J., Thomas-Caesar, R., Toledo, M., Torello-Raventos, M., Umetsu, R. K., Van Der Heijden, G. M. F., Van Der Hout, P., Guimarães Vieira, I. C., Vieira, S. A., Vilanova, E., Vos, V. A. and Zagt, R. J.: Long-term decline of the Amazon carbon sink, Nature, 519(7543), 344–348, doi:10.1038/nature14283, 2015.

Brum, M., Vadeboncoeur, M. A., Ivanov, V., Asbjornsen, H., Saleska, S., Alves, L. F., Penha, D., Dias, J. D., Aragão, L. E. O. C., Barros, F., Bittencourt, P., Pereira, L. and Oliveira, R. S.: Hydrological niche segregation defines forest structure and drought tolerance strategies in a seasonal Amazon forest, J. Ecol., 107(1), 318–333, doi:10.1111/1365-2745.13022, 2019.

Brunner, I., Herzog, C., Dawes, M. A., Arend, M. and Sperisen, C.: How tree roots respond to drought, Front. Plant Sci., 6(JULY), 1–16, doi:10.3389/fpls.2015.00547, 2015.

Canadell, J., Jackson, R. B., Ehleringer, J. R., Mooney, H. A., Sala, O. E. and Schulze, E.-D.: Max rooting depth of vegetation types at the global scale, Oecologica, 108, 583–595, doi:10.1007/s10705-016-9812-z, 1996.

Chave, J., Condit, R., Aguilar, S., Hernandez, A., Lao, S. and Perez, R.: Error propagation and scaling for tropical forest biomass estimates, Philos. Trans. R. Soc. B Biol. Sci., 359(1443), 409–420, doi:10.1098/rstb.2003.1425, 2004.

Carvalhais, N., Forkel, M., Khomik, M., Bellarby, J., Jung, M., Migliavacca, M., Saatchi, S., Santoro, M., Thurner, M. and Weber, U.: Global covariation of carbon turnover times with climate in terrestrial ecosystems, Nature, 514(7521), 213–217, 2014.

Ciemer, C., Boers, N., Hirota, M., Kurths, J., Müller-Hansen, F., Oliveira, R. S. and Winkelmann, R.: Higher resilience to climatic disturbances in tropical vegetation exposed to more variable rainfall, Nat. Geosci., 12(March), doi:10.1038/s41561-019-0312-z, 2019.

Cosby, B. J., Hornberger, G. M., Clapp, R. B. and Ginn, T.: A statistical exploration of the relationships of soil moisture characteristics to the physical properties of soils, Water Resour. Res., 20(6), 682–690, 1984.

Costa, M. H., Biajoli, M. C., Sanches, L., Malhado, A. C. M., Hutyra, L. R., Da Rocha, H. R., Aguiar, R. G. and De Araújo, A. C.: Atmospheric versus vegetation controls of Amazonian tropical rain forest evapotranspiration: Are the wet and seasonally dry rain forests any different?, J. Geophys. Res. Biogeosciences, 115(4), 1–9, doi:10.1029/2009JG001179, 2010.

Dee, D. P., Uppala, S. M., Simmons, A. J., Berrisford, P., Poli, P., Kobayashi, S., Andrae, U., Balmaseda, M. A., Balsamo, G., Bauer, P., Bechtold, P., Beljaars, A. C. M., van de Berg, L., Bidlot, J., Bormann, N., Delsol, C., Dragani, R., Fuentes, M., Geer, A. J., Haimberger, L., Healy, S. B., Hersbach, H., Hólm, E. V., Isaksen, L., Kållberg, P., Köhler, M., Matricardi, M., Mcnally, A. P., Monge-Sanz, B. M., Morcrette, J. J., Park, B. K., Peubey, C., de Rosnay, P., Tavolato, C., Thépaut, J. N. and Vitart, F.: The ERA-Interim reanalysis: Configuration and performance of the data assimilation system, Q. J. R. Meteorol. Soc., 137(656), 553–597, doi:10.1002/qj.828, 2011.

Ek, M. B., Mitchell, K. E., Lin, Y., Rogers, E., Grunmann, P., Koren, V., Gayno, G. and Tarpley, J. D.: Implementation of Noah land surface model advances in the National Centers for Environmental Prediction operational mesoscale Eta model, J. Geophys. Res. D Atmos., 108(22), 1–16, doi:10.1029/2002jd003296, 2003.

Eshel, A. and Grünzweig, J. M.: Root-shoot allometry of tropical forest trees determined in a large-scale aeroponic system, Ann. Bot., 112(2), 291–296, doi:10.1093/aob/mcs275, 2013.

Espírito Santo, F. D. B., Gloor, M., Keller, M., Malhi, Y., Saatchi, S., Nelson, B., Junior, R. C. O., Pereira, C., Lloyd, J., Frolking, S., Palace, M., Shimabukuro, Y. E., Duarte, V., Mendoza, A. M., López González, G., Baker, T. R., Feldpausch, T. R., Brienen, R. J. W., Asner, G. P., Boyd, D. S. and Phillips, O. L.: Size and frequency of natural forest disturbances and the Amazon forest carbon balance, Nat. Commun., 5, 1–6, doi:10.1038/ncomms4434, 2014.

Fan, Y., Miguez-Macho, G., Jobbágy, E. G., Jackson, R. B. and Otero-Casal, C.: Hydrologic regulation of plant rooting depth., Proc. Natl. Acad. Sci. U. S. A., 114(40), 10572–10577, doi:10.1073/pnas.1712381114, 2017.

Fearnside, P. M.: Brazil's Amazonian forest carbon: the key to Southern Amazonia's significance for global climate, Reg. Environ. Chang., 18(1), 47–61, doi:10.1007/s10113-016-1007-2, 2016.

Forkel, M., Carvalhais, N., Schaphoff, S., Bloh, W. V., Migliavacca, M., Thurner, M. and Thonicke, K.: Identifying environmental controls on vegetation greenness phenology through model-data integration, Biogeosciences, 11(23), 7025–7050, doi:10.5194/bg-11-7025-2014, 2014.

~~Forkel, M., Migliavacca, M., Thonicke, K., Reichstein, M., Schaphoff, S., Weber, U. and Carvalhais, N.: Codominant water control on global interannual variability and trends in land surface phenology and greenness, Glob. Chang. Biol., 21(9), 3414–3435, doi:10.1111/gcb.12950, 2015.~~

Guimberteau, M., Zhu, D., Maignan, F., Huang, Y., Yue, C., Dantec-Nédélec, S., Ottlé, C., Jornet-Puig, A., Bastos, A., Laurent, P., Goll, D., Bowring, S., Chang, J., Guenet, B., Tifafi, M., Peng, S., Krinner, G., Ducharne, A., Wang, F., Wang, T., Wang, X., Wang, Y., Yin, Z., Lauerwald, R., Joetzjer, E., Qiu, C., Kim, H. and Ciais, P.: ORCHIDEE-MICT (revision 4126), a land surface model for the high-latitudes: model description and validation, Geosci. Model Dev. Discuss., (June), 1–65, doi:10.5194/gmd-2017-122, 2017.

Harris, I., Jones, P. D., Osborn, T. J. and Lister, D. H.: Updated high-resolution grids of monthly climatic observations - the CRU TS3.10 Dataset, Int. J. Climatol., 34(3), 623–642, doi:10.1002/joc.3711, 2014.

Hijmans, R. J. and van Etten, J.: raster: Geographic data analysis and modeling, R Packag. version, 2(8), 2016.

Hirota, M., Holmgren, M., Van New, E. H. and Scheffer, M.: Global Resilience of Tropical Forest, Science (80-.)., 334(October), 232–235, doi:10.1126/science.1210657, 2011.

Huang, S., Titus, S. J. and Wiens, D. P.: Comparison of nonlinear height–diameter functions for major Alberta tree species, Can. J. For. Res., 22(9), 1297–1304, 1992.

Huntingford, C., Zelazowski, P., Galbraith, D., Mercado, L. M., Sitch, S., Fisher, R., Lomas, M., Walker, A. P., Jones, C. D., Booth, B. B. B., Malhi, Y., Hemming, D., Kay, G., Good, P., Lewis, S. L., Phillips, O. L., Atkin, O. K., Lloyd, J., Gloor, E., Zaragoza-Castells, J., Meir, P., Betts, R., Harris, P. P., Nobre, C., Marengo, J. and Cox, P. M.: Simulated resilience of tropical rainforests to CO 2 -induced climate change, Nat. Geosci., 6(4), 268–273, doi:10.1038/ngeo1741, 2013.

Ichii, K., Hashimoto, H., White, M. A., Potter, C., Hutyra, L. R., Huete, A. R., Myneni, R. B. and Nemani, R. R.: Constraining rooting depths in tropical rainforests using satellite data and ecosystem modeling for accurate simulation of gross primary production seasonality, Glob. Chang. Biol., 13(1), 67–77, doi:10.1111/j.1365-2486.2006.01277.x, 2007.

Jackson, R. B., Canadell, J., Ehleringer, J., Mooney, H., Sala, O. and Schulze, E.: A global analysis of root distributions for terrestrial biomes, Oecologica, 108, 389–411, 1996.

Jenik, J.: Roots and root systems in tropical trees, Trop. trees as living Syst., 323, 2010.

Jobbágy, E. G. and Jackson, R. B.: the Vertical Distribution of Soil Organic Carbon and Its Relation To Climate and Vegetation, Ecol. Appl., 10(2), 423–436, doi:10.1890/1051-0761(2000)010[0423:TVDOSO]2.0.CO;2, 2000.

Johnson, D. M., Domec, J. C., Carter Berry, Z., Schwantes, A. M., McCulloh, K. A., Woodruff, D. R., Wayne Polley, H., Wortemann, R., Swenson, J. J., Scott Mackay, D., McDowell, N. G. and Jackson, R. B.: Co-occurring woody species have diverse hydraulic strategies and mortality rates during an extreme drought, Plant Cell Environ., 41(3), 576–588, doi:10.1111/pce.13121, 2018.

~~Johnson, M. O., Galbraith, D., Gloor, M., De Deurwaerder, H., Guimberteau, M., Rammig, A., Thonicke, K., Verbeeck, H., von Randow, C., Monteagudo, A., Phillips, O. L., Brienen, R. J. W., Feldpausch, T. R., Lopez Gonzalez, G., Fauset, S., Quesada, C. A., Christoffersen, B., Ciais, P., Sampaio, G., Kruijt, B., Meir, P., Moorcroft, P., Zhang, K., Alvarez Davila, E., Alves de Oliveira, A., Amaral, I., Andrade, A., Aragao, L. E. O. C., Araujo Murakami, A., Arets, E. J. M. M., Arroyo, L., Aymard, G. A., Baraloto, C., Barroso, J., Bonal, D., Boot, R., Camargo, J., Chave, J., Cogollo, A., Cornejo Valverde, F., Lola da Costa, A. C., Di Fiore, A., Ferreira, L., Higuchi, N., Honorio, E. N., Killeen, T. J., Laurance, S. G., Laurance, W. F., Licona, J., Lovejoy, T., Malhi, Y., Marimon, B., Marimon, B. H., Matos, D. C. L., Mendoza, C., Neill, D. A., Pardo, G.,~~

Peña-Claros, M., Pitman, N. C. A., Poorter, L., Prieto, A., Ramirez-Angulo, H., Roopsind, A., Rudas, A., Salomao, R. P., Silveira, M., Stropp, J., ter Steege, H., Terborgh, J., Thomas, R., Toledo, M., Torres Lezama, A., van der Heijden, G. M. F., Vasquez, R., Guimarães Vieira, I. C., Vilanova, E., Vos, V. A. and Baker, T. R.: Variation in stem mortality rates determines patterns of above-ground biomass in Amazonian forests: implications for dynamic global vegetation models, Glob. Chang. Biol., 22(12), 3996–4013, doi:10.1111/gcb.13315, 2016.

Kattge, J., Bönisch, G., Díaz, S., Lavorel, S., Prentice, I. C., Leadley, P., Tautenhahn, S., Werner, G. D. A., Aakala, T. and Abedi, M.: TRY plant trait database–enhanced coverage and open access, Glob. Chang. Biol., 2020.

Kelley, D. I., Prentice, I. C., Harrison, S. P., Wang, H., Simard, M., Fisher, J. B. and Willis, K. O.: A comprehensive benchmarking system for evaluating global vegetation models, Biogeosciences, 10(5), 3313–3340, doi:10.5194/bg-10-3313-2013, 2013.

Kim, H., Watanabe, E.-C., Chang, K., Yoshimura, Y., Hirabayashi, J., Famiglietti, T. and Oki, T.: Century long observation constrained global dynamic downscaling and hydrologic implication, n.d.

Kim, Y., Knox, R. G., Longo, M., Medvigy, D., Hutyra, L. R., Pyle, E. H., Wofsy, S. C., Bras, R. L. and Moorcroft, P. R.: Seasonal carbon dynamics and water fluxes in an Amazon rainforest, Glob. Chang. Biol., 18(4), 1322–1334, doi:10.1111/j.1365-2486.2011.02629.x, 2012.

Kleidon, A. and Heimann, M.: A method of determining rooting depth from a terrestrial biosphere model and its impacts on the global water and carbon cycle, Glob. Chang. Biol., 4(3), 275–286, doi:10.1046/j.1365-2486.1998.00152.x, 1998.

Kleidon, A. and Heimann, M.: Deep-rooted vegetation, Amazonian deforestation, and climate: Results from a modelling study, Glob. Ecol. Biogeogr., 8(5), 397–405, doi:10.1046/j.1365-2699.1999.00150.x, 1999.

Kleidon, A. and Heimann, M.: Assessing the role of deep rooted vegetation in the climate system with model simulations: Mechanism, comparison to observations and implications for Amazonian deforestation, Clim. Dyn., 16(2–3), 183–199, doi:10.1007/s003820050012, 2000.

Krysanova, V., Müller-Wohlfeil, D.-I. and Becker, A.: Development and test of a spatially distributed hydrological/water quality model for mesoscale watersheds, Ecol. Modell., 106(2–3), 261–289, 1998.

Langan, L., Higgins, S. I. and Scheiter, S.: Climate-biomes, pedo-biomes or pyro-biomes: which world view explains the tropical forest–savanna boundary in South America?, J. Biogeogr., 44(10), 2319–2330, doi:10.1111/jbi.13018, 2017.

Lawrence, D. M., Oleson, K. W., Flanner, M. G., Thornton, P. E., Swenson, S. C., Lawrence, P. J., Zeng, X., Yang, Z.-L., Levis, S., Sakaguchi, K., Bonan, G. B. and Slater, A. G.: Parameterization improvements and functional and structural advances in Version 4 of the Community Land Model, J. Adv. Model. Earth Syst., 3(3), 1–27, doi:10.1029/2011ms000045, 2011.

Lee, J. E., Oliveira, R. S., Dawson, T. E. and Fung, I.: Root functioning modifies seasonal climate, Proc. Natl. Acad. Sci. U. S. A., 102(49), 17576–17581, doi:10.1073/pnas.0508785102, 2005.

Leuschner, C., Moser, G., Bertsch, C., Röderstein, M. and Hertel, D.: Large altitudinal increase in tree root/shoot ratio in tropical mountain forests of Ecuador, Basic Appl. Ecol., 8(3), 219–230, 2007.

Lewis, S. L., Brando, P. M., Phillips, O. L., Van Der Heijden, G. M. F. and Nepstad, D.: The 2010 Amazon drought, Science (80-.)., 331(6017), 554, doi:10.1126/science.1200807, 2011.

Li, W., Houghton, R. A., Bontemps, S., MacBean, N., Lamarche, C., Ciais, P., Peng, S. and Defourny, P.: Gross and net land cover changes in the main plant functional types derived from the annual ESA CCI land cover maps (1992–2015), Earth Syst. Sci. Data, 10(1), 219–234, doi:10.5194/essd-10-219-2018, 2018.

Liu, L., Peng, S., AghaKouchak, A., Huang, Y., Li, Y., Qin, D., Xie, A. and Li, S.: Broad Consistency Between Satellite and Vegetation Model Estimates of Net Primary Productivity Across Global and Regional Scales, J. Geophys. Res. Biogeosciences, 123(12), 3603–3616, doi:10.1029/2018JG004760, 2018.

Liu, Y., Piao, S., Lian, X., Ciais, P. and Smith, W. K.: Seasonal responses of terrestrial carbon cycle to climate variations in

CMIP5 models: Evaluation and projection, J. Clim., 30(16), 6481–6503, doi:10.1175/JCLI-D-16-0555.1, 2017.

Liu, Y. Y., Dorigo, W. A., Parinussa, R. M., De Jeu, R. A. M., Wagner, W., McCabe, M. F., Evans, J. P. and Van Dijk, A. I. J. M.: Trend-preserving blending of passive and active microwave soil moisture retrievals, Remote Sens. Environ., 123(October 2006), 280–297, doi:10.1016/j.rse.2012.03.014, 2012.

Liu, Y. Y., van Dijk, A. I. J. M., McCabe, M. F., Evans, J. P. and de Jeu, R. A. M.: Global vegetation biomass change (1988-2008) and attribution to environmental and human drivers, Glob. Ecol. Biogeogr., 22(6), 692–705, doi:10.1111/geb.12024, 2013.

Malhi, Y., Aragao, L. E. O. C., Galbraith, D., Huntingford, C., Fisher, R., Zelazowski, P., Sitch, S., McSweeney, C. and Meir, P.: Exploring the likelihood and mechanism of a climate-change-induced dieback of the Amazon rainforest, Proc. Natl. Acad. Sci., 106(49), 20610–20615, doi:10.1073/pnas.0804619106, 2009.

Markewitz, D., Devine, S., Davidson, E. A., Brando, P. and Nepstad, D. C.: Soil moisture depletion under simulated drought in the Amazon: Impacts on deep root uptake, New Phytol., 187(3), 592–607, doi:10.1111/j.1469-8137.2010.03391.x, 2010.

Martens, B., Miralles, D. G., Lievens, H., Van Der Schalie, R., De Jeu, R. A. M., Fernández-Prieto, D., Beck, H. E., Dorigo, W. A. and Verhoest, N. E. C.: GLEAM v3: Satellite-based land evaporation and root-zone soil moisture, Geosci. Model Dev., 10(5), 1903–1925, doi:10.5194/gmd-10-1903-2017, 2017.

Masson, V., Champeaux, J. L., Chauvin, F., Meriguet, C. and Lacaze, R.: A global database of land surface parameters at 1-km resolution in meteorological and climate models, J. Clim., 16(9), 1261–1282, doi:10.1175/1520-0442-16.9.1261, 2003.

Miralles, D. G., Holmes, T. R. H., De Jeu, R. A. M., Gash, J. H., Meesters, A. G. C. A. and Dolman, A. J.: Global land-surface evaporation estimated from satellite-based observations, Hydrol. Earth Syst. Sci., 15(2), 453–469, doi:10.5194/hess-15-453-2011, 2011.

~~Mitchard, E. T. A., Feldpausch, T. R., Brienen, R. J. W., Lopez-Gonzalez, G., Monteagudo, A., Baker, T. R., Lewis, S. L., Lloyd, J., Quesada, C. A., Gloor, M., ter Steege, H., Meir, P., Alvarez, E., Araujo-Murakami, A., Aragão, L. E. O. C., Arroyo, L., Aymard, G., Banki, O., Bonal, D., Brown, S., Brown, F. I., Cerón, C. E., Chama Moscoso, V., Chave, J., Comiskey, J. A., Cornejo, F., Corrales Medina, M., Da Costa, L., Costa, F. R. C., Di Fiore, A., Domingues, T. F., Erwin, T. L., Frederickson, T., Higuchi, N., Honorio Coronado, E. N., Killeen, T. J., Laurance, W. F., Levis, C., Magnusson, W. E., Marimon, B. S., Marimon Junior, B. H., Mendoza Polo, I., Mishra, P., Nascimento, M. T., Neill, D., Núñez Vargas, M. P., Palacios, W. A., Parada, A., Pardo Molina, G., Peña Claros, M., Pitman, N., Peres, C. A., Poorter, L., Prieto, A., Ramirez-Angulo, H., Restrepo Correa, Z., Roopsind, A., Roucoux, K. H., Rudas, A., Salomão, R. P., Schietti, J., Silveira, M., de Souza, P. F., Steininger, M. K., Stropp, J., Terborgh, J., Thomas, R., Toledo, M., Torres-Lezama, A., Van Andel, T. R., van der Heijden, G. M. F., Vieira, I. C. G., Vieira, S., Vilanova-Torre, E., Vos, V. A., Wang, O., Zartman, C. E., Malhi, Y. and Phillips, O. L.: Markedly divergent estimates of Amazon forest carbon density from ground plots and satellites, Glob. Ecol. Biogeogr., 23(8), 935–946, doi:10.1111/geb.12168, 2014.~~

Mokany, K., Raison, R. J. and Prokushkin, A. S.: Critical analysis of root: Shoot ratios in terrestrial biomes, Glob. Chang. Biol., 12(1), 84–96, doi:10.1111/j.1365-2486.2005.001043.x, 2006.

Nachtergaele, F. van, Velthuizen, H., Verelst, L., Batjes, N., Dijkshoorn, K. van Engelen, V., Fischer, G., Jones, A., Montanarella, L. and Petri, M.: Harmonized world soil database, Food and Agriculture Organization of the United Nations, [online] Available from: http://www.fao.org/soils-portal/soil-survey/soil-maps-and-databases/harmonized-world-soil-database-v12/en/, 2009.

Nemani, R. R., Keeling, C. D., Hashimoto, H., Jolly, W. M., Piper, S. C., Tucker, C. J., Myneni, R. B. and Running, S. W.: Climate-driven increases in global terrestrial net primary production from 1982 to 1999, Science (80-.)., 300(5625), 1560–1563, doi:10.1126/science.1082750, 2003.

Nepstad, D. C., de Carvalho, C. R., Davidson, E. A., Jipp, P. H., Lefebvre, P. A., Negreiros, G. H., da Silva, E. D., Stone, T. A., Trumbore, S. E. and Vieira, S.: The role of deep roots in the hydrological and carbon cycles of Amazonian forests and

pastures, Nature, 372(6507), 666–669, doi:10.1038/372666a0, 1994.

New, M., Hulme, M. and Jones, P.: Representing twentieth century space-time climate variability. Part II: development of a 1901-1996 monthly grids of terrestrial surface climate, J. Clim., 13, 2217–2238, 2000.

Nikolova, P. S., Zang, C. and Pretzsch, H.: Combining tree-ring analyses on stems and coarse roots to study the growth dynamics of forest trees: A case study on Norway spruce (Picea abies [L.] H. Karst), Trees - Struct. Funct., 25(5), 859–872, doi:10.1007/s00468-011-0561-y, 2011.

Oliveira, R. S., Bezerra, L., Davidson, E. A., Pinto, F., Klink, C. A., Nepstad, D. C. and Moreira, A.: Deep root function in soil water dynamics in cerrado savannas of central Brazil, Funct. Ecol., 19(4), 574–581, doi:10.1111/j.1365-2435.2005.01003.x, 2005.

Ostle, N. J., Smith, P., Fisher, R., Ian Woodward, F., Fisher, J. B., Smith, J. U., Galbraith, D., Levy, P., Meir, P., McNamara, N. P. and Bardgett, R. D.: Integrating plant-soil interactions into global carbon cycle models, J. Ecol., 97(5), 851–863, doi:10.1111/j.1365-2745.2009.01547.x, 2009.

Pelletier, J. D., Broxton, P. D., Hazenberg, P., Zeng, X., Troch, P. A., Niu, G.-Y., Williams, Z., Brunke, M. A. and Gochis, D.: A gridded global data set of soil, intact regolith, and sedimentary deposit thicknesses for regional and global land surface modeling, J. Adv. Model. Earth Syst., 8, 41–65, doi:10.1002/2017MS001065, 2016.

Pillet, M., Joetzjer, E., Belmin, C., Chave, J., Ciais, P., Dourdain, A., Evans, M., Hérault, B., Luyssaert, S. and Poulter, B.: Disentangling competitive vs. climatic drivers of tropical forest mortality, J. Ecol., 106(3), 1165–1179, doi:10.1111/1365-2745.12876, 2018.

Poorter, H., Niklas, K. J., Reich, P. B., Oleksyn, J., Poot, P. and Mommer, L.: Biomass allocation to leaves, stems and roots: meta-analyses of interspecific variation and environmental control, New Phytol., 193(1), 30–50, 2012.

Prentice, I. C., Sykes, M. T. and Cramer, W.: A simulation model for the transient effects of climate change on forest landscapes, Ecol. Modell., 65(1–2), 51–70, 1993.

Quesada, C. A., Phillips, O. L., Schwarz, M., Czimczik, C. I., Baker, T. R., Patiño, S., Fyllas, N. M., Hodnett, M. G., Herrera, R., Almeida, S., Alvarez Dávila, E., Arneth, A., Arroyo, L., Chao, K. J., Dezzeo, N., Erwin, T., Di Fiore, A., Higuchi, N., Honorio Coronado, E., Jimenez, E. M., Killeen, T., Lezama, A. T., Lloyd, G., López González, G., Luizão, F. J., Malhi, Y., Monteagudo, A., Neill, D. A., Núñez Vargas, P., Paiva, R., Peacock, J., Peñuela, M. C., Peña Cruz, A., Pitman, N., Priante Filho, N., Prieto, A., Ramírez, H., Rudas, A., Salomão, R., Santos, A. J. B., Schmerler, J., Silva, N., Silveira, M., Vásquez, R., Vieira, I., Terborgh, J. and Lloyd, J.: Basin-wide variations in Amazon forest structure and function are mediated by both soils and climate, Biogeosciences, 9(6), 2203–2246, doi:10.5194/bg-9-2203-2012, 2012.

Rammig, A., Heinke, J., Hofhansl, F., Verbeeck, H., Baker, T. R., Christoffersen, B., Ciais, P., De Deurwaerder, H., Fleischer, K., Galbraith, D., Guimberteau, M., Huth, A., Johnson, M., Krujit, B., Langerwisch, F., Meir, P., Papastefanou, P., Sampaio, G., Thonicke, K., Von Randow, C., Zang, C. and Rödig, E.: A generic pixel to point comparison for simulated large scale ecosystem properties and ground based observations: An example from the Amazon region, Geosci. Model Dev., 11(12), 5203–5215, doi:10.5194/gmd-11-5203-2018, 2018.

R Core Team: R: A language and environment for statistical computing. R Foundatoin for Statistical Computing, [online] Available from: https://www.r-project.org/, 2019.

Restrepo-Coupe, N., Levine, N. M., Christoffersen, B. O., Albert, L. P., Wu, J., Costa, M. H., Galbraith, D., Imbuzeiro, H., Martins, G., da Araujo, A. C., Malhi, Y. S., Zeng, X., Moorcroft, P. and Saleska, S. R.: Do dynamic global vegetation models capture the seasonality of carbon fluxes in the Amazon basin? A data-model intercomparison, Glob. Chang. Biol., 23(1), 191–208, doi:10.1111/gcb.13442, 2017.

da Rocha, H. R., Goulden, M. L., Miller, S. D., Menton, M., Pinto, L. D. V. O., Freitas, H. C. De and Figueira Silva E M., A.: Seasonality of water and heat fluxes over a tropical forest in eastern Amazonia, Ecol. Appl., 14(4), 22–32, doi:10.1890/02-6005, 2004.

Rodell, M., Houser, P. R., Jambor, U., Gottschalck, J., Mitchell, K., Meng, C.-J., Arsenault, K., Cosgrove, B., Radakovich, J., Bosilovich, M., Entin, J. K., Walker, J. P., Lohmann, D. and Toll, D.: The Global Land Data Assimilation System, Bull. Am. Meteorol. Soc., 85(March), 381–394, 2004.

Saatchi, S~~., Mascaro, J., Xu, L., Keller, M., Yang, Y., Duffy, P., Espírito-Santo, F., Baccini, A., Chambers, J. and Schimel, D.: Seeing the forest beyond the trees, Glob. Ecol. Biogeogr., 24(5), 606–610, doi:10.1111/geb.12256, 2015.~~

~~Saatchi, S~~. S., Harris, N. L., Brown, S., Lefsky, M., Mitchard, E. T. A., Salas, W., Zutta, B. R., Buermann, W., Lewis, S. L., Hagen, S., Petrova, S., White, L., Silman, M. and Morel, A.: Benchmark map of forest carbon stocks in tropical regions across three continents, Proc. Natl. Acad. Sci., 108(24), 9899–9904, doi:10.1073/pnas.1019576108, 2011.

Saleska, S. R., Da Rocha, H. R., Huete, A. R., Nobre, A. D., Artaxo, P. E. and Shimabukuro, Y. E.: LBA-ECO CD-32 Flux Tower Network Data Compilation, Brazilian Amazon: 1999-2006, , doi:10.3334/ORNLDAAC/1174, 2013.

Schaphoff, S., von Bloh, W., Rammig, A., Thonicke, K., Biemans, H., Forkel, M., Gerten, D., Heinke, J., Jägermeyr, J., Knauer, J., Langerwisch, F., Lucht, W., Müller, C., Rolinski, S. and Waha, K.: LPJmL4 – a dynamic global vegetation model with managed land – Part 1: Model description, Geosci. Model Dev., 11(4), 1343–1375, doi:10.5194/gmd-11-1343-2018, 2018.

Schymanski, S. J., Sivapalan, M., Roderick, M. L., Beringer, J. and Hutley, L. B.: An optimality-based model of the coupled soil moisture and root dynamics, Hydrol. Earth Syst. Sci., 12(3), 913–932, doi:10.5194/hess-12-913-2008, 2008.

Sheffield, J., Goteti, G. and Wood, E. F.: Development of a 50-year high-resolution global dataset of meteorological forcings for land surface modeling, J. Clim., 19(13), 3088–3111, doi:10.1175/JCLI3790.1, 2006.

Shinozaki, K., Yoda, K. and Kira, T.: A quantitative analysis of plant form - The pipe model theory, Japanese J. Ecol., 14(3), 1964.

Smith, B., Wärlind, D., Arneth, A., Hickler, T., Leadley, P., Siltberg, J. and Zaehle, S.: Implications of incorporating N cycling and N limitations on primary production in an individual-based dynamic vegetation model, Biogeosciences, 11(7), 2027–2054, doi:10.5194/bg-11-2027-2014, 2014.

Sörensson, A. A. and Ruscica, R. C.: Intercomparison and Uncertainty Assessment of Nine Evapotranspiration Estimates Over South America, Water Resour. Res., 54(4), 2891–2908, doi:10.1002/2017WR021682, 2018.

Staal, A., Tuinenburg, O. A., Bosmans, J. H. C., Holmgren, M., Van Nes, E. H., Scheffer, M., Zemp, D. C. and Dekker, S. C.: Forest-rainfall cascades buffer against drought across the Amazon, Nat. Clim. Chang., 8(6), 539–543, doi:10.1038/s41558-018-0177-y, 2018.

Stahl, C., Hérault, B., Rossi, V., Burban, B., Bréchet, C. and Bonal, D.: Depth of soil water uptake by tropical rainforest trees during dry periods: Does tree dimension matter?, Oecologia, 173(4), 1191–1201, doi:10.1007/s00442-013-2724-6, 2013.

Staver, A. C., Archibald, S. and Levin, S. A.: The global extent and determinants of savanna and forest as alternative biome states, Science (80-.)., 334(6053), 230–232, doi:10.1126/science.1210465, 2011.

Tans, P. and Keeling, R.: Trends in Atmospheric Carbon Dioxide, Natl. Ocean. Atmos. Adm. Earth Syst. Res. Lab. [online] Available from: http://www.esrl.noaa.gov/gmd/ccgg/trends, 2015.

Thonicke, K., Venevsky, S., Sitch, S. and Cramer, W.: The role of fire disturbance for global vegetation dynamics: Coupling fire into a dynamic global vegetation model, Glob. Ecol. Biogeogr., 10(6), 661–677, doi:10.1046/j.1466-822X.2001.00175.x, 2001.

Waring, R. H., Schroeder, P. E. and Oren, R.: Application of the pipe model theory to predict canopy leaf area, Can. J. For. Res., 12(3), 556–560, doi:https://doi.org/10.1139/x82-086, 1982.

Warren, J. M., Hanson, P. J., Iversen, C. M., Kumar, J., Walker, A. P. and Wullschleger, S. D.: Root structural and functional dynamics in terrestrial biosphere models - evaluation and recommendations, New Phytol., 205(1), 59–78, doi:10.1111/nph.13034, 2015a.

Warren, J. M., Hanson, P. J., Iversen, C. M., Kumar, J., Walker, A. P. and Wullschleger, S. D.: Root structural and functional dynamics in terrestrial biosphere models - evaluation and recommendations, New Phytol., 205(1), 59–78, doi:10.1111/nph.13034, 2015b.

Weber, U., Jung, M., Reichstein, M., Beer, C., Braakhekke, M. C., Lehsten, V., Ghent, D., Kaduk, J., Viovy, N., Ciais, P., Gobron, N. and Rödenbeck, C.: The interannual variability of Africa's ecosystem productivity: A multi-model analysis, Biogeosciences, 6(2), 285–295, doi:10.5194/bg-6-285-2009, 2009.

Weedon, G. P., Gomes, S., Viterbo, P., Shuttleworth, W. J., Blyth, E., Österle, H., Adam, J. C., Bellouin, N., Boucher, O. and Best, M.: Creation of the WATCH Forcing Data and Its Use to Assess Global and Regional Reference Crop Evaporation over Land during the Twentieth Century, J. Hydrometeorol., 12(5), 823–848, doi:10.1175/2011jhm1369.1, 2011.

Weedon, G. P., Balsamo, G., Bellouin, N., Gomes, S., Best, M. J. and Viterbo, P.: Data methodology applied to ERA-Interim reanalysis data, Water Resour. Res., 50, 7505–7514, doi:10.1002/2014WR015638.Received, 2014.

Wu, J., Albert, L. P., Lopes, A. P., Restrepo-Coupe, N., Hayek, M., Wiedemann, K. T., Guan, K., Stark, S. C., Christoffersen, B., Prohaska, N., Tavares, J. V., Marostica, S., Kobayashi, H., Ferreira, M. L., Campos, K. S., Dda Silva, R., Brando, P. M., Dye, D. G., Huxman, T. E., Huete, A. R., Nelson, B. W. and Saleska, S. R.: Leaf development and demography explain photosynthetic seasonality in Amazon evergreen forests, Science (80-.)., 351(6276), 972–976, doi:10.1126/science.aad5068, 2016.

Wuyts, B., Champneys, A. R. and House, J. I.: Amazonian forest-savanna bistability and human impact, Nat. Commun., 8(May), 1–11, doi:10.1038/ncomms15519, 2017.

Xiao, C. W., Yuste, J. C., Janssens, I. A., Roskams, P., Nachtergale, L., Carrara, A., Sanchez, B. Y. and Ceulemans, R.: Above- and belowground biomass and net primary production in a 73-year-old Scots pine forest, Tree Physiol., 23(8), 505–516, doi:10.1093/treephys/23.8.505, 2003.

Xiao, X., Hagen, S., Zhang, Q., Keller, M. and Moore, B.: Detecting leaf phenology of seasonally moist tropical forests in South America with multi-temporal MODIS images, Remote Sens. Environ., 103(4), 465–473, doi:10.1016/j.rse.2006.04.013, 2006.

Zemp, D. C., Schleussner, C. F., Barbosa, H. M. J., Hirota, M., Montade, V., Sampaio, G., Staal, A., Wang-Erlandsson, L. and Rammig, A.: Self-amplified Amazon forest loss due to vegetation-atmosphere feedbacks, Nat. Commun., 8, 1–10, doi:10.1038/ncomms14681, 2017.

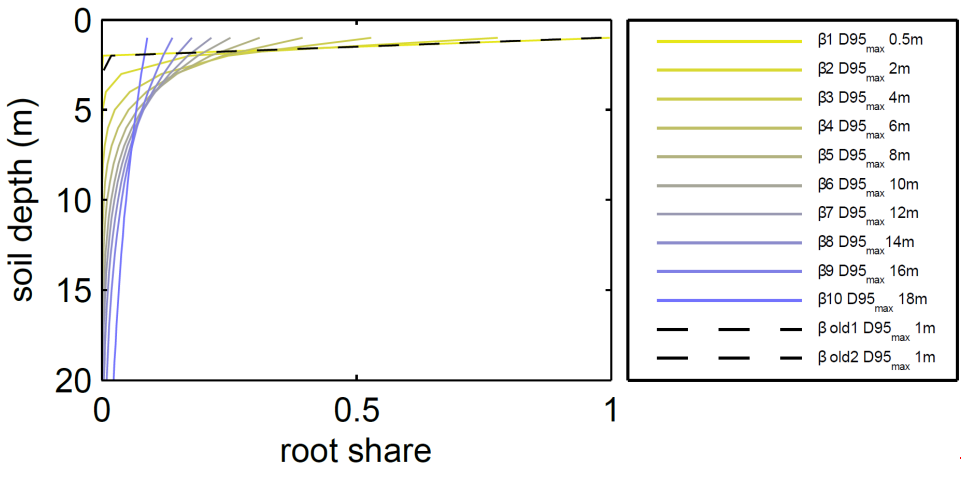

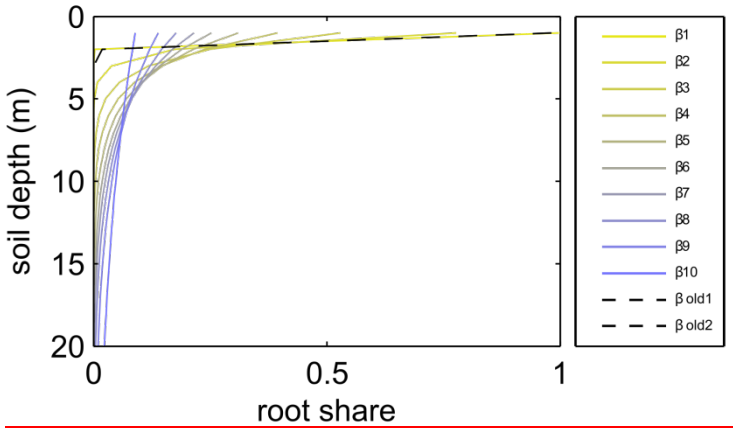

Figure 1: ~~Fine root distributions~~**Relative amount of fine roots in each soil layer for different β-values in LPJmL4.0 and** ~~fine root distribution at maximum rooting depth in~~ **LPJmL4.0-VR** ~~as the relative amount of fine roots over soil depth.~~ **In the legend "β old1-2" correspond to the β-values of the 2 tropical tree PFTs (deciduous and evergreen)** ~~employed~~**simulated in LPJmL4.0. The corresponding graphs lie on top of each other due to marginal differences in their β-values. "β1-10" correspond to the 10 β-values used in LPJmL4.0-VR (**~~table 2~~**Table 1) used to create the 10 sub-PFTs of the tropical evergreen and deciduous tree PFTs (**~~see Sect. 2.2.2).~~**3). For LPJmL4.0-VR the fine root distribution at maximum rooting depth is shown. Please note, the first 3 soil layer (as described in 2.2.1) in this visualization are treated as 1 layer of 1 m thickness for reasons of visual clarity.**

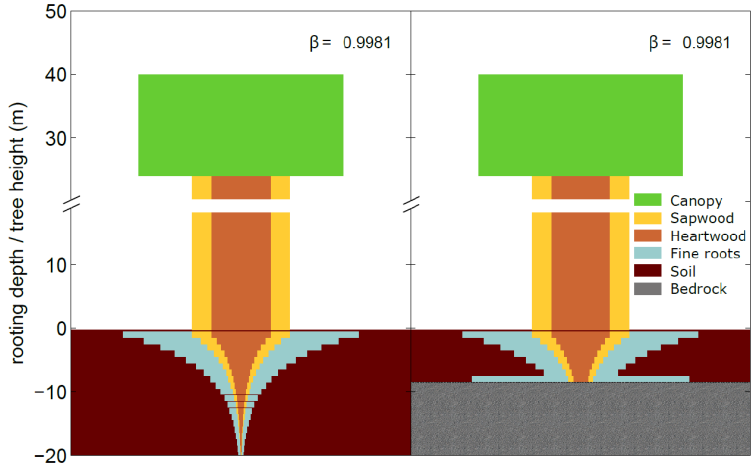

Figure 2: Visualization of belowground carbon allocation to different carbon pools of a tree PFT in LPJmL4.0-VR with a height of 40m and a D_{95_max} of 14m (sub-PFT no. 8 in Table ~~2~~**1) growing in a grid cell with a soil depth of 20m (left panel) and a soil depth of 7m (right panel). As for stem sapwood, also root sapwood needs to satisfy the pipe model. In the first soil layer root sapwood cross-sectional area is equal to stem sapwood cross-sectional area, as all water taken up by fine roots needs to pass this layer. In each following soil layer the root sapwood cross-sectional area is reduced by the sum of the relative amount of fine roots of all soil layers above, thus adjusting the amount of sapwood needed to satisfy the pipe model. Please also see Supplementary Video 1 for a visualization of root growth and development of belowground carbon pools over time under http://www.pik-potsdam.de/~borissa/LPJmL4_VR/Supplementary_Video_1.pptx.**

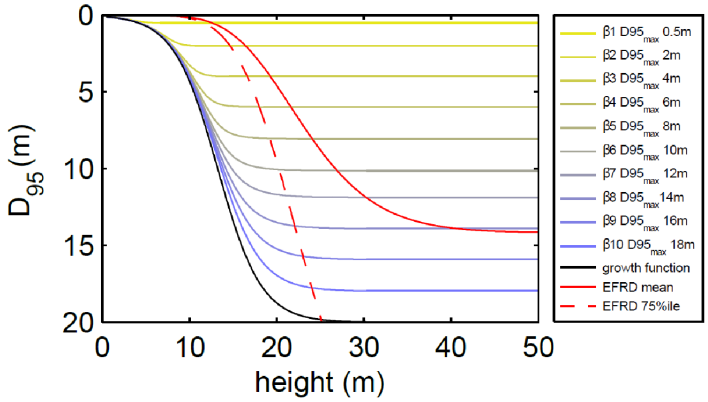

Figure 3: Relation between tree height and rooting depth in LPJmL4.0-VR. Black line: Implemented general growth function of rooting depth (Eq. 5). Lines with colour scale from yellow to blue: Growth functions of rooting depth for each of the 10 sub-PFTs (~~see~~**Sect. 2.2.**~~2~~**3). Here temporal rooting depth is expressed as D_{95} and eventually reaches D_{95_max} (Eq. 3). Red solid line: Mean effective functional rooting depth over tree height (EFRD) adapted from Brum *et al.* (2019) using Eq.** ~~6~~**5. Red dashed line: Respective 75%ile EFRD over tree height adapted from Brum *et al.* (2019). Please also see Supplementary Video 1 for a**

visualization of root growth and development of belowground carbon pools over time under http://www.pik-potsdam.de/~borissa/LPJmL4_VR/Supplementary_Video_1.pptx.

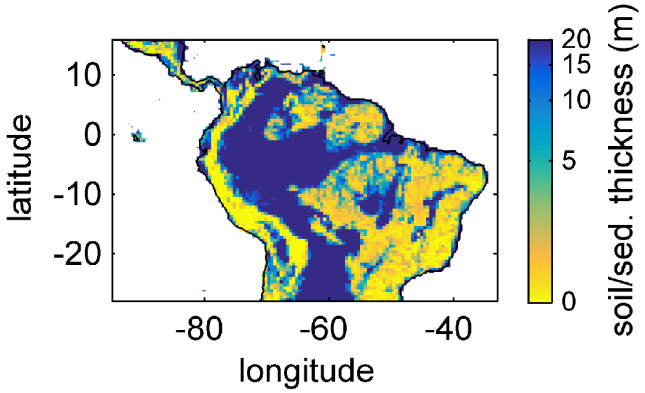

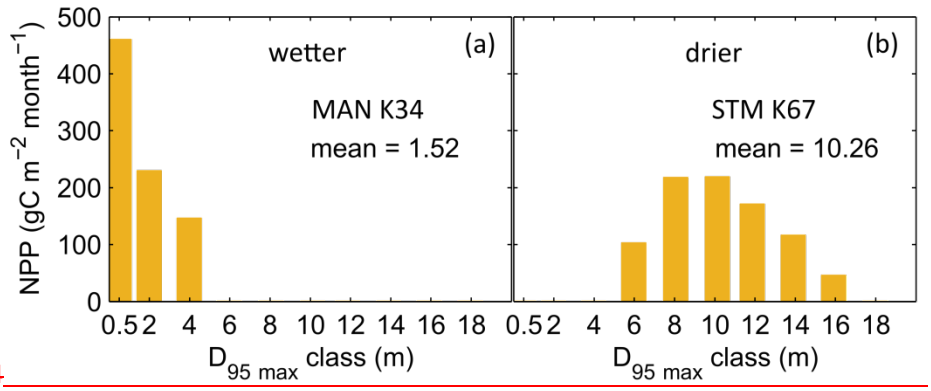

~~Figure 4~~

~~**Figure 4: Soil/sediment thickness from (Pelletier et al., 2016) regridded to the 0.5° x 0.5° longitude latitude grid of LPJmL4.0-VR and restricted to a maximum of 20 m. Colorbar in decadic logarithm.**~~

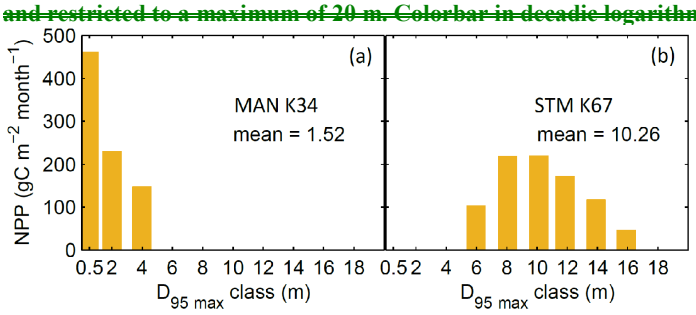

~~Figure 5~~**: Distributions of simulated mean monthly NPP for each D_{95_max}-class for 2001-2010 under CRU climate input at two FluxNet sites. a) Site MAN K34 near the city of Manaus. b) Site STM K67 near the city of Santarem. For more site information see ~~table 3~~Table A2 and ~~figure 9a).~~Fig. 7a.**

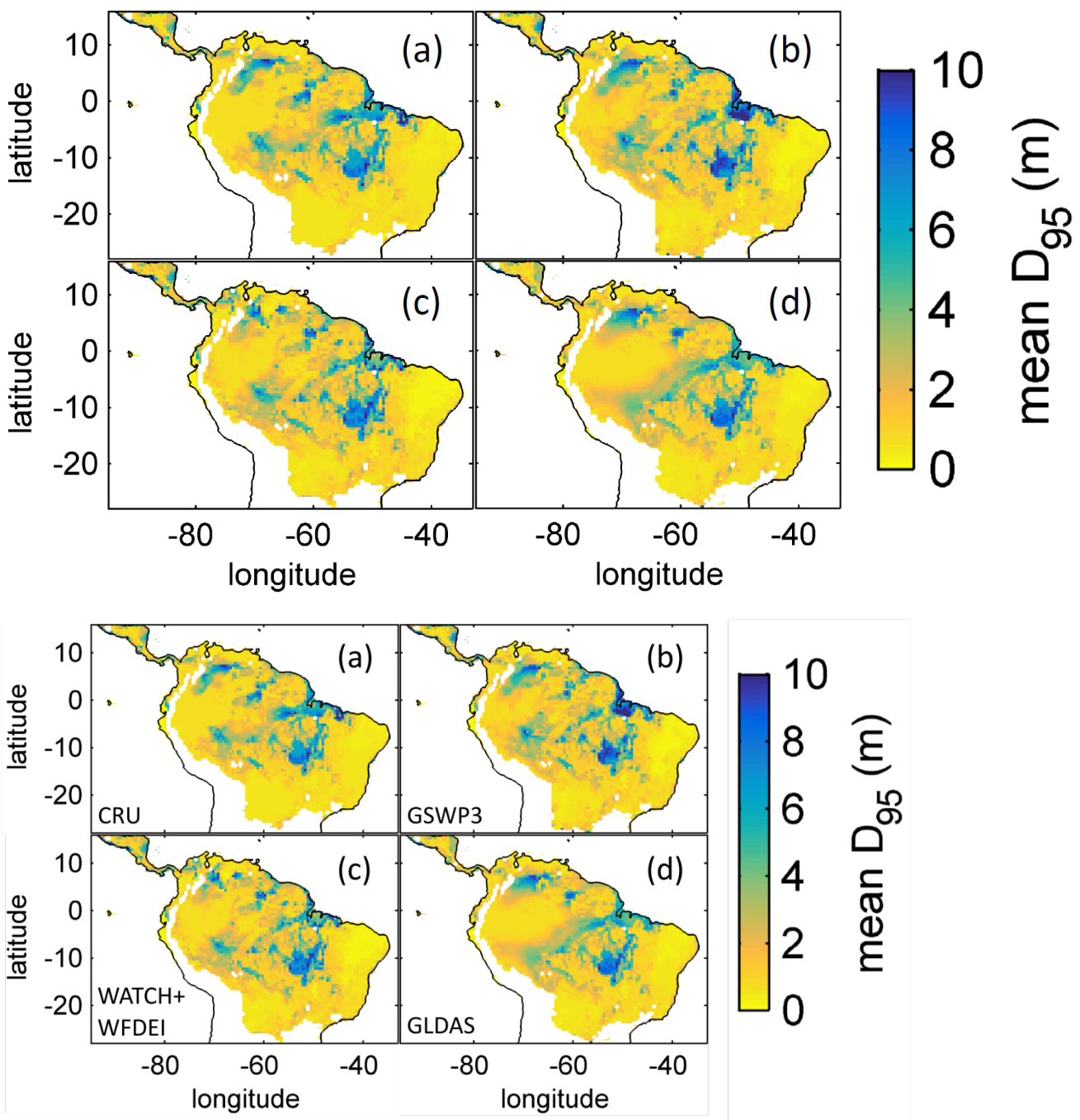

Figure ~~6~~5: Regional NPP-weighted mean rooting depth ($\overline{D_{95}}$) of all sub-PFTs (evergreen and deciduous PFTs combined) for 2001-2010 and different climate inputs simulated with LPJmL4.0-VR. a) CRU climate input. b) GSWP3 climate input. c) WATCH+WFDEI climate input. d) GLDAS climate input. The color scale maximum is set to 10 m.

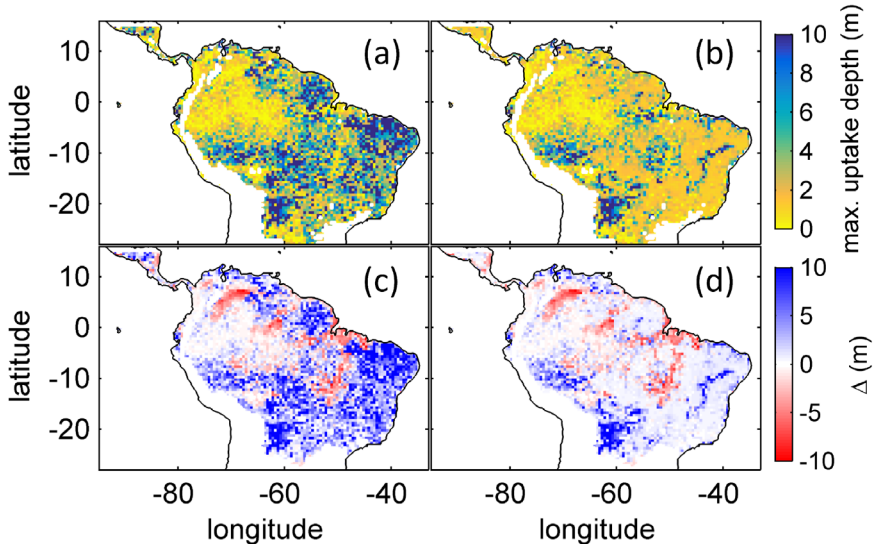

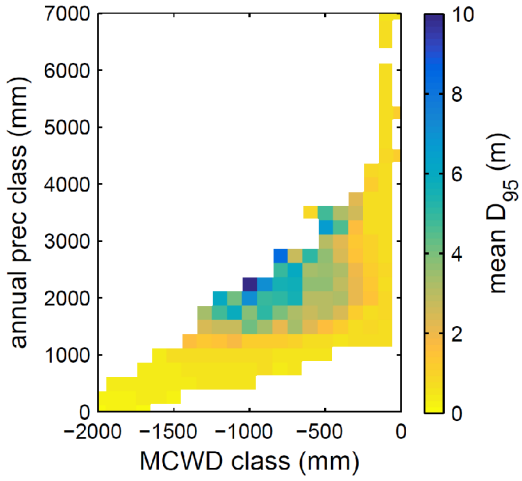

~~Figure 7~~

~~Figure 6: Comparison of simulated $\overline{D_{95}}$ to product of maximum tree root water uptake depth (MDRU). a) Original (Fan et al., 2017) MDRU regridded to 0.5°x0.5° resolution of LPJmL4.0-VR. b) Same as a) but adjusted to soil depth input used in this study (see 2.3.2), in cases where values of (Fan et al., 2017) exceeded this soil depth. The color scale maximum for a) and b) is set to 10 m. c) Difference between a) and $\overline{D_{95}}$ simulated with LPJmL4.0-VR under CRU climate forcing (Fig. 6a). d) Difference between b) and $\overline{D_{95}}$ simulated with LPJmL4.0-VR under CRU climate forcing (Fig. 6a). Red/blue colors denote higher/lower rooting depths in LPJmL4.0-VR.~~

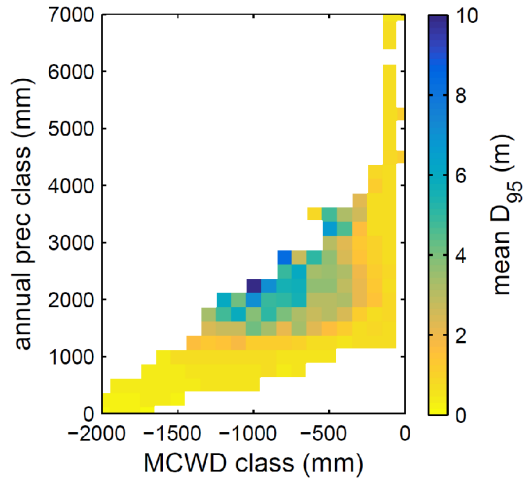

~~Figure 8~~**: Mean rooting depth depicted as mean $\overline{D_{95}}$ over classes of MCWD and annual precipitation sums. Class step size for precipitation was set to 250 mm and class size for MCWD was set to 50 mm. Regions with high amounts of annual rainfall and lower seasonality exclusively favour shallow rooted forests (low $\overline{D_{95}}$). $\overline{D_{95}}$ increases with decreasing MCWD (increasing seasonal drought stress) and decreasing sums of annual precipitation. Below 1200 mm of annual rainfall or -1100 mm of MCWD $\overline{D_{95}}$ sharply decreases again. Note this figure does not consider soil depth. The color scale maximum is set to 10 m.**

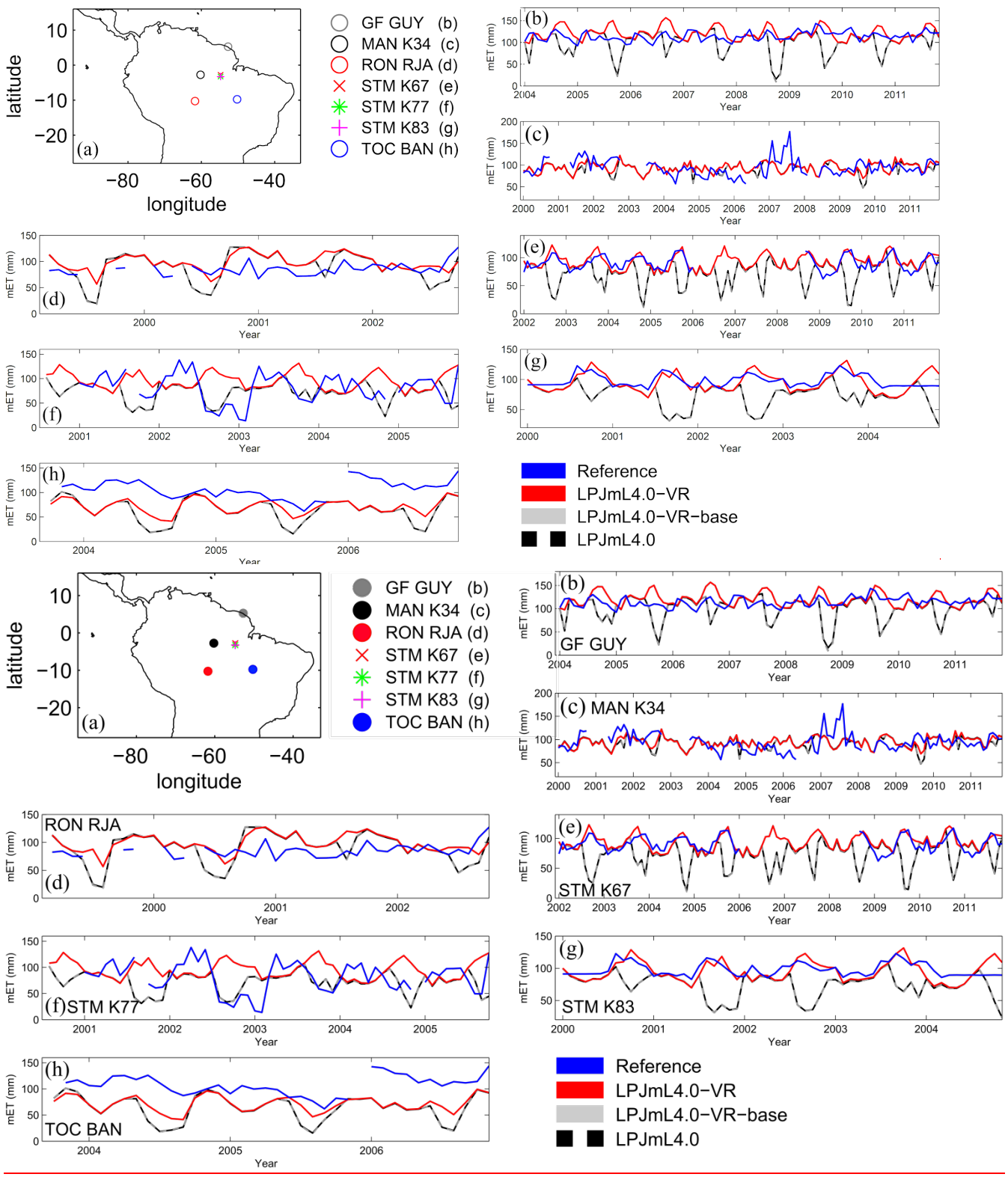

Figure ~~9~~7: Comparisons of monthly ET between different Fluxnet sites and respective simulation output of the different LPJmL model versions used in this study forced with CRU climate. a) Geographical location of different Fluxnet sites (see also ~~table 3~~Table A2). For statistical measures of the individual comparison see Table ~~4~~A3.

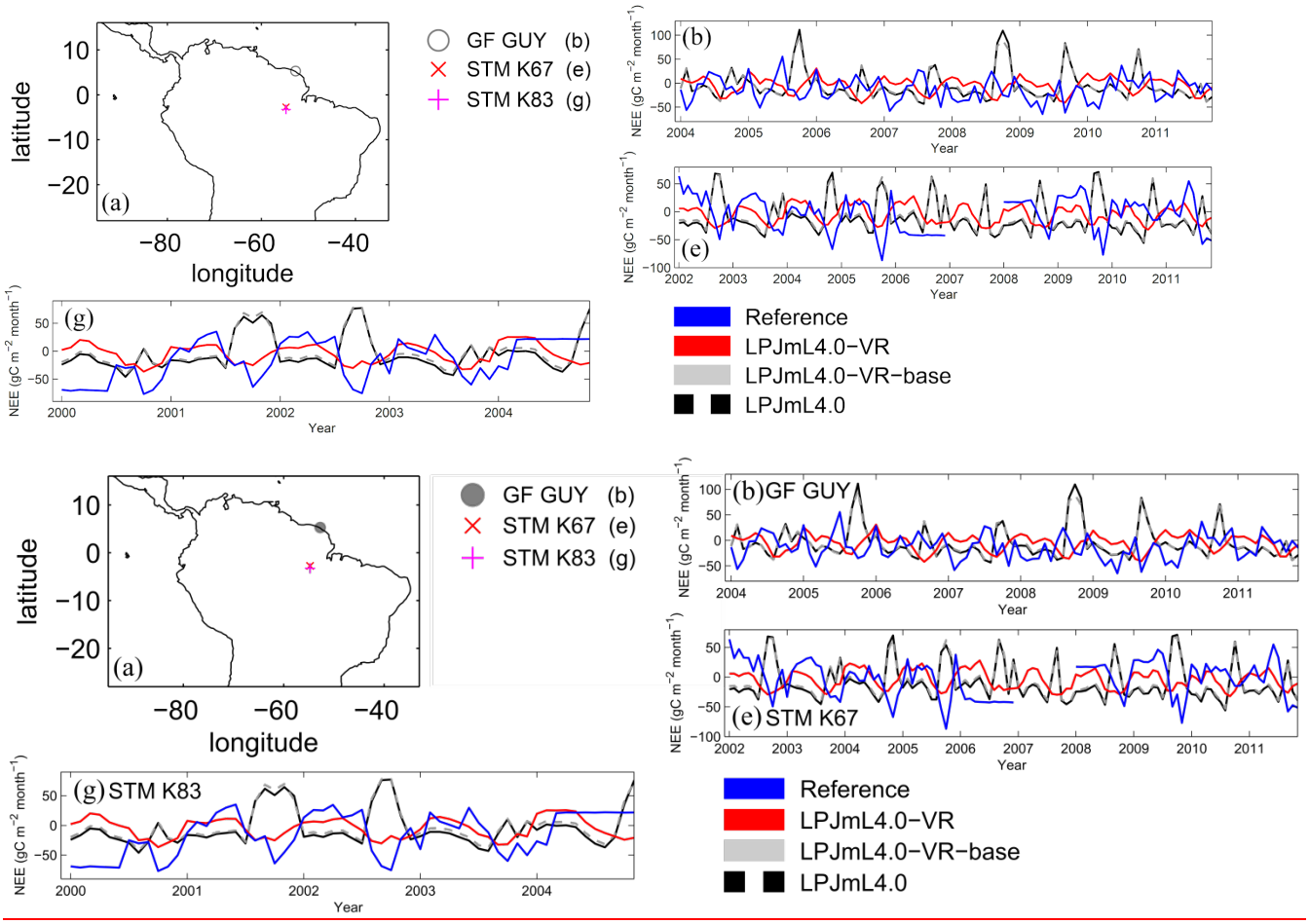

Figure 108: Comparisons of monthly NEE between different Fluxnet sites and respective simulation output of the different LPJmL model versions used in this study forced with CRU climate. a) Geographical location of different Fluxnet sites (see also table 3Table A2). For statistical measures of the individual comparison see table 5Table A4. Note due to data scarcity only 3 Fluxnet sites are shown. Plots of all sites are shown in Fig. S3A5. We kept panel labelling as in Fig. 97 to ensure easy comparability.

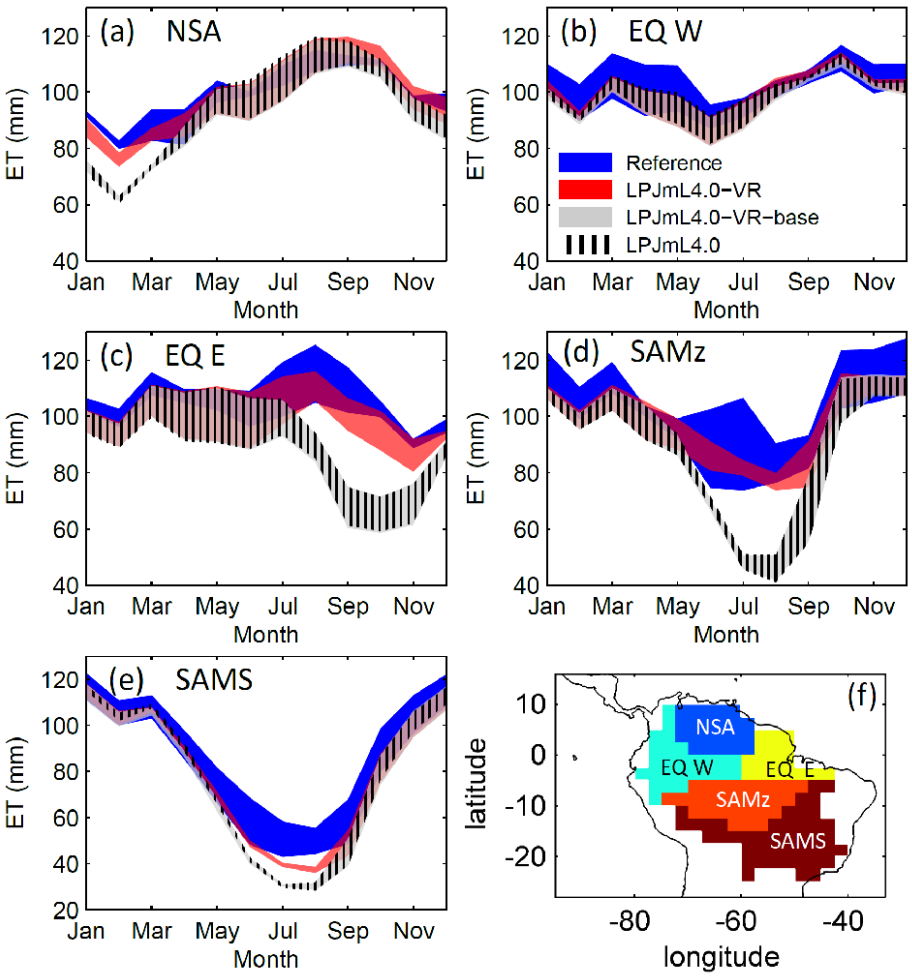

Figure ~~11~~9: Comparisons of continental scale gridded ET products ~~(2.4.2)~~ against simulated ET within 5 regional climatological clusters (a-e) as defined in Sect. 2.~~4.2)~~5.1. Shown is the mean annual cycle of 1981-2010 and the mean for the whole cluster area. Corridors denote the minimum-maximum range between either the ET products or the model outputs under the different climate forcings used in this study. f) Geographical extent of climatological clusters (adapted from Sörensson and Ruscica, 2018). Statistical measures of the individual comparisons can be found in Table ~~6~~A5 (comparisons of corridor means).

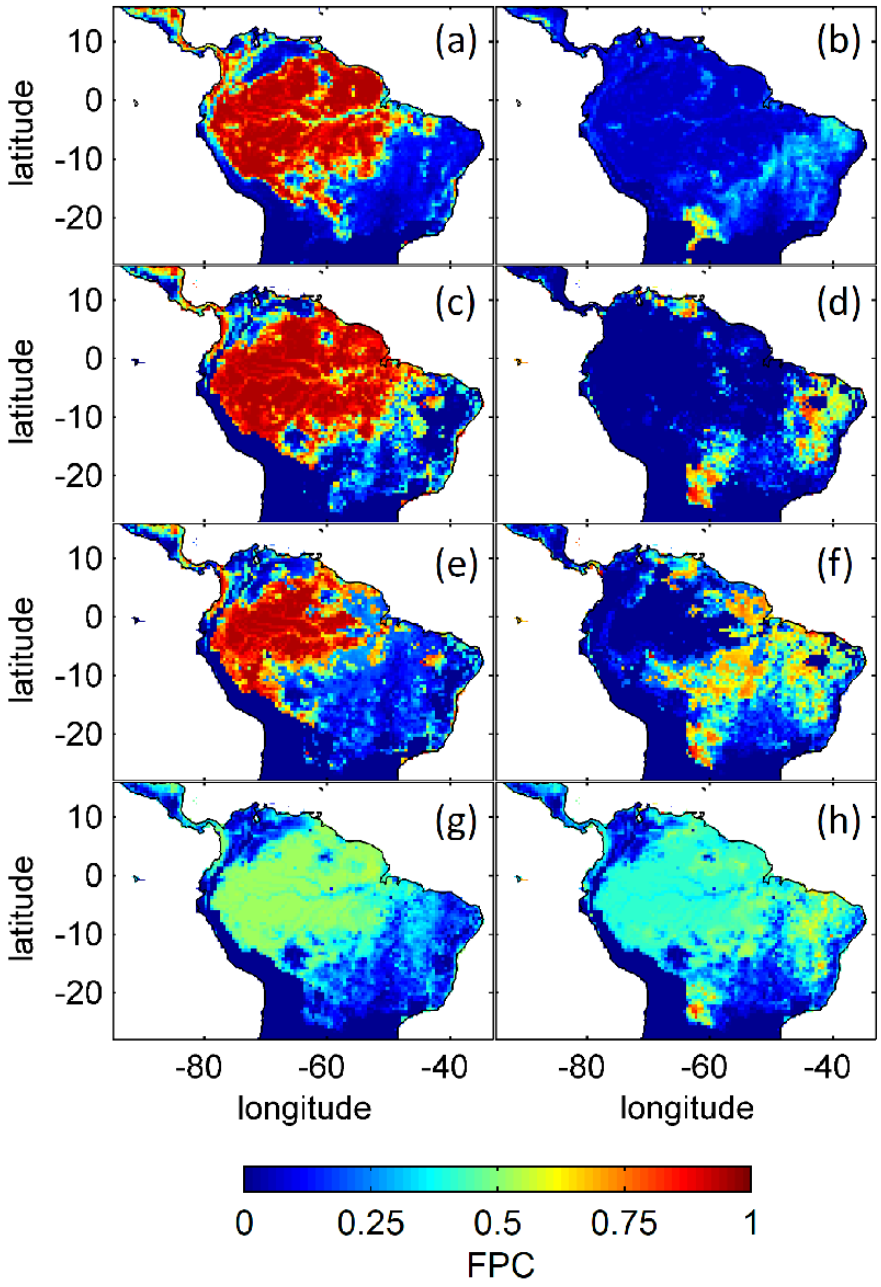
(a)
(b)
(c)
(d)
(e)
(f)
(g)
(h)
latitude
10
0
-10
-20
-80
-60
-40
longitude
0
0.25
0.5
0.75
1
FPC

1297

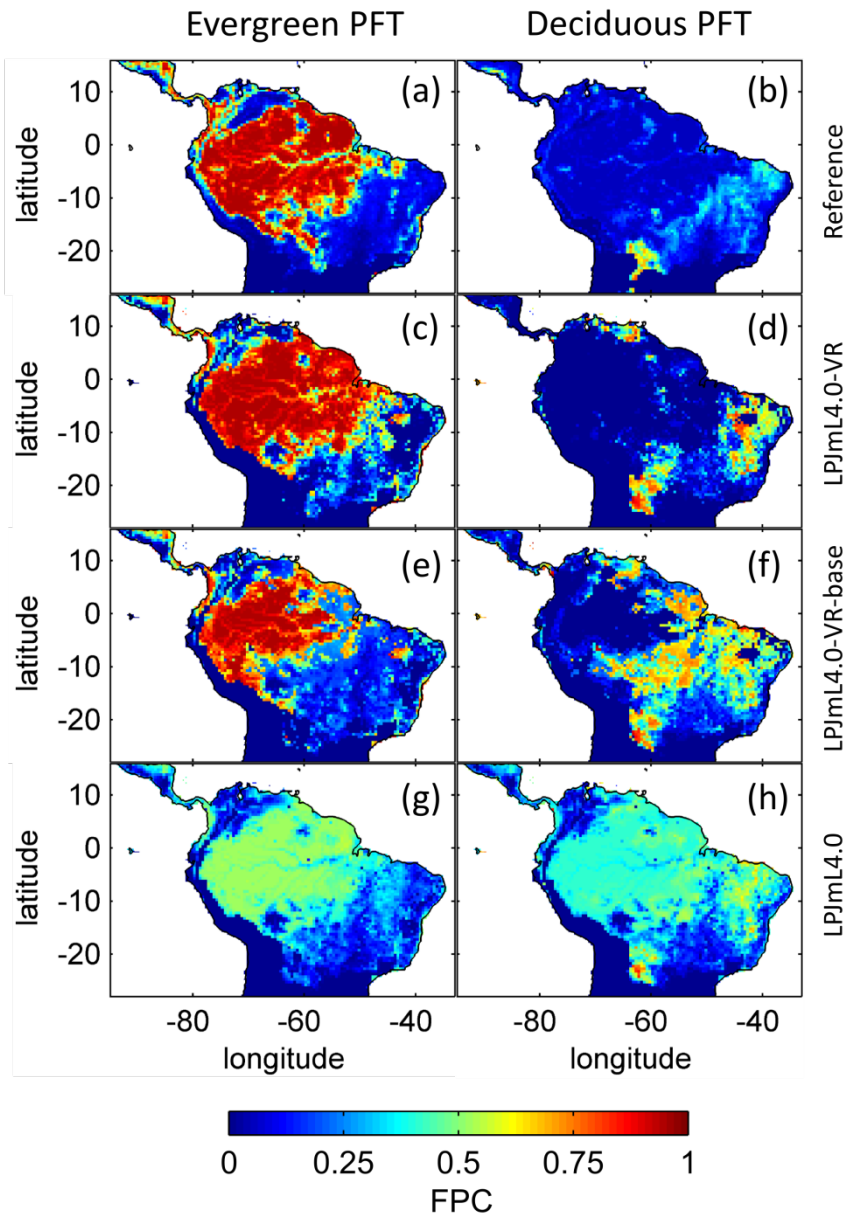

Fig. ~~12~~10: Foliage projected cover (FPC) of evergreen (a, c, e~~,~~ g) and deciduous (b, d, f, h) PFTs over the study region. a)-b) Satellite-derived vegetation composition from ESA Land cover CCI V2.0.7 (Li et al., 2018) **reclassified to the PFTs of LPJmL as in** (Forkel et al., 2014)**. b)-c) LPJmL4.0-VR. d)-e) LPJmL4.0-VR-base. f)-g) LPJmL4.0. All LPJmL model versions were forced with CRU climate input. The shown FPC for all models refers to 2001-2010. For statistical measures of individual comparisons between model versions (c-h) and satellite derived vegetation composition (a-b) see Table ~~7~~A6.**

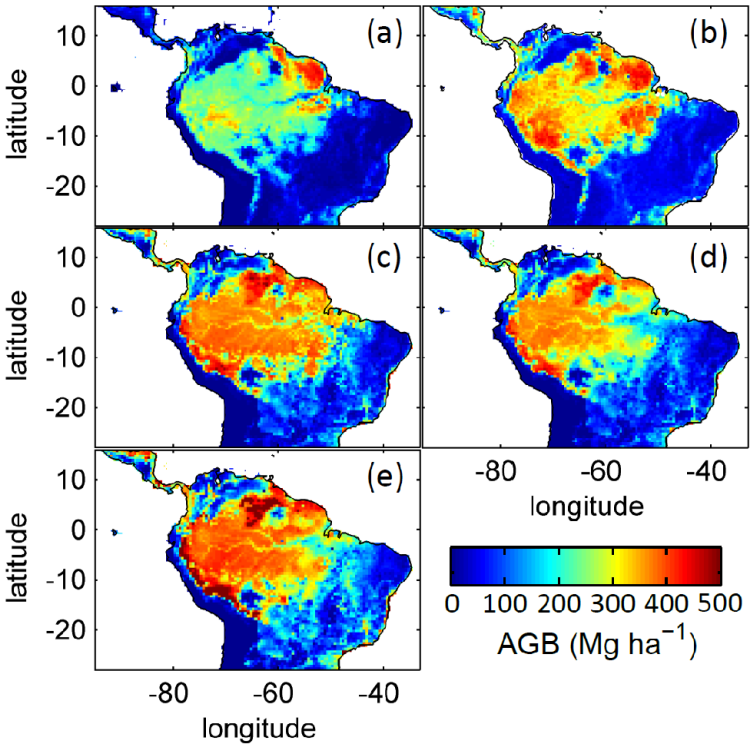

Fig. 13: Comparison of simulated AGB and satellite derived AGB validation products regridded to the spatial resolution of LPJmL models. a) Biomass validation product from Avitabile *et al.* (2016b). b) AGB validation product from Saatchi *et al.*, (2011). c) e) Mean AGB simulated for the time span 2001-2010 with c) LPJmL4.0-VR, d) LPJmL4.0-VR-base and e) LPJmL4.0. For statistical measures of individual comparisons between model versions (c-e) and satellite derived AGB evaluation products (a-b) see Table 8.

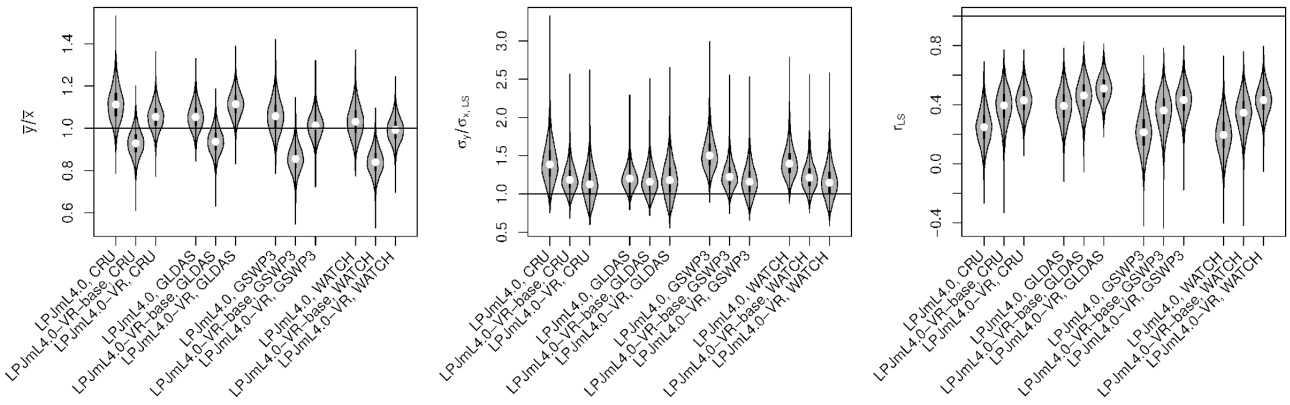

Fig. 14: Comparison of simulated large-scale average AGB (Y) from LPJmL4.0, LPJmL4.0-VR-base and LPJmL4.0-VR for different climate datasets to forest inventory data (X) from Brienen et al. (2015) using the method from Rammig et al. (2019). Three metrics are shown: the ratio of means ($\overline{y}/\overline{x}$) as a measure for the agreement of pattern average (left), the ratio of standard deviations of large scale AGB patterns ($\sigma_y/\sigma_{x,LS}$) as a measure for the agreement of pattern amplitude (middle), the corrected Pearson correlation coefficient (r_{LS}) as a measure for the agreement of pattern shape (right).

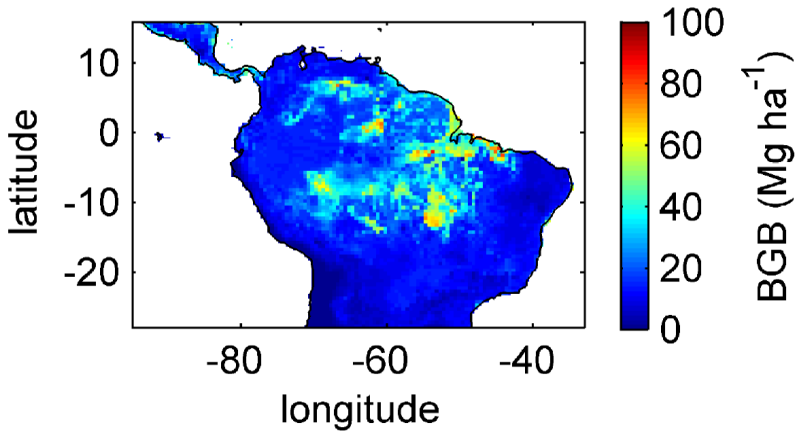

~~Fig. 15: Mean sum (2001-2010) of belowground biomass (BGB; sum of tree coarse and fine roots) of evergreen and deciduous tree PFTs simulated with LPJmL4.0-VR under CRU climate forcing.~~

Table 1: β-values assigned to the 10 sub-PFTs of each tropical PFT (evergreen and deciduous) in LPJmL4.0-VR and the corresponding maximum rooting depth reached by 95% of the roots (D_{95_max}).

sub-PFT number	β-value	D_{95_max} (m)
1	0.9418	0.5
2	0.9851	2
3	0.9925	4
4	0.995	6
5	0.9963	8
6	0.9971	10
7	0.9976	12
8	0.9981	14
9	0.9986	16
10	0.9993	18

12 Appendix A

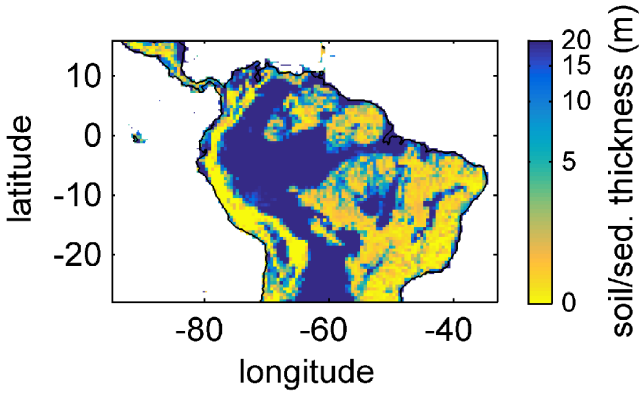

Figure A1: Soil/sediment thickness from (Pelletier et al., 2016) **regridded to the 0.5° x 0.5° longitude-latitude grid of LPJmL4.0-VR and restricted to a maximum of 20 m. Colorbar in decadic logarithm.**

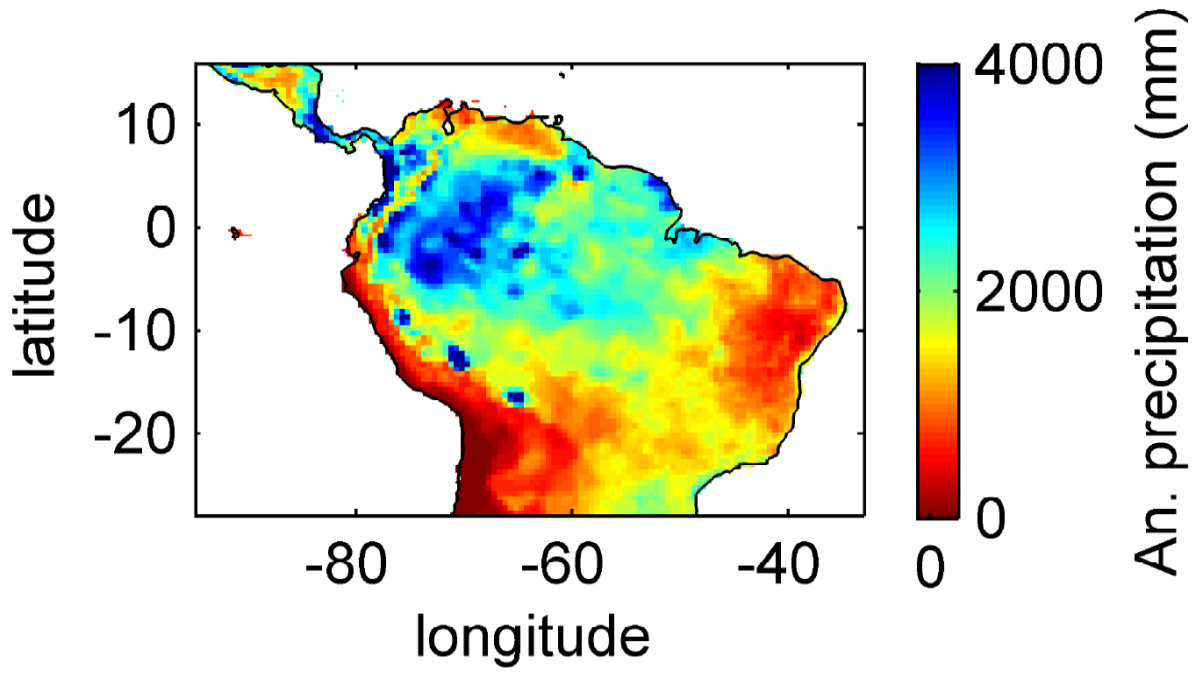

Figure A2: Mean annual precipitation for 2001-2010 under CRU climate input.

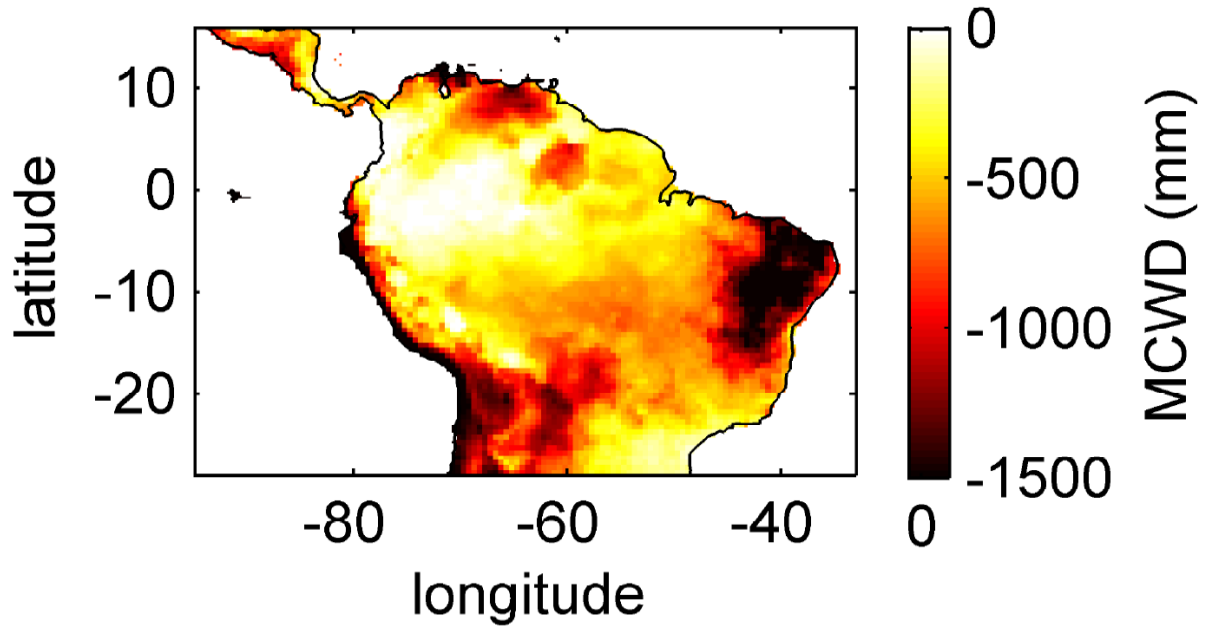

Figure A3: Mean annual MCWD for 2001-2010 under CRU climate input.

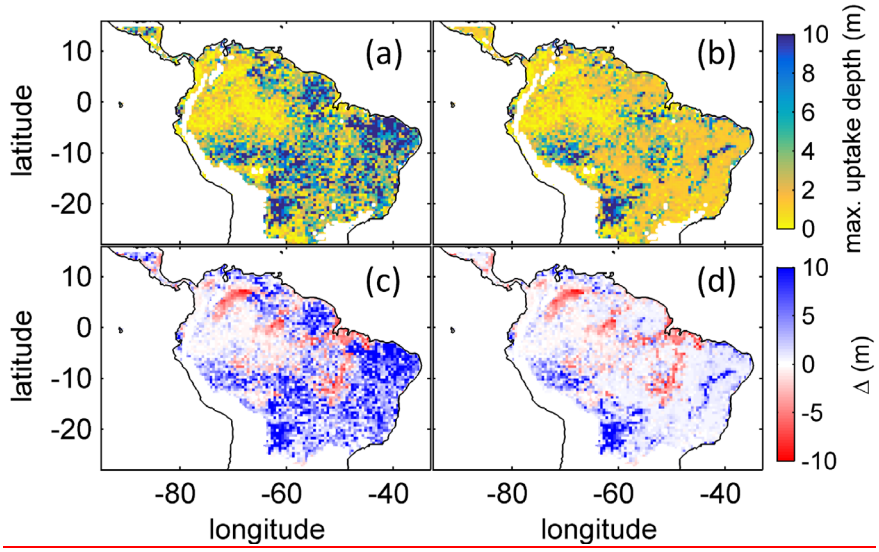

Figure A4: Comparison of simulated $\overline{D_{95}}$ to product of maximum tree root water uptake depth (MDRU). a) Original (Fan et al., 2017) MDRU regridded to 0.5°x0.5° resolution of LPJmL4.0-VR. b) Same as a) but adjusted to soil depth input used in this study (see 2.3.2), in cases where values of (Fan et al., 2017) exceeded this soil depth. The color scale maximum for a) and b) is set to 10 m. c) Difference between a) and $\overline{D_{95}}$ simulated with LPJmL4.0-VR under CRU climate forcing (Fig. 6a). d) Difference between b) and $\overline{D_{95}}$ simulated with LPJmL4.0-VR under CRU climate forcing (Fig. 5a). Red/blue colors denote higher/lower rooting depths in LPJmL4.0-VR.

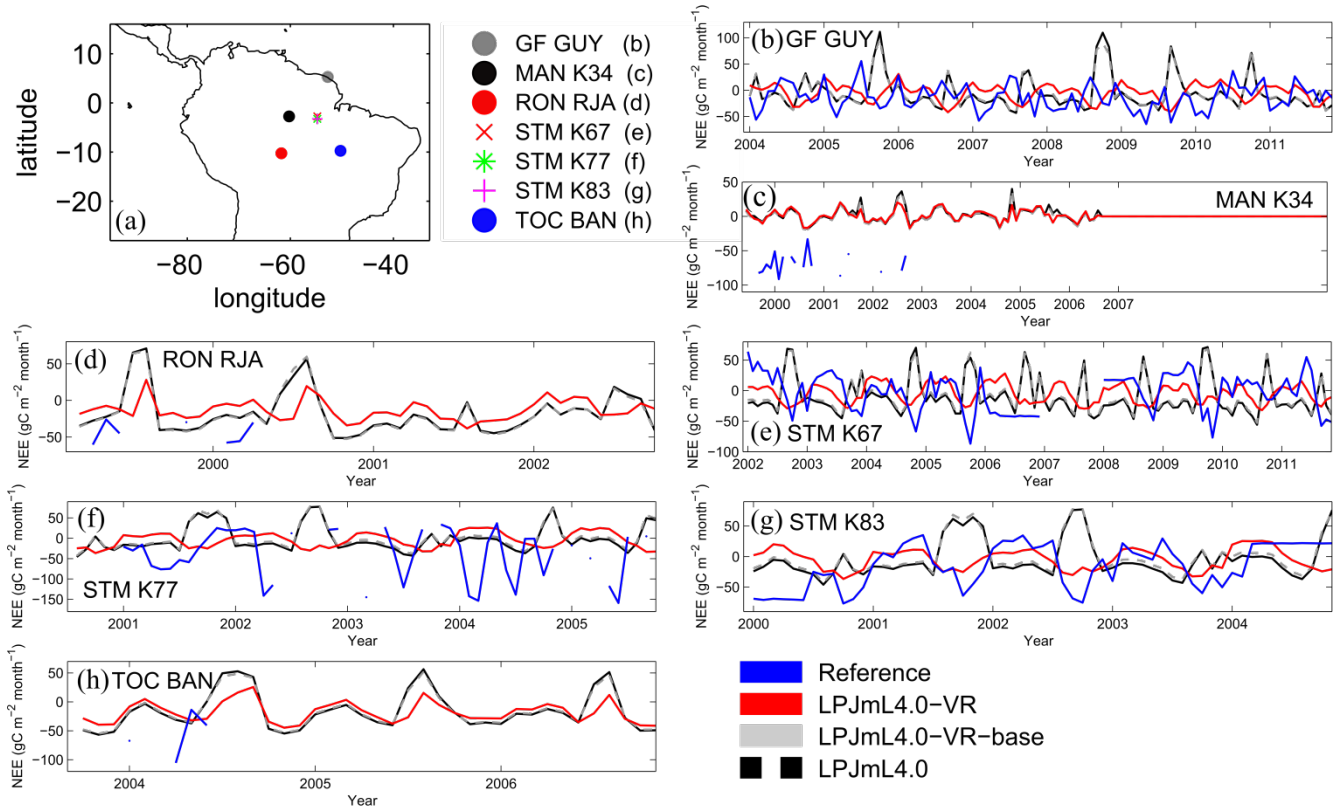

Fig. A5: Comparisons of monthly NEE between different Fluxnet sites and respective simulation output of the different LPJmL model versions used in this study forced with CRU climate. a) Geographical location of different Fluxnet sites (see also Table A2).

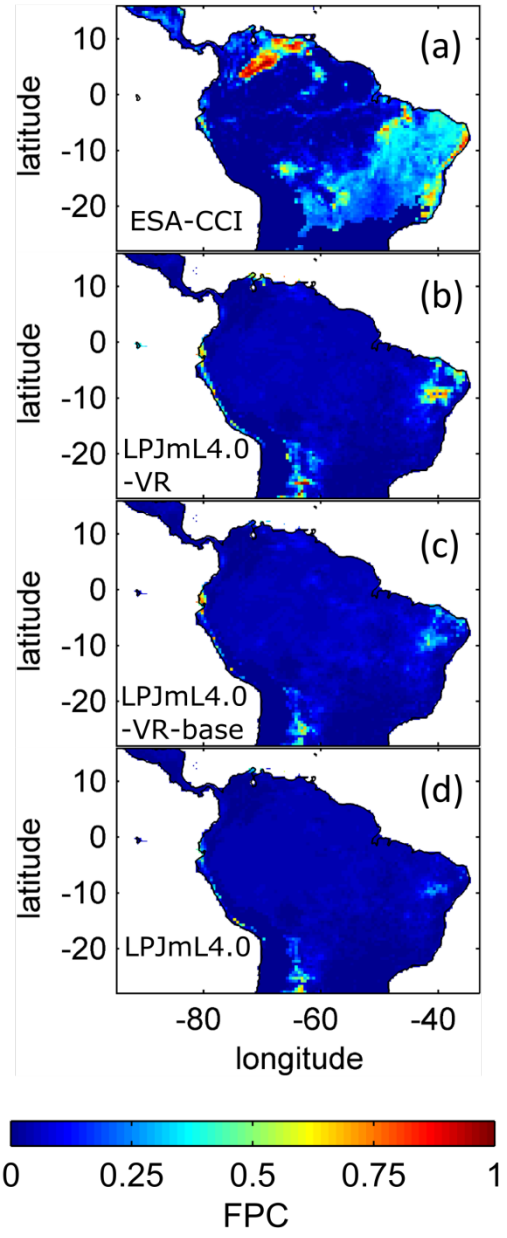

Figure A6: Foliage projected cover (FPC) of the tropical herbaceous PFT over the study region. a) Satellite-derived vegetation composition from ESA Land cover CCI V2.0.7 (Li et al., 2018) **reclassified to the PFTs of LPJmL as in** (Forkel et al., 2014)**. b) LPJmL4.0-VR. c) LPJmL4.0-VR-base. d) LPJmL4.0. All LPJmL model versions were forced with CRU climate input. The shown FPC for all models refers to 2001-2010.**

Regional pattern of simulated above- and belowground biomass

The simulated mean AGB pattern (2001-2010) of LPJmL4.0-VR (Fig. A7) shows that variable tree rooting strategies lead to a contiguous high biomass over the Amazon region. Especially towards the borders of the South-Eastern Amazon region in the climatological clusters EQ E and SAMz, AGB values appear rather homogenous in contrast to constant shallow tree rooting strategies simulated in the other 2 model versions (Fig. A7d-e). In connection with the significantly improved underlying vegetation composition (Fig. 10e-f) it is clear that LPJmL4.0-VR is the only model version capable of simulating high AGB evergreen rainforests across the climatic gradient of the Amazon region (Fig. A2-A3). This pattern is also found by one satellite derived AGB product chosen for evaluation of our model results (Saatchi *et al.*, 2011; Fig A7b) which yields a corresponding NME close to 0 (Table A7). However, compared to this product low NME values are found for all model versions. Surprisingly, in comparison to the other AGB validation product (Avitabile et al., 2016a; Fig. A7a) LPJmL4.0-VR-base yields a smaller NME than LPJmL4.0-VR. Considering the significantly less accurate underlying vegetation composition of LPJmL4.0-VR-base as well as LPJmL4.0 (Fig. 10) we regard such comparisons as critical in this context.

Simulating diverse tree rooting strategies in connection with investment into coarse root structures in LPJmL4.0-VR allows analysing carbon investment into the newly implemented root carbon pools (Sect. 2.2.4). As expected, belowground biomass (BGB; Fig. A8) follows the simulated pattern $\overline{D_{95}}$ (Fig. 5). Highest BGB is found at maximum values of $\overline{D_{95}}$ and vice versa. It is important to note that LPJmL4.0-VR appears to underestimate BGB compared to empirical findings in the Amazon region. While LPJmL4.0-VR shows BGB making up a range of 3.6-16.2% of total biomass across the Amazon region, different site specific empirical studies found mean values at the upper end or significantly exceeding this range (Fearnside, 2016). The most plausible explanation for underestimating BGB is that LPJmL4.0-VR does not account for root structures needed for tree statics. Acknowledging tree statics would increase below ground carbon investment and therefore BGB. Nevertheless, below-ground carbon investment for tree statics would apply for all sub-PFTs simultaneously and would therefore most likely not significantly change competition dynamics and resulting distributions of tree rooting strategies found in this study.

Comparisons of AGB pattern between all model versions of this study and different biomass products are difficult, since only LPJmL4.0-VR shows a reasonable geographical distribution of underlying PFTs across the study area (Fig. 10, Table A6). Therefore, differences in biomass are not solely the consequence of different productivities directly related to diversity in tree rooting strategies, but also the consequence of simulated PFT dominance, i.e. rather an indirect effect of diversity in tree rooting strategies. Concentrating on LPJmL4.0-VR only, the model matches substantially better with the gridded biomass product of Saatchi et al. (2011; Table A7), since this product shows generally higher biomass values across the Amazon region which are more similar to LPJmL4.0-VR. Therefore, the higher NME found in the comparison to the biomass product of Avitabile et al. (2016) is mainly caused by divergence of mean biomass values of the evergreen PFT across the whole study area rather than pattern divergence. Thus, we argue lowering overall biomass values in LPJmL4.0-VR would improve its match with Avitabile et al. (2016) which is a matter of adjusting overall maximum tree mortality rates (Sect. 2.2.7).

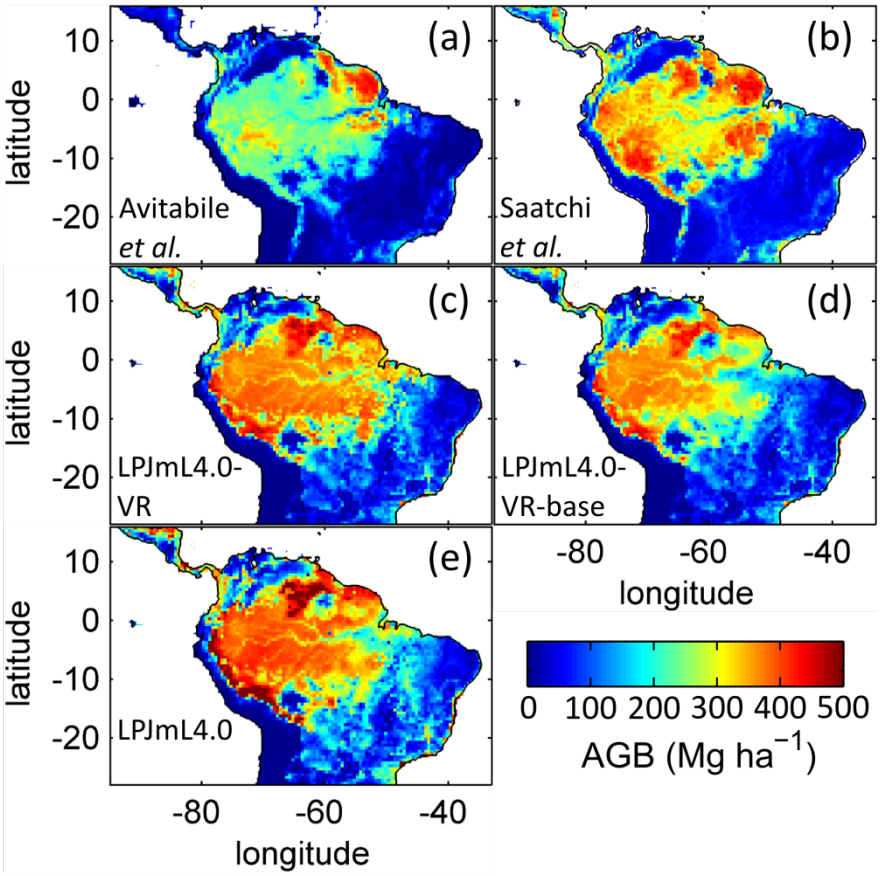

Fig. A7: Comparison of simulated AGB and satellite derived AGB validation products regridded to the spatial resolution of LPJmL models. a) Biomass validation product from Avitabile *et al.* (2016b). b) AGB validation product from Saatchi *et al.*, (2011). c)-e) Mean AGB simulated for the time span 2001-2010 with c) LPJmL4.0-VR. d) LPJmL4.0-VR-base and e) LPJmL4.0. For statistical measures of individual comparisons between model versions (c-e) and satellite derived AGB evaluation products (a-b) see Table A7.

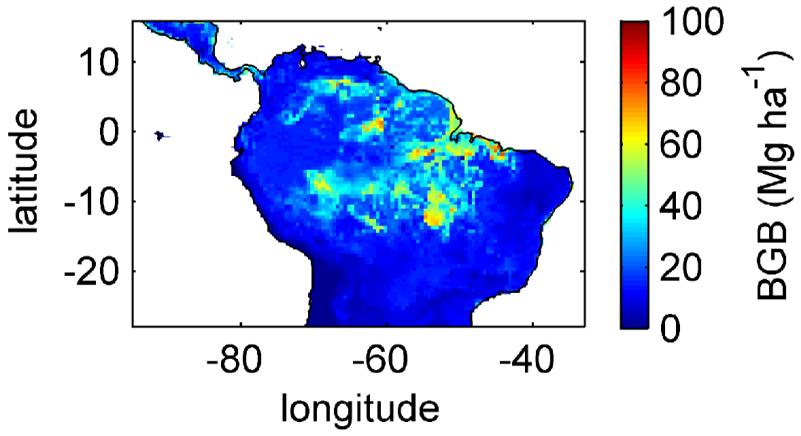

Fig. A8: Mean sum (2001-2010) of belowground biomass (BGB; sum of tree coarse and fine roots) of evergreen and deciduous tree PFTs simulated with LPJmL4.0-VR under CRU climate forcing.

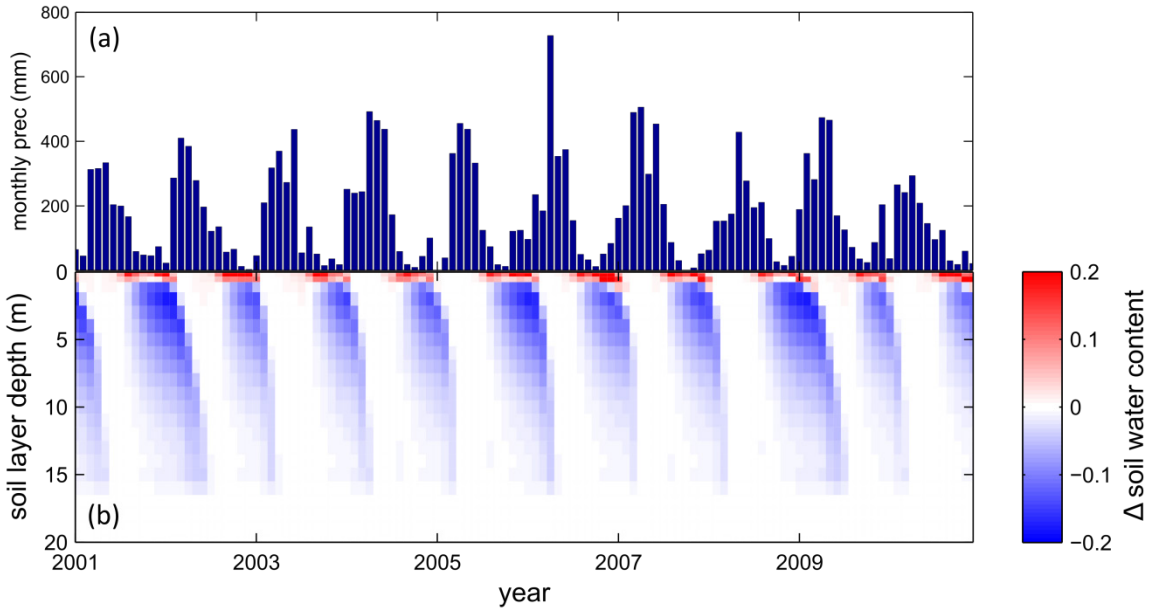

Figure A9: Difference in soil water reaction to seasonal precipitation between LPJmL4.0-VR-base and LPJmL4.0-VR at Fluxnet site STM_KM67 a) Mean monthly precipitation input from CRU for 2001-2010. b) Difference in monthly relative soil water content between LPJmL4.0-VR-base and LPJmL4.0-VR forced with CRU climate for 2001-2010. The underlying model output variable "soil water content" of each model version is a number between 0 and 1 depicting the relative water saturation of the soil. Blue colors denote lower soil water content in LPJmL4.0-VR and red colors a lower soil water content in LPJmL4.0-VR-base.

~~Table 1~~Table A1:~~:~~ **Soil layer partitioning scheme used in LPJmL4.0-VR. The first meter of the soil column is split into 3 soil layers and after 1m of soil depth each following soil layer is assigned a thickness of 1 m as in LPJmL4.0. Whereas LPJmL4.0's last soil layer reaches 3 m, LPJmL4.0-VR's last soil layer reaches 20 m.**

Soil layer number	Soil layer boundary (m)	Soil layer thickness (m)
1	0.2	0.2
2	0.5	0.3
3	1	0.5

4	2	1
…	…	…
23	20	1

Table A2: Description of Fluxnet sites used for the evaluation of simulated ET.

~~**Table 2: β values assigned to the 10 sub-PFTs of each tropical PFT (evergreen and deciduous) in LPJmL4.0-VR and the corresponding maximum rooting depth reached by 95% of the roots (D_{95_max}).**~~

Site name	Short name	Country	LPJmL coordinate	
			latitude	longitude
Ecotone Bananal Island/BR-Ban	TOC_BAN	Brazil	-9.75	-50.25
Manaus-ZF2 K34/BR-Ma2	MAN_K34	Brazil	-2.75	-60.25
Santarem-Km67-Primary Forest/BR-Sa1	STM_K67	Brazil	-2.75	-54.75
Santarem-Km77-Pasture/BR-Sa2	STM_K77	Brazil	-3.25	-54.75
Santarem-Km83-Logged Forest/BR-Sa3	STM_K83	Brazil	-3.25	-54.75
Rond.- Rebio Jaru Ji Parana-Tower B/BR-Ji3	RON_RJA	Brazil	-10.25	-61.75
Guyaflux	GF_GUY	French Guiana	5.25	-52.75

~~**Table 3: Description of Fluxnet sites used for the evaluation of simulated ET.**~~

Table A3: Normalized mean error (NME), coefficient of determination (r^2) and p-value of F-statistic piecewise calculated for simulated ET of the different LPJmL model versions used in this study forced with CRU climate input and Fluxnet data of ET at 7 Fluxnet sites (in accordance with Fig. 7).

Statistic	Model	TOC_BAN	MAN_K34	STM_K67	STM_K77	STM_K83	RON_RJA	GF_GUY
NME	LPJmL4.0-VR	2.41	1.11	0.75	1.38	1.10	2.28	1.57
	LPJmL4.0-VR-base	2.92	1.22	2.29	0.98	2.74	2.73	2.38
	LPJmL4.0	2.93	1.23	2.27	0.98	2.74	2.70	2.36
r^2	LPJmL4.0-VR	0.09	0.03	0.53	0.17	0.43	0.01	0.08
	LPJmL4.0-VR-base	0.10	0.00	0.33	0.14	0.03	0.01	0.01
	LPJmL4.0	0.09	0.00	0.33	0.14	0.03	0.01	0.01
p-value	LPJmL4.0-VR	0.075	0.041	< 0.001	0.002	< 0.001	0.575	0.005
	LPJmL4.0-VR-base	0.067	0.585	< 0.001	0.005	0.221	0.517	0.277
	LPJmL4.0	0.068	0.672	< 0.001	0.005	0.221	0.514	0.274

Table ~~4~~A4: Normalized mean error (NME), coefficient of determination (r^2) and p-value of F-statistic piecewise calculated for simulated ~~ET~~NEE of the different LPJmL model versions used in this study forced with CRU climate input and Fluxnet data of ~~ET~~NEE at ~~7~~3 Fluxnet sites (in accordance with Fig. 8).

Statistic	Model	STM_K67	STM_K83	GF_GUY
NME	LPJmL4.0-VR	0.90	0.84	1.30
	LPJmL4.0-VR-base	1.62	1.36	1.52
	LPJmL4.0	1.68	1.39	1.52
r^2	LPJmL4.0-VR	0.16	0.14	0.00
	LPJmL4.0-VR-base	0.32	0.06	0.03
	LPJmL4.0	0.33	0.07	0.03
p-value	LPJmL4.0-VR	< 0.001	0.003	0.515
	LPJmL4.0-VR-base	< 0.001	0.055	0.046
	LPJmL4.0	< 0.001	0.047	0.059

~~Table 5: Normalized mean error (NME), coefficient of determination (r^2) and p-value of F-statistic piecewise calculated for simulated NEE of the different LPJmL model versions used in this study forced with CRU climate input and Fluxnet data of NEE at 3 Fluxnet sites (in accordance with Fig. 10).~~

~~Statistic~~	~~Model~~	~~NSA~~	~~EQ W~~	~~EQ E~~	~~SAmz~~	~~SAMS~~
~~NME~~	~~LPJmL4.0-VR~~	~~0.08~~	~~0.26~~	~~0.62~~	~~0.20~~	~~0.06~~
	~~LPJmL4.0-VR-base~~	~~0.37~~	~~0.42~~	~~1.95~~	~~0.58~~	~~0.13~~
~~-~~	~~LPJmL4.0~~	~~0.34~~	~~0.26~~	~~1.92~~	~~0.58~~	~~0.11~~
~~r^2~~	~~LPJmL4.0-VR~~	~~0.98~~	~~0.94~~	~~0.91~~	~~0.98~~	~~1.00~~
	~~LPJmL4.0-VR-base~~	~~0.94~~	~~0.96~~	~~0.20~~	~~0.91~~	~~0.99~~
~~-~~	~~LPJmL4.0~~	~~0.93~~	~~0.96~~	~~0.21~~	~~0.90~~	~~0.99~~
~~p-value~~	~~LPJmL4.0-VR~~	~~< 0.001~~	~~< 0.001~~	~~< 0.001~~	~~< 0.001~~	~~< 0.001~~
	~~LPJmL4.0-VR-base~~	~~< 0.001~~	~~< 0.001~~	~~0.143~~	~~< 0.001~~	~~< 0.001~~
	~~LPJmL4.0~~	~~< 0.001~~	~~< 0.001~~	~~0.135~~	~~< 0.001~~	~~< 0.001~~

~~Table 6~~**Table A5:~~** **Normalized mean error (NME), coefficient of determination (r^2) and p-value of F-statistic piecewise calculated for the simulated ET of the different LPJmL model versions used in this study and continental scale gridded ET products within 5 regional climatological clusters. With respect to Fig. ~~11~~9 comparisons are based on the monthly mean of corridors shown, i.e. 1) the monthly mean of all outputs produced by one LPJmL model version but forced with different climate inputs and 2) the monthly mean of all continental scale gridded ET data products.**

Statistic	Model	NSA	EQ W	EQ E	SAmz	SAMS
NME	LPJmL4.0-VR	0.08	0.26	0.62	0.20	0.06
	LPJmL4.0-VR-base	0.37	0.42	1.95	0.58	0.13
-	LPJmL4.0	0.34	0.26	1.92	0.58	0.11
r^2	LPJmL4.0-VR	0.98	0.94	0.91	0.98	1.00
	LPJmL4.0-VR-base	0.94	0.96	0.20	0.91	0.99
-	LPJmL4.0	0.93	0.96	0.21	0.90	0.99
p-value	LPJmL4.0-VR	< 0.001	< 0.001	< 0.001	< 0.001	< 0.001
	LPJmL4.0-VR-base	< 0.001	< 0.001	0.143	< 0.001	< 0.001
	LPJmL4.0	< 0.001	< 0.001	0.135	< 0.001	< 0.001

~~Statistic~~	~~Model~~	~~FPC Evergreen~~	~~FPC Deciduous~~
~~NME~~	~~LPJmL4.0-VR~~	~~0.31~~	~~1.01~~
	~~LPJmL4.0-VR-base~~	~~0.38~~	~~1.5~~
	~~LPJmL4.0~~	~~0.47~~	~~1.76~~

Table ~~7~~A6: Normalized mean error (NME) of FPC comparison piecewise calculated between 1) the satellite-derived vegetation composition from ESA Land cover CCI V2.0.7 (Li et al., 2018) **reclassified to the PFTs of LPJmL as in Forkel et al. (2014) and 2) all LPJmL model versions used in this study forced with CRU climate data (in accordance with Fig. 10).**

Statistic	Model	FPC Evergreen	FPC Deciduous
NME	LPJmL4.0-VR	0.31	1.01
	LPJmL4.0-VR-base	0.38	1.5
	LPJmL4.0	0.47	1.76

~~Statistic~~	~~Model~~	~~Avitabile *et al.*~~	~~Saatchi *et al.*~~
~~NME~~	~~LPJmL4.0-VR~~	~~0.78~~	~~0.12~~
	~~LPJmL4.0-VR-base~~	~~0.69~~	~~0.11~~
	~~LPJmL4.0~~	~~1.09~~	~~0.14~~

Table ~~8~~A7: Normalized mean error (NME) of AGB comparison piecewise calculated between 1) the satellite-derived AGB validation products and 2) all LPJmL model versions used in this study forced with CRU climate data (in accordance with Fig. ~~12).~~A7).

Statistic	Model	Avitabile *et al.*	Saatchi *et al.*
NME	LPJmL4.0-VR	0.78	0.12
	LPJmL4.0-VR-base	0.69	0.11
	LPJmL4.0	1.09	0.14